DEVELOPMENT OF ELECTRIC CAR PROTOTYPE: ELECTRIC VEHICLE INTELLIGENT CONTROL SYSTEM (EVICS)

GAN GUO DONG

A project report submitted in partial fulfilment of the requirements for the award of Bachelor of Engineering (Hons.) Electrical and Electronic Engineering

Faculty of Engineering and Science
Universiti Tunku Abdul Rahman

May 2011

DECLARATION

I hereby declare that this project report is based on my original work except for citations and quotations which have been duly acknowledged. I also declare that it has not been previously and concurrently submitted for any other degree or award at UTAR or other institutions.

Signature : ____________________

Name : Gan Guo Dong

ID No. : 07UEB06446

Date : 13th May 2011

APPROVAL FOR SUBMISSION

I certify that this project report entitled **"DEVELOPMENT OF ELECTRIC CAR PROTOTYPE: ELECTRIC VEHICLE INTELLIGENT CONTROL SYSTEM (EVICS)"** was prepared by **GAN GUO DONG** has met the required standard for submission in partial fulfilment of the requirements for the award of Bachelor of Engineering (Hons.) Electrical and Electronic Engineering at Universiti Tunku Abdul Rahman.

Approved by,

Signature : _______________________________

Supervisor : Dr. Chew Kuew Wai

Date : 13th May 2011

ACKNOWLEDGEMENTS

I would like to thank everyone who had contributed to the successful completion of this project.

First and foremost, I would like to express my sheer gratitude to my research supervisor and beloved mentor of the UTAR EV Team, Dr. Chew Kuew Wai for his invaluable advice, guidance and his enormous patience throughout the development of the research. Through his wide knowledge, kind understanding and directional leadership, I am able to experience a lot more than I have imagined, such as industrial visits to companies (Tai Kwong-Yokohama Battery Industries Sdn. Bhd.and Proton Sdn. Bhd.) and attend paper publication conference.

Furthermore, I would like to thank Universiti Tunku Abdul Rahman (UTAR) in providing the adequate support and facilities for me to complete my final year project. Moreover, I would like to thank Tai Kwong-Yokohama Battery Industries Sdn. Bhd. in providing us sponsorship in terms of lead acid batteries and brushless DC motors.

Besides, I would like to thank my fellow team-mates (Gan Yu Han, Vincent Cheah Beng Keat, Jayson Phuan Zheng Yi, Leong Chee Ken and Yoong Mun Kiat) who have been very helpful and kind in giving advice and offering their utmost hard work, attention and patience in completing this project together.

Additionally, I would like to thank my dear parents in giving me the support that I needed to have my tertiary education and consequently giving me the passion and drive to strive harder in completing this final year project.

Lastly, I would like to express gratitude to those who I have not mentioned here for your great help in assisting and guiding me throughout this project.

ELECTRIC VEHICLE INTELLIGENT CONTROL SYSTEM

ABSTRACT

Electric Vehicle Intelligent Control System (also known as EVICS) is the brainchild of the UTAR EV Team in prototyping the implementation of an intelligent control and monitoring system for a light-weight, urban-dwell electric vehicle. EVICS's main control processing unit is the Intel® Atom Desktop Board D510M0 and the desktop board offers flexibility for the integration of different kinds of monitoring modules. In this report of the project, the main discussed topics are the Battery Temperature Monitoring Module, the Vehicle Speed Monitoring Module and the Wireless Remote Desktop Control Module. In addition, the Reverse Parking Sensor Module will also be thoroughly discussed in this report of the project. The Battery Temperature Monitoring Module is important in any electric vehicle owing to the fact that the battery's lifetime is affected greatly by temperatures during charging and discharging, thus it must be monitored and controlled strictly. The Vehicle Speed Monitoring Module is also an imperative part of any vehicle. Thus, EVICS offers an ingenious and cost-effective way to monitor the speed of the electric motor and the electric vehicle. Furthermore, the Wireless Remote Desktop Control Module is an innovative integral of EVICS in providing real time problem solving and maintenance work done on the electric vehicle more effective and efficient without leaving the comfort of the engineer's seat.

Keyword: EVICS

TABLE OF CONTENTS

LIST OF TABLES

LIST OF FIGURES

LIST OF SYMBOLS / ABBREVIATIONS

V	Voltage
S	Rotational Speed
T	Temperature
n	RPM, gear speed
Cp	Specific Heat of Air
W	mass flow
CFM	air flow
P	Static Pressure
K	load factor
r	fluid density
Q	flow
N_A	Number of Gear Teeth
VR	Velocity Ratio
TV	Train Value
f	frequency
R	resistance
C	capacitance
v	velocity, speed (km/h)

EVICS	Electric Vehicle Intelligent Control System
EV	Electric Vehicle
VNC	Virtual Network Computing
ADC	Analogue-to-Digital Conversion
GUI	Graphical User Interface
FTP	File Transfer Protocol
OS	Operating System
IR	Infrared
BLDC	Brushless DC Motor
IM	Induction Motor
SRM	Switch Reluctance Motor
PMDC	Permanent Magnet DC Motor

LIST OF APPENDICES

CHAPTER 1

INTRODUCTION

1.1 Background

The emergence of the electric vehicles came during the time of technological advancement in the field of battery. Moreover, the introduction of more advanced electric motors spurs the rise of electric vehicle even though the electric vehicles have been around since the mid-1800s as the electric motor came before the internal combustion engine. The electric vehicles were manufactured in volume in the late 1800s and early 1900s, and just to decline only with the emergence and the ready availability of cheap gasoline (Leitman, 2009). Below is the history of the electric vehicles:

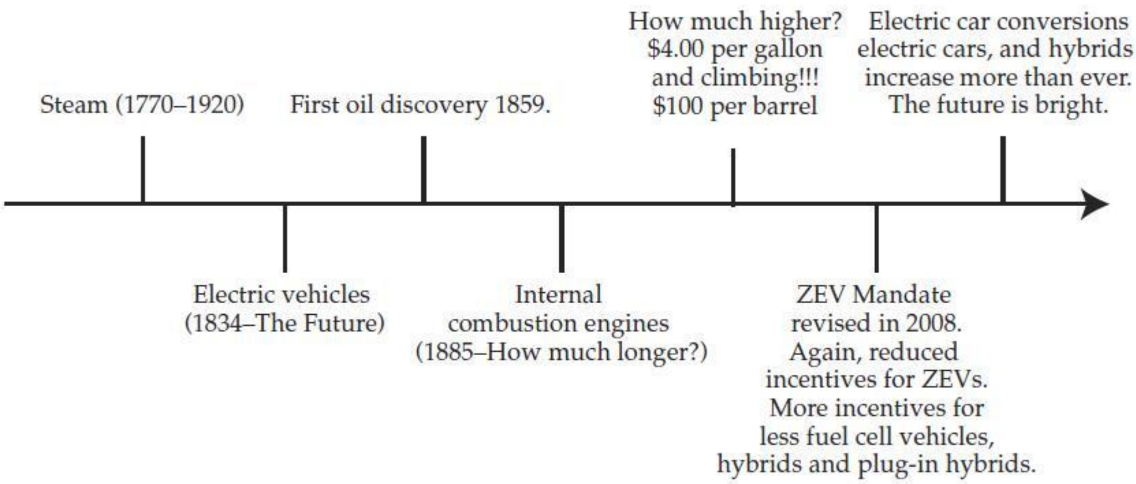

Figure 1.1 History of Electric Vehicle (Leitman, 2009)

The ZEV Mandate was commenced by the California's Air Resources Board in accordance with Low-Emission Vehicle (LEV) Regulations passed in 1990. The mandate required an increase percentage of Zero-Emission Vehicles (ZEV) to be sold in California. ZEV are battery-powered EVs, because they are the only demonstrated automobile technology with no tailpipe emissions (Korthof, 2005).

California's Air Resources Board was able to do perform this action owing to two reasons (Korthof, 2005):

1. General Motors had shown in 1990 that EVs were possible with the "Impact" which is a streamlined car using a (at that time) new type of battery, and the “Impact” was driven into an auto show by the GM CEO. This demonstration showed that previous arguments that EVs were not feasible were not sound.
2. The Clean Air act mandates penalties for California's failure to meet standards.

Figure 1.2 GM EV1 “Impact” (EV1)

Meeting air quality standards remains a challenge due to a growing state population with more vehicles per capita, and more miles travelled per vehicle. ZEVs have no tailpipe emissions, no evaporative emissions, and have a radically lower full fuel-cycle emission, including re-fuelling and fuel generation. Unlike Internal Combustion Engine (ICE) Vehicles, whose emission control systems deteriorate over time, ZEVs remain benign from cradle to grave (Korthof, 2005).

Currently, car manufacturers such as Toyota, Honda, Tesla Motors, General Motors, Proton Sdn. Bhd. and many more have determined that the depletion of the fossil fuel as a huge impact to their future business plans and also a great threat to the automobile industry. Besides, the technological advancement of the EV industry and the increasing demand for EVs are great opportunities for them to re-introduce the electric vehicle to the world as a new form of transportation and maybe a new replacement for the internal combustion engine (ICE) vehicles. For instance, Tesla Motors and Shelby Supercars have proved to the world that electric cars can also be labelled as supercars.

Figure 1.3 Ultimate Aero EV with Top Speed of 334.74km/h and 1000horse power (Telegraph, 2009)

Figure 1.4 Tesla Roadster Sport with Top Speed of 209.21km/h and 288horse power (Tesla, 2010)

Moreover, in Malaysia's Budget 2011 announcement, the Prime Minister has announced that import duty and excise duty is now fully exempted for hybrid and electric cars until the end of the year 2011 (Tan, 2010) and this is a great initiative in encouraging the purpose of zero-emissions. Thus, Proton Sdn. Bhd. took note of the words of our leader and expanded their research in the field of EVs with collaborations from their South Korean counterparts, LG Corporation (Tan, 2009).

Figure 1.5 Proton Saga EV

On the other hand, batteries and electric motors come hand in hand for being the fundamental drive in the advancement of electrical and hybrid vehicles.

There are four major types of batteries used for EVs (Thompson):

1. Free Maintenance Deep Cycle Lead Acid Batteries
2. Nickel Metal Hydride (NiMH) Batteries
3. Lithium Ion Polymer Batteries
4. Molten Salt Batteries

The Free Maintenance Deep Cycle Lead Acid Batteries are common in EVs and have an efficiency of 70-75% and energy density of 30-40Wh/kg in EV application while the most current one, the Lithium Ion Polymer Batteries have an impressive energy density of 200+Wh/kg. In addition, the Nickel Metal Hydride (NiMH) Batteries have a lower efficiency of 60-70% with higher energy density of 30-80 Wh/kg.

In addition, there are three major types of electric motors:

1. AC Induction Motor (IM)
2. Brushless DC Motor (BLDC)
3. Permanent Magnet DC Motor (PMDC)

The AC Induction (Squirrel Cage) motors are more commonly used in EV compared to its counterparts due to their reliability, robustness, almost maintenance-free characteristics, low manufacturing cost and the ability to work in various conditions. However, the controller and driver circuit used to control the AC Induction motor are more complicated and the components used are expensive as the technology are not as matured as its DC counterparts (Gan, 2010).

Brushless DC Motors are the most efficient out of all of the motors mentioned above due to the fact that the brush/commutator assembly is replaced by an intelligent electronic controller (Gan, 2010). And, the controller and driver circuit for controlling a DC motor is usually easier than the AC Induction motors because the technological maturity of DC-based driver circuits are far more established. Hence, BLDC has an advantage in offering a more straightforward approach to speed and torque control (Gan, 2010).

Permanent Magnet DC Motor is the most affordable and readily available current production motor. Also known as the Brushed DC motors, they are good in achieving high torque at low speed and their torque–speed characteristics suitable for the high starting torque situation and high load conditions. However, the biggest weakness of the PMDC is that it requires high maintenance cost and maintenance work have be done frequently to maintain efficiency owing to its brush/commutator assembly. Hence, BLDCs are maturing in the direction to overcome this problem caused by PMDCs.

One of the EVICS's roles in this project is a monitoring system for the motor speed and the battery capacity, including measuring and displaying the running time of battery and the distance left for the EV to travel. EVICS complements the implementation of the measurement modules and the Intel Atom Desktop Board, thus displaying real time information about the batteries and speed.

The Intel® Desktop Board D510MO is designed to unleash the power of the new Intel® Atom™ processor D510 which supports the new revolutionary two–chip layout. This new chipset layout reduces the package footprint by 70%, enabling easier routing and better heat flow. The Intel® NM10 Express Chipset also provides additional flexibility and upgradability with two slots of single channel DDR2 memory at 800/667 MHz supporting up to 4GB maximum (Intel, 2009).

With breakthrough low-power silicon, the Intel Desktop Board D510MO can be used with a passive thermal solution based on the recommended boundary conditions.

Thus, the Intel Desktop Board D510MO represents a fundamental shift in system design—small, yet powerful (Intel, 2009).

1.2 Aims and Accomplishments

This project has several aims and milestones that have been achieved:

1. This project ultimate purpose is to initiate an innovation through prototyping an EV system by utilizing different kinds of monitoring modules. Hence, the project brought us EVICS which is a prototype system ready to be implemented into current electric vehicles.

2. Also, this project is aimed to be a research-based, continuous developing and nonstop project that can be passed down to future UTAR students.

3. This project also open up to many doors for collaborations between UTAR EV Team and many EV related industry leaders. For instance, the continuous collaboration between UTAR EV Team and Tai Kwong-Yokohama Battery Industries Sdn. Bhd. in the field of lead acid batteries. Furthermore, the technical consultations and visits between UTAR EV Team and Proton Sdn. Bhd. Moreover, the discussion regarding electric motorcycles between BKZ (Bikerz) Sdn. Bhd.

4. The UTAR EV Team has joined the Innovate Malaysia 2011 Design Competition under the Intel Atom category with a hope to bring victorious recognition to the UTAR EV Team and its university in terms of vehicular researches. Now, the team has strive through hardships and have risen up to the competition's challenge by being chosen to represent UTAR in the grand finale after being shortlisted as the top five teams from 60 teams from the whole of Malaysia. The grand finale will be held on 11th June 2011 at Altera, Penang.

5. From doing researches for this pioneer-project, altogether there are six paper publications approved and published to the public:
    - Ultra-Fast Charging System On Lithium Ion Battery (IEEE STUDENT 2010 Conference)
    - Studies of Regenerative Braking In Electric Vehicle IEEE STUDENT 2010 Conference)
    - EV Controller and Power Management System (Malaysian Universities Transportation Research Forum and Conference, MUTRFC 2010)
    - Studies on Electric Car Chassis and Design Principle (Malaysian Universities Transportation Research Forum and Conference, MUTRFC 2010)
    - Studies of Electric Motor for Light-Weight Electric Vehicle (Malaysian Universities Transportation Research Forum and Conference, MUTRFC 2010)
    - Design of Battery Pack based on Lithium ion Technology (Malaysian Universities Transportation Research Forum and Conference, MUTRFC 2010)

6. Lastly, hopefully in the future this project will be developed into an operating electric vehicle with the implementation of a fully functional EVICS.

1.3 Research Objectives

The objectives of doing the research and this project are to:

1. Investigate the battery temperature during charging and discharging and its effect during critical temperature.
2. Perform cooling measures for battery temperature beyond optimized level.
3. Investigate methods to measure the rpm of the wheel and electric motor.
4. Translate rpm of wheel into km/h for displaying the speedometer.
5. Determine innovative ideas to troubleshoot EVICS conveniently.

1.4 Scope of Project

This project is divided into a few main modules as below:

1. EVICS
2. Battery Charger Module – Fast Charging and Normal Charging
3. Solar Charging Module
4. Regenerative Braking Module
5. Reverse Parking Sensor Module

1.5 Structure of the Project Report

This project report consists of five chapters, which are described below:

Chapter 1: Introduction
Chapter 2: Literature Review
Chapter 3: Methodology
Chapter 4: Results and Discussions
Chapter 5: Conclusion and Recommendations

CHAPTER 2

LITERATURE REVIEW

2.1 The Overall System Configuration of an Electric Vehicle

The modern electric vehicle drive train is conceptually described in figure 2.1. The drive train consists of three major subsystems: electric motor propulsion, energy source and auxiliary.

The Electric Motor Propulsion Subsystem is comprised of:

a. The vehicle controller
b. The power electronic converter
c. The electric motor
d. Mechanical transmission
e. Driving wheels

The Energy Source Subsystem involves:

a. The energy source (Battery)
b. Energy management unit
c. Energy refuelling unit (Battery Charging Unit)

The Auxiliary Subsystem consists of:

a. The power steering unit
b. The climate control unit
c. The auxiliary supply unit

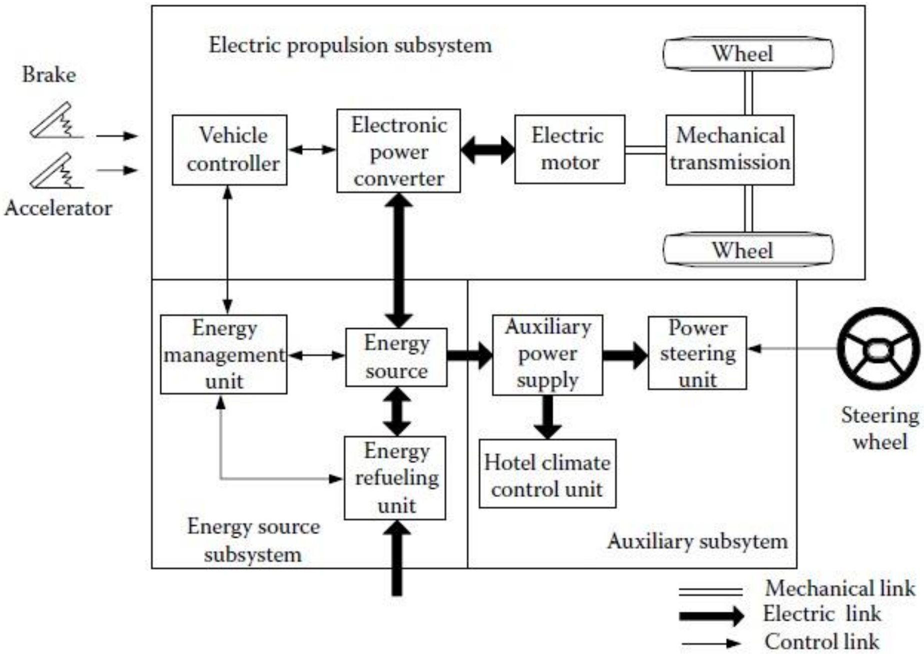

Figure 2.1 Conceptual Illustration of a General EV Configuration (Mehrad, 2005)

The real-time monitoring system of EVICS revolves around parts of the general EV configuration, such as the Energy Source Subsystem and the Electric Motor Propulsion Subsystem.

In addition, the monitoring or the sensing system for the electric vehicle is shown as below in figure 2.2.

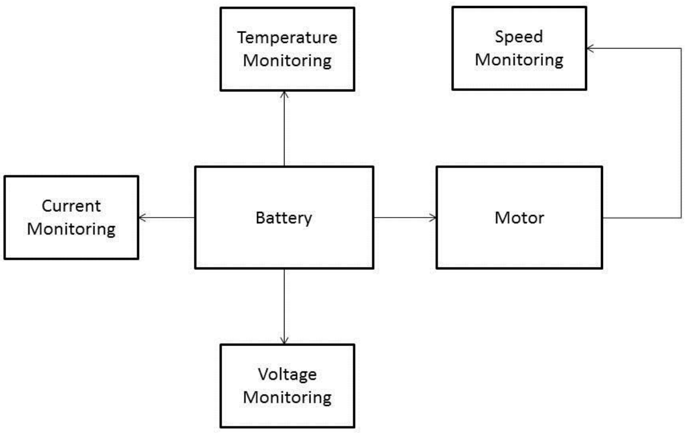

Figure 2.2 Simple Monitoring and Sensing System for EV

Voltage and current monitoring system is implemented in EVs to measure the capacity of the batteries as a fully charged battery will draw less current and its voltage level is same as its nominal value compared to an empty battery having a lower voltage level and it will draw a lot of current from the charger. Thus, we can know whether a particular battery has done charging by measuring its current and voltage.

Additionally, the temperature monitoring module is also important to eschew any overheating of battery during charging and discharging as the critical temperature of batteries will dangerously affect the battery lifetime and condition.

Moreover, the speed monitoring module is also another vital part of the system as measuring the speed of the electric motor requires precision and sensitivity. From the measurement of the raw motor and wheel speed, we can translate the corresponding values into km/h for the travelling speed of the EV.

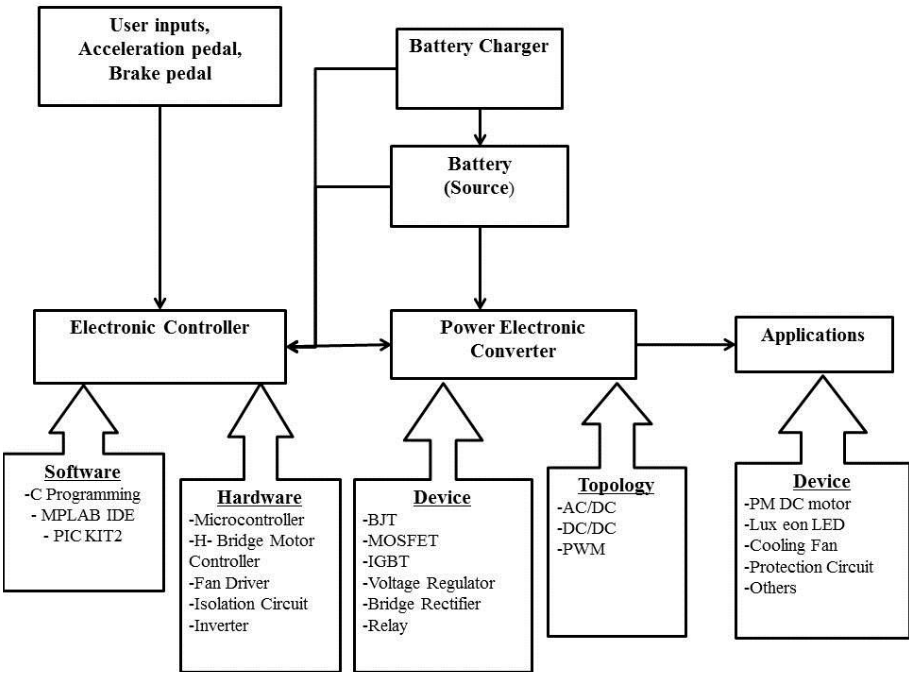

Figure 2.3 Functional Block Diagram of a Typical Electric Propulsion System (Chong, 2009).

The electric propulsion systems are at the heart of the electric vehicles, they consist of:

- Electric motors
- Power converters
- Electronic controllers

The electric motor converts the electric energy into mechanical energy in order the vehicle. The significant advantage that electric motors have over internal combustion engine is regenerative braking to generate electricity when the supply to motor is cut off and the motor slows down on free-running manner. Hence, by utilizing this free-running momentum, it is able to charge the on-board energy storage (batteries). Next, the power converter is used to supply the electric motor with sufficient voltage and most importantly sufficient current to overcome initial torque/stalling torque. On the other hand, the electronic controller commands the power converter by providing control signals to it and consequently controlling the operation of the motor.

Furthermore, there are also sensors and detection devices used to measure the parameters of the entire EV status and the detected results are sent to the microcontroller for generating the appropriate signal output to control the devices for their applications.

An EV control system is very complicated as there are a lot of circuitry and parameters that needed to be taken account. Hence, in figure 2.4 illustrates a rough idea on the interconnections and relationships between the parts and components of an EV.

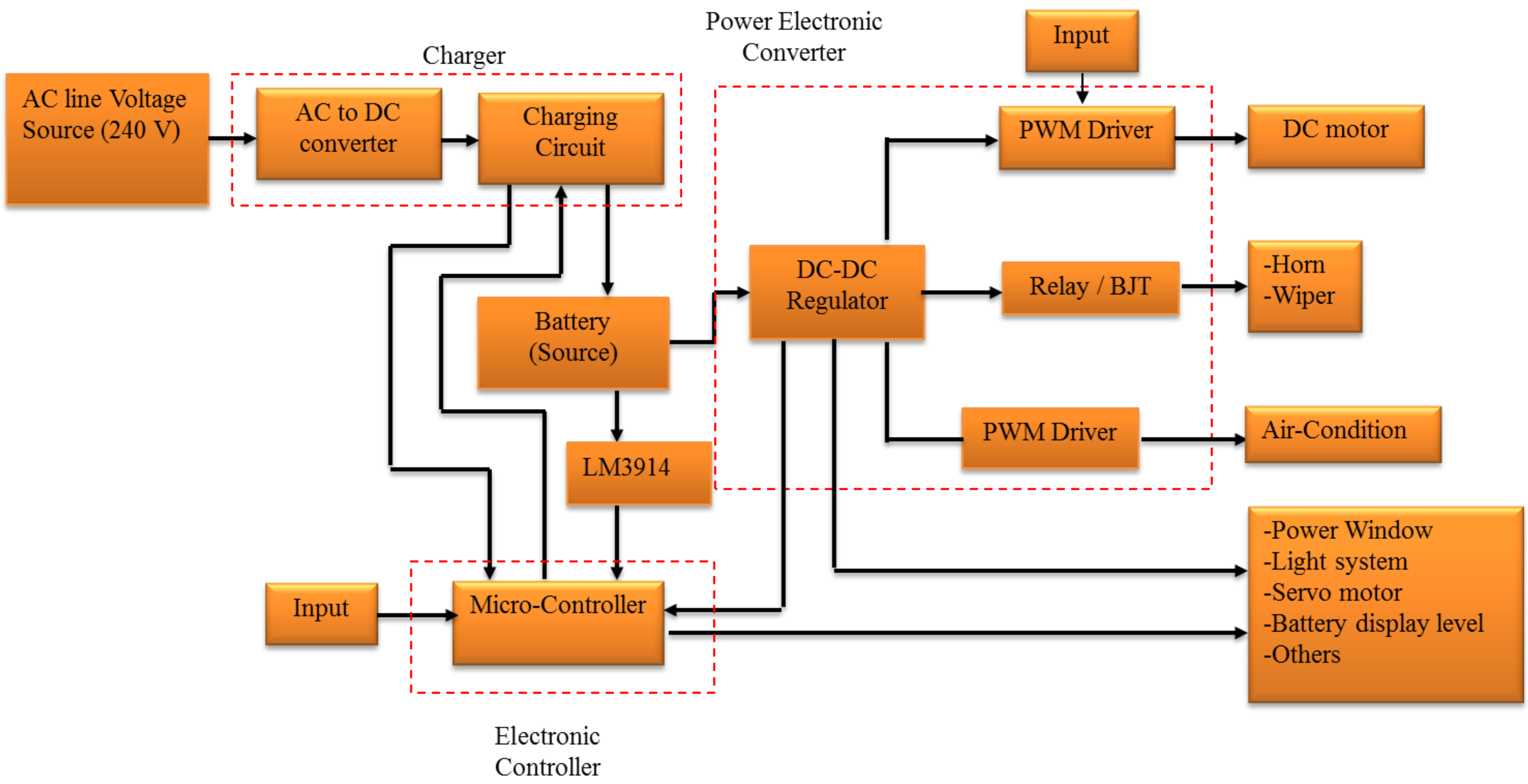

Figure 2.4 Relationships between Different Parts of the EV Car System (Chong, 2009).

2.2 Studies of Electric Motors for Light-Weight Electric Vehicle

According to a new study from the Centre for Entrepreneurship and Technology at University of California, Berkeley, electric cars could comprise 64-86% of US light vehicle sales by 2030. As seen in figure 2.5, the study shows rapid adoption for electric vehicles with switchable batteries, quantifies how the electrification of the U.S. transportation system will decrease America's dependence on foreign oil, increase employment, and reduce the environmental impact of transportation emissions. From this study, the electric vehicle and the development of high performance electric motor is a force to be reckoned with (Gan, 2010).

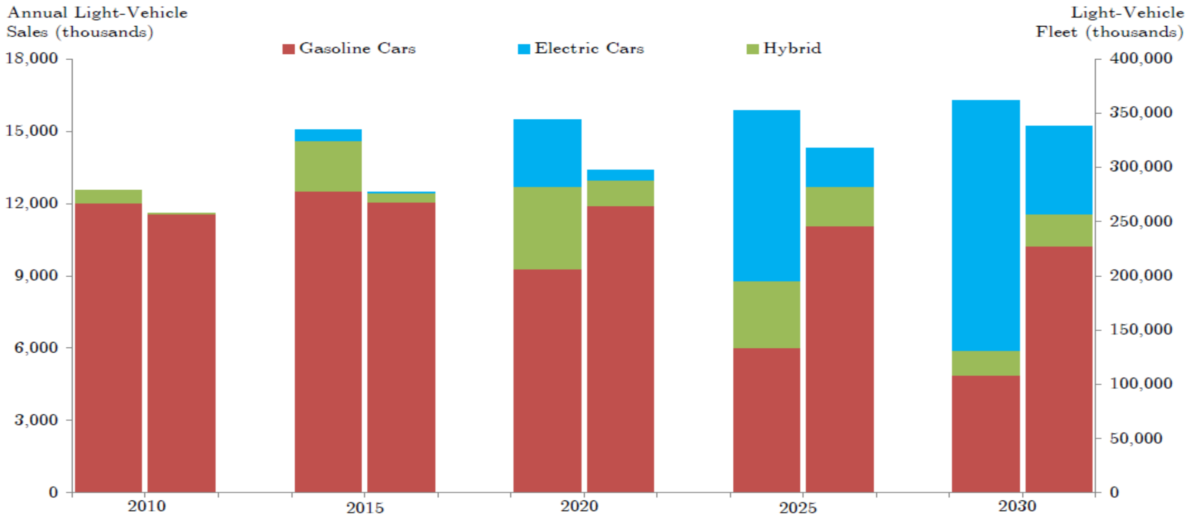

Figure 2.5 US Light Vehicle Sales and Fleet Composition under Baseline Scenario (Gan, 2010)

Therefore, the electric motor has many criteria such as efficiency, cost, reliability, power density, maturity of technology and controllability must be taken into consideration. Usually, electric cars are driven by large electric motors usually rated between 3.5 and 28 horsepower. For those accustomed to gas engines, this may not seem like much power, but the rating systems used for gas engines and electric motors are so different that the numbering system is almost meaningless. Gas engines are rated at their peak horse power while electric motors are rated at their continuous horse power. The peak horse power of an electric motor is usually 8 to 10 times its continuous rating. Electric vehicle drive motors can be divided into two basic groups, DC or direct current motors, and AC or alternating current motors (Gan, 2010).

2.2.1 EV Demands and Design Outline of EPS

Table 2.1 EV's Basic Requirement on Electric Drive Train and their Implications on Performance

Requirement	Implications
High torque at low speeds and constant power at high speed.	Driving performance.
Continuous and smooth drive control.	Comfort.
High efficiency, regenerative braking.	Longer driving range.
High specific power and specific torque.	Overall efficiency and consistency.
Maintenance free.	Safety and maintenance cost.
Reasonable Cost.	Price and Budget.

With this, a description of motor parameters and control strategy can be discussed and also to identify the parameters according to the performance requirement. Lastly, optimization can be made to improve the drive train and efficiency (Gan, 2010).

2.2.2 Characteristics of Electric Motor for EV

In EV, the vehicle performance is completely determined by the torque-speed characteristic of the motor which is much closer to the ideal as compared to ICE (Internal Combustion Engine). In order to meet EV requirement, operation entirely in constant power is needed. However, operation fully in constant power may be impossible for any practical vehicle. For EVs, the desired output characteristics of electric motor drives are illustrated in figure 2.6. It can be observed that the electric motor is expected to be able to produce a high torque at low speed for starting and acceleration because as it increase to the base speed, the voltage increases to its rated voltage while the flux remain constant. Also, electric motor generates a high power at high speed for cruising due to the fact that beyond the base speed, the voltage remains constant and the flux is weakened. The result is constant output power while the torque declines hyperbolically with speed. Thus, a single-gear transmission will be enough for a light-weight EV. In figure 2.6, as we know from above, the electric motor can generate constant rated torque up to its base speed. At this speed, the motor reaches its rated power limit. The operation beyond the base speed up to the maximum speed is limited to the constant power region. This region of the constant power operation depends primarily on the particular motor type and its control strategy (Gan, 2010).

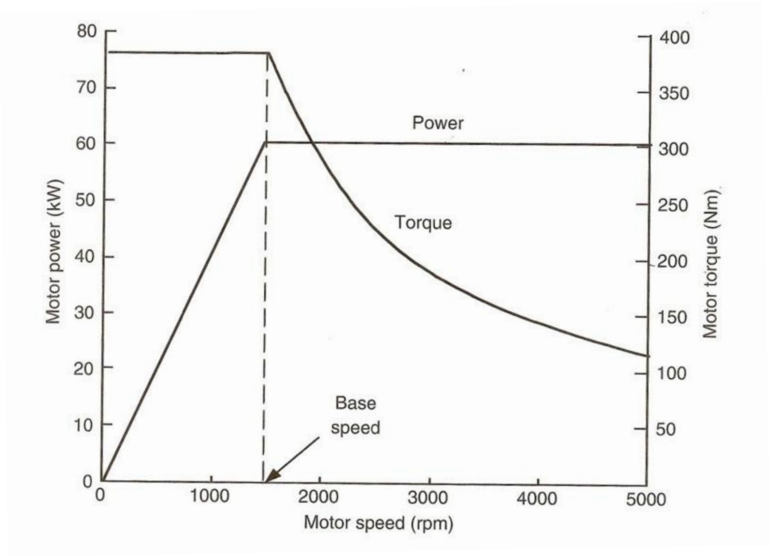

Figure 2.6 Typical Performance Characteristics of Electric Motor for Traction (Gan, 2010).

From the output characteristics of electric motor for EVs, the following valuable results can be concluded as follows:

a) The power requirement (rated power) for acceleration performance (acceleration time and acceleration distance) decreases as constant power region ratio increases.
b) Conversely, the torque requirement (rated torque) for acceleration increases as constant power region ratio increases. This results in a larger motor size and volume.
c) The maximum speed of electric motor has a pronounced effect on the required torque of the motor. Low speed motors with the extended constant

power speed range have a much higher rated shaft torque. Consequently, they need more iron and copper to support this higher flux and torque.

d) As motor power decreases (due to extending the range of constant power operation), the required torque is increasing. Therefore, although the converter power requirement (hence the converter cost) will decrease when increasing the constant power range, the motor size, volume, and cost will increase.

e) Increasing the maximum speed of the motor can reduce the motor size by allowing gearing to increase shaft torque. However, the motor maximum speed cannot be increased indefinitely without incurring more cost and transmission requirements. Thus, there is multitude of system level conflicts when extending the constant power range.

Next, it is the tractive effort of the electric motor is discussed. The tractive effort which is also known as tractive force is described as the pulling force exerted by a vehicle. The tractive effort generated by a traction motor on driven wheels and vehicle velocity are expressed as:

$$F_t = \frac{T_m \, i_g i_o \eta}{r_d} \ (N)$$

And

$$V = \frac{\pi \, N_m \, r_d}{30 \, i_g \, i_o} \ (m/s)$$

where T_m and N_m are respectively the motor torque output and speed (rpm), i_g is the gear ratio of transmission, i_o is the gear ratio of final drive, η is the efficiency of the whole driveline from the motor to the driven wheels and r_d is the radius of the drive wheels.

The efficiency of an electric motor varies with the operating conditions on the speed-torque curve as shown in figure 2.6 below where the most efficient operating area exist. Thus, the EPS design should be at least be as close as possible to the area with the most efficiency.

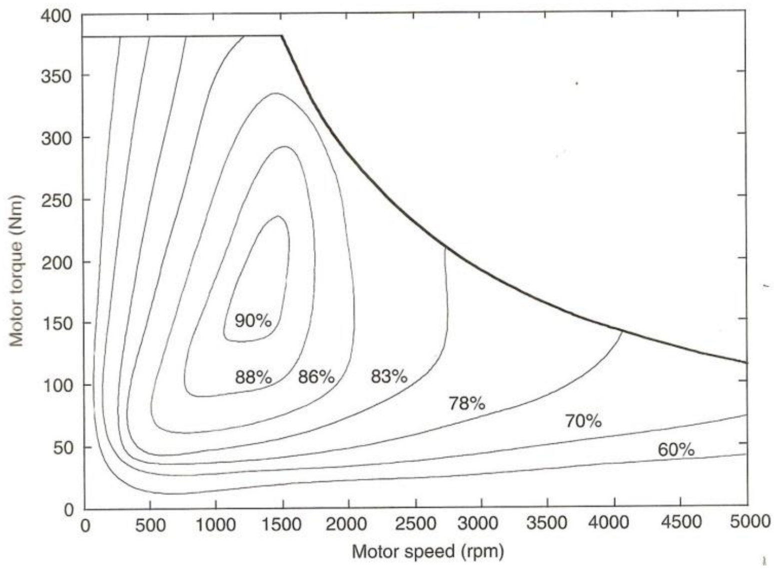

Figure 2.7 Typical Electric Motor Efficiency Characteristics (Gan, 2010)

2.2.3 Comparative Study about the Specific Type of Electric Motors for EV

In this section, there will be comparisons between electric motors and their advantages and drawbacks of implementing them in the EV (Gan, 2010).

1. Brushed DC Motor

The brushed series DC motor is the most affordable and readily available current production motor. Brushed DC motors are good in achieving high torque at low speed and their torque–speed characteristics suitable for the high starting torque situation and high load conditions. And, these motors are easy to control their speed through variation of voltage levels. The characteristic of series, shunt and compound motors are shown in figure 2.7. Series motors are good in applications requiring high starting torque and heavy torque overload. Shunt motors have better controllability than series motors. Shunt motors also known as separately excited motors are suited for field weakened operation, due to its decoupled torque and flux control characteristics. Moreover, a range of extended constant power operation is obtained by separate field weakening.

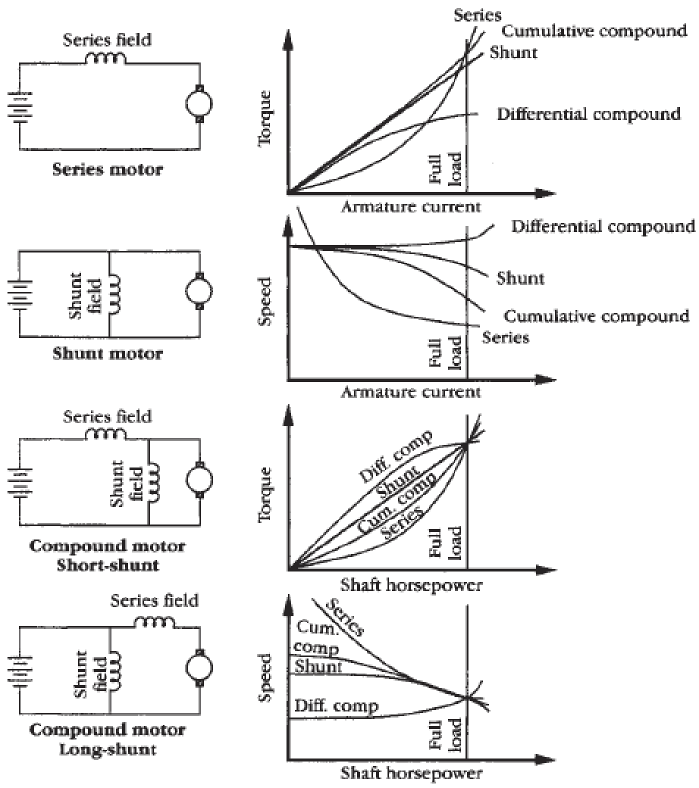

Figure 2.8 Characteristics of DC Motor Types (Gan, 2010)

Moreover, the speed characteristics of DC motors can be observed in the figure 2.8 below.

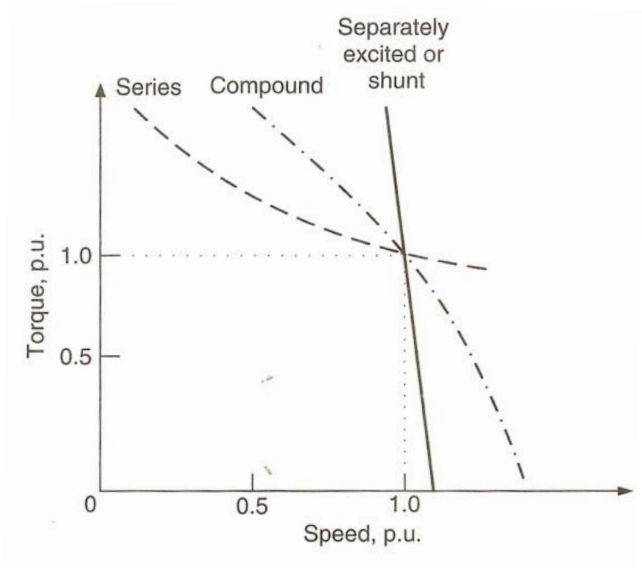

Figure 2.9 Speed Characteristics of DC motors (Gan, 2010)

On the other hand, permanent magnet motors are very efficient, but only in a very narrow rpm band, and quickly lose their efficiency in the varying speeds of normal driving. Permanent magnet motors resemble the shunt motor in their torque, speed, reversing, and regenerative braking characteristics. However, the permanent magnet motors have starting torques several times that of shunt motors and their speed versus load characteristics are more linear and easier to predict.

2. Brushless DC Motor (BLDC)

In a BLDC, the brush-system/commutator assembly is replaced by an intelligent electronic controller and making the BLDC the most efficient of all electric motor. The controller performs the same power-distribution found in a brushed DC-motor, only without using a commutator/brush system. The controller may contain a bank of MOSFET devices to drive high-current DC power, and a microcontroller to precisely orchestrate the rapid-changing current-timings. Because the controller must follow the rotor, the controller needs some means of determining the rotor's orientation/position (relative to the stator coils.) Some designs use Hall Effect sensors to directly measure the rotor's position. Others measure the back EMF in the undriven coils to infer the rotor position, eliminating the need for separate Hall Effect sensors, and therefore are often called "sensorless" controllers.

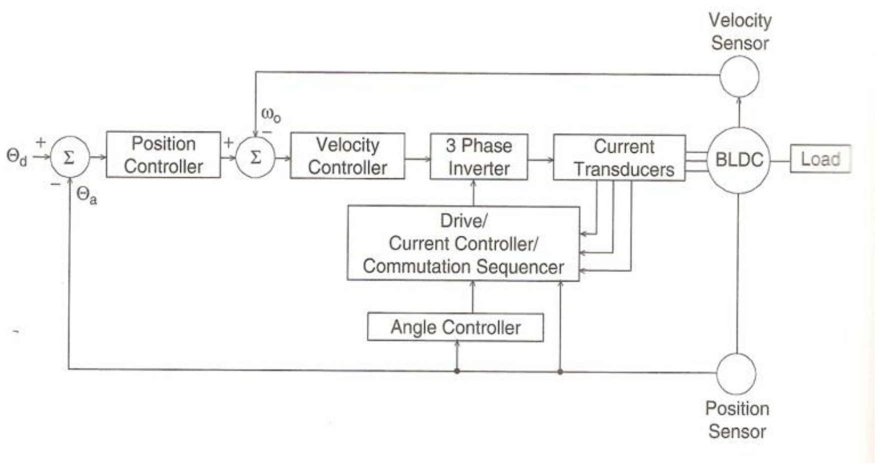

Figure 2.10 Basic Block Diagram of a Classical Speed and Position Control for BLDC (Gan, 2010)

BLDC motors can be constructed in two different physical configurations: In the 'conventional' configuration, the permanent magnets are mounted on the spinning armature (rotor) and the stator coils surround the rotor. In the 'outrunner' configuration, the radial relationship between the coils and magnets are reversed; the stator coils form the center (core) of the motor, while the permanent magnets spin on an overhanging rotor which surrounds the core. In all BLDC motors, the stator-coils are stationary and thus making current circulation only in the stator and not the rotor, making the rotor to not heat up. This will further ease the cooling design for the BLDC as the stator in conventional configuration is on the periphery of the motor and it will be easier to cool when the stator heats up. Improvement of efficiency can be done using the inverted rotor topology/”outrunner” (where the rotor rotates on the outside of the stator) has a larger magnetic field. The additional radius provides higher torque and power density and leads to better efficiency.

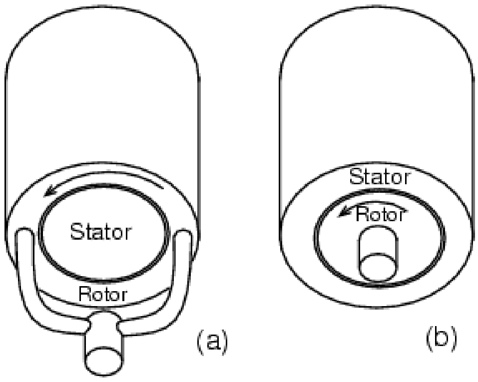

Figure 2.11 (a) Out-runner configuration. (b) Conventional configuration (Gan, 2010)

3. AC Induction Motor (IM)

Squirrel cage IM have been the most suitable candidate due to their reliability, robustness, almost maintenance-free characteristics, low manufacturing cost and the ability to work in various conditions. The IMs are the only AC motor that has the most mature technology in EV industry and having several features such as lightweight, small volume, low maintenance, high reliability and efficiency. Besides, the IM offers a higher efficiency in the regenerative effect.

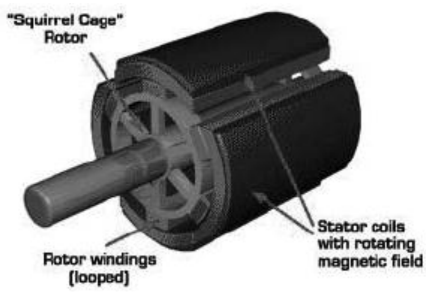

Figure 2.12 AC Squirrel Cage IM (Gan, 2010)

The absence of brush friction allows the motors to have higher maximum speed, and the higher rating of speed enable these motors to develop high output. Thus, IM does not have so much of the speed limitation as in the dc motors. Frequency of the voltage is varied to offer the speed control of the IM. Extended speed range operation beyond base speed is accomplished by flux weakening, once the motor has reached its rated power capability. Field orientation control (FOC) of IM can decouple its torque control from field control. This allows the motor to behave in the same manner as a separately excited dc motor. A properly designed IM, with field oriented control can achieve field weakened range of 3-5 times the base speed (Gan, 2010).

However, the controllers of IMs are at higher cost than the ones of DC motors. Moreover, the breakdown torque limits its extended constant-power operation. At the critical speed, the breakdown torque is reached and any attempt to operate the motor at the maximum current beyond this speed will stall the motor. Although FOC may extend constant power operation, it results in an increased breakdown torque thereby resulting in an over-sizing of the motor. In addition, efficiency at a high speed range may suffer in addition to the fact that its efficiency is lower than that of permanent magnetic (PM) motors and switched reluctance motors (SRMs) due to the absence of rotor winding and rotor copper losses (Gan, 2010).

4. Switched Reluctance Motor (SRM)

The SRM is an interesting candidate in the EV industry due to the high performance, low cost, rugged structure, fault tolerant, outstanding torque-speed characteristics and reliable converter topology. The design of SRM is similar as the stepper motor. Also, SRM drives can run in extremely long constant power range and the torque-speed characteristic matches with the needs of the EV. SRM has high starting torque and high torque-inertia ratio. The simplicity of the design owes to the rotor without any windings, magnets, commutators or brushes. The fault tolerance of SRM is also extremely good.

Owing to its simple construction and low rotor inertia, SRM has very rapid acceleration and extremely high speed operation. And, SRM is suitable for single gear transmission in EV propulsion due to its wide speed range operation. One important feature of the SRM is the different number of poles on the stator and the rotor. The windings of diametrically opposite stator poles are connected in a series to form the electric phases of the motor. For each electric phase, a power electronic circuit with one or two electronic switches is necessary for the control of unidirectional current flowing during appropriate intervals for the torque production. Exciting the stator coils in sequence produces the torque in the motor. This requires an inverter (i.e. a set of low cost electronic switches such MOSFETs or IGBTs) that drives the motor from the battery's DC voltage supply (Gan, 2010).

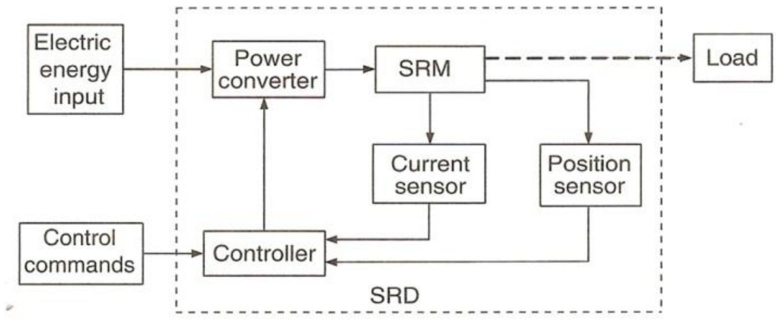

Figure 2.13 SRM Drive System (Gan, 2010)

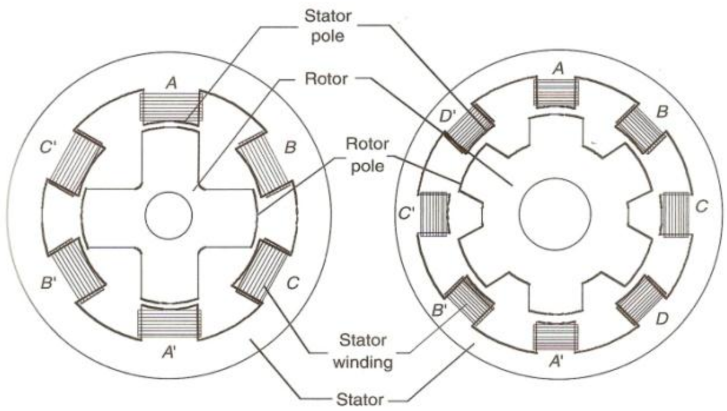

Figure 2.14 Cross Section of Common SRM (Gan, 2010)

5. Comparisons between Motors

DC motor will continue to be used in EVs because DC motor drives are available at the lowest cost. From the point of view of efficiency, BLDC motors are the best choice as BLDCs have several advantages over brushed DC-motors, including higher reliability, longer lifetime (no brush erosion), elimination of ionizing sparks from the commutator, and overall reduction of electromagnetic interference (EMI.).

However, among the four types of motors discussed, the lightest of all is the SRM which is a bonus point for EVs. If the choice of motor for EVs is determined by weight, efficiency and cost, it is clear that SRM is the victor. Besides of the efficiency, weight and cost, SRM also have the upper hand in cooling, maximum speed, fault tolerance, and reliability. However, of the four major electric EV motors, BLDC motor has the highest torque density, but if compared to SRM which have better speed-torque characteristic for traction application.

Even though the BLDC has a higher efficiency than SRM, taking into that the SRM's fault tolerance plays a big role in EV. SRM are naturally fault tolerant. As for IM and BLDC motors, their electromechanical energy conversion is interdependent upon proper excitation. While, SRM drives have discrete phase windings and thus phase windings are independent of each other.

Therefore, if one phase in the SRM fails the SRM drive can still operate at a lower performance until repair work is done on it. Additionally, the converter topology used for an SRM protects it from serious electrical fault of shoot-through, which is not eliminated fully in IM and PM BLDC motor drives (Gan, 2010).

2.2.4 Study Results and Outcome

As the comparisons stated, the DC motors seems to be more mature in the industry of electric vehicles and less expensive in constructing the prototype itself. AC motor driver circuit is very complicated and the components are expensive since the technology is not yet mature.

DC motor driver offers a more straightforward approach to speed and torque control while BLDCs are maturing to replace DC brushed motors to overcome the problems of high maintenance.

However, even though AC motor controller technology is not yet mature in the electric vehicle industry, thus making the cost very high. There are several car companies are pushing their way and creating their own path in developing this technology as the AC motor are still can be improved further and someday overtake DC motors in the EV industry.

However, the SRM which is a very powerful candidate in the EV motor struggle proves to have the upper hand in nearly every category of the comparisons:

- Lower weight than BLDC and IM.
- Lower cost than BLDC and IM due to the absence of winding and rare-earth permanent magnets.
- Fault tolerance and safety.
- Higher reliability and efficiency than brushed-DC motor.

The only losing points of SRM are the cost of manufacturing is lower than brushed DC motors while the efficiency of BLDC is higher than SRM and the lacking of maturity of SRM in the EV industry as most car companies opt for BLDC and IM while EV enthusiasts favour the low cost brushed DC motor (Gan, 2010).

2.3 Studies on the Effects of Temperature on Battery Performance and Lifetime

The temperature of the lead acid battery is an important element to be monitored for an electric vehicle as the temperature of the battery plays a big role in maintaining the lifetime and efficiency of the battery. Even in all other types of batteries, different temperatures will affect its internal chemical reaction rates, internal resistance and efficiency in different manner.

The run times of the battery will tend to vary as the temperature changes. The run time of battery will increase to a certain stage as the temperature rises above $25^{O}C$ while the run time of the battery tend decrease as temperature plunge below $25^{O}C$. Thus, the efficiency of the battery will significantly decrease during heavy discharge at lower temperature (Discover, 2009). To be more specific, the electric current generated by a battery is produced when a connection is made between its positive and negative terminals. When the terminals are connected, a chemical reaction is initiated that generates electrons to supply the flow of current of the battery. Lowering the temperature causes chemical reactions to proceed more slowly, so if a battery is used at a low temperature then less current is produced than at a higher temperature. As the batteries run down they quickly reach the point where they cannot deliver enough current to keep up with the demand. If the battery is warmed up again it will operate normally (Phuan, 2010).

Furthermore, the charge times will also vary when the temperature changes. The efficiency of charging the battery will be less when it is in lower temperature. As the same pattern in analysing the run times, the charge time tends to increase as the temperature drops below $25^{O}C$ while the charge time will tend to decrease to a certain threshold when the temperature rises above $25^{O}C$ (Discover, 2009).

However, there is also a certain threshold for the increasing battery temperature as degradation of the battery will take place in higher temperature and consequently resulting in capacity loss.

Moreover, continuous operation at higher temperatures will shorten the battery life. Hence, the optimized temperature for lead acid battery to run is at approximately 25^{O}C.

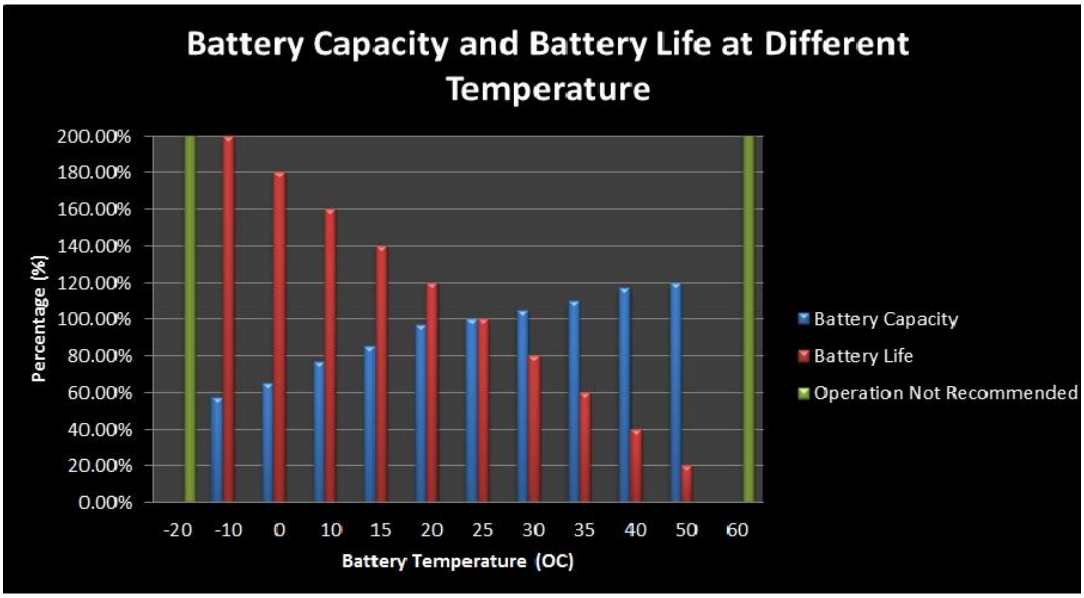

Figure 2.15 Battery Capacities and Battery Life at Different Temperature (Discover, 2009)

Thus, an intelligent air cooling ventilation system is implemented to maintain the battery temperature at optimized level, preferably between 20^{O}C and 40^{O}C as the critical temperature for the lead acid battery is at 40^{O}C. Furthermore, the system will eschew the battery to overheat when supplying power (discharging) to the load which is the complete electric vehicle monitoring system and during charging of the battery pack.

2.3.1 Establishing Cooling Requirements

Before a fan can be specified, the airflow required to dissipate the heat generated has to be approximated. Both the amount of heat to be dissipated and the density of the air must be known.

1. The basic heat transfer equation is:

   q= Cp x W x DT

   Where:
   q = amount of heat transferred
   Cp = specific heat of air
   DT = temperature rise within the cabinet
   W = mass flow

2. Mass flow is defined as:

   W = CFM x Density

By incorporating conversion factors and specific heat and density for sea level are, the heat dissipation equation is arrived at:

CFM = 3.16 x Watts / DT (°F)

This yields a rough estimate of the airflow needed to dissipate a given amount of heat at sea level. It should be noted that the mass of air, not its volume, governs the amount of cooling.

3. Determining System Impedance

After the airflow has been determined, the amount of resistance to it must be found. This resistance to flow is referred to as system impedance and is expressed in static pressure as a function of flow in CFM. A typical system impedance curve, in most electronic equipment, follows what is called the "square law," which means that static pressure changes as a square function of changes in the CFM. Figure 2.8 describes typical impedance curves.

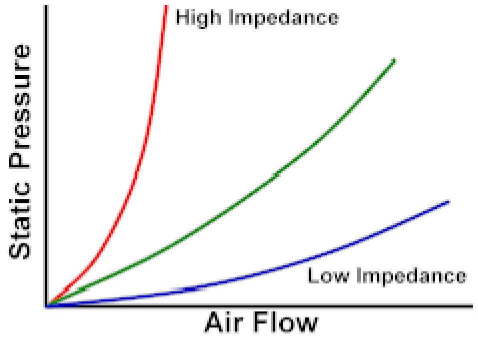

Figure 2.16 System Impedance Curve (Comair Rotron, n.d).

For most forced air cooling application, the system curve is calculated by:

$P = KrQ^n$

Where:

P = static pressure

K = load factor

r = Fluid Density

Q = Flow

n = constant; Let n=2; approximating a turbulent system.

Static pressure through complex systems cannot be easily arrived at by calculation. In any system, measurement of the static pressure will provide the most accurate result.

4. System Flow

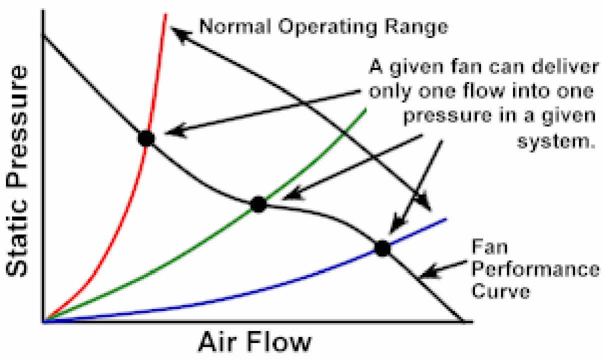

Figure 2.17 Fans over Operating Range (Comair Rotron, n.d)

Once the volume of air and the static pressure of the system to be cooled are known, it is possible to specify a fan. The governing principle in fan selection is that any given fan can only deliver one flow at one pressure in a given system.

Figure 2.9 shows a typical fan pressure versus flow curve along with what is considered as normal operating range of the fan. The fan, in any given system, can only deliver as much air as the system will pass for a given pressure. Thus, before increasing the number of fans in a system, or attempting to increase the air volume using a larger fan, the system should be analysed for possible reduction in the overall resistance to airflow.

Other considerations, such as available space and power, noise, reliability and operating environment should also be brought to bear on fan choice.
Impact of Varying System Impedance

To demonstrate the impact of system resistance on fan performance, figure 2.10 shows three typical fans used in the computer industry.

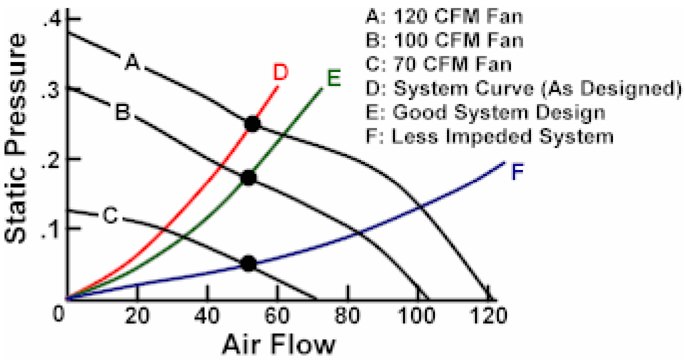

Figure 2.18 System Impedance Impact (Comair Rotron, n.d)

A is a 120 CFM fan, B is a 100 CFM fan and C is a 70CFM fan. Line D represents system impedance within a given designed system. If 50 CFM of air are needed, fan A will meet the need. However, fan A is a high performance, higher noise fan that will likely draw more power and be more costly.

If the system impedance could be improved to curve E, then fan B would meet the 50 CFM requirement, with a probable reduction in cost, noise and power draw. And if the system impedance could be optimized to where curve F were representative, then fan C would meet the airflow requirement, at a dramatically lower power, noise and cost level.

This would be considered a well-designed system from a forced convection cooling viewpoint. Keeping in mind that a given fan can only deliver a single airflow into a given system impedance, the importance of system design on fan selection is critical.

System impedance thus must be minimized whereas in practical condition, for best performance, noise, power and cost characteristics.

5. Series and Parallel Operation

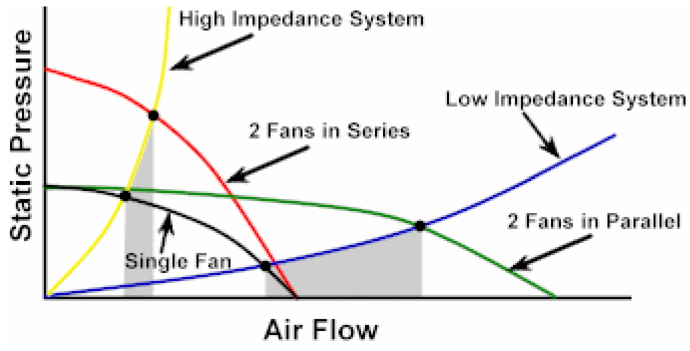

Figure 2.19 Series vs. Parallel Performance (Comair Rotron, n.d)

Combining fans in series of parallel can achieve the desired airflow without greatly increasing the system package size or fan diameter. Parallel operation is defined as having two or more fans blowing together side by side.

The performance of two fans in parallel will result in doubling the volume flow, but only at free delivery. As figure 2.11 shows that when a system curve is overlaid on the parallel performance curves, the higher the system resistance, the less increase in flow results with parallel fan operation.

Thus, this type of application should only be used when the fans can operate in low impedance near free delivery.

Series operation can be defined as using multiple fans in a push-pull arrangement. By staging two fans in series, the static pressure capability at a given airflow can be increased, but again, not doubled at every flow point, as Figure 2.12 displays. In series operation, the best results are achieved in systems with high impedance.

In both series and parallel operation, particularly with multiple fans, certain areas of the combined performance curve will be unstable and should be avoided. This instability is unpredictable and is a function of the fan and motor construction and the operating point.

6. Speed and Density Changes

By using dimensional analysis and fluid dynamic equations, basic fan laws can be derived giving a relationship between airflow, static pressure, horsepower, speed, density and noise. The table below shows the most useful of these fan laws.

Table 2.2 Basic Fan Laws

Variable	**When Speed Changes**	**When Density Changes**
Air Flow	Varies directly with speed ratio: $CFM_2 = CFM_1\ (RPM_2 / RPM_1)$	Varies directly with density ratio: $CFM_2 = CFM_1\ (r_2 / r_1)$
Pressure	Varies with square of speed ratio: $P_2 = P_1\ (RPM_2 / RPM_1)^2$	Varies directly with density ratio: $P_2 = P_1\ (r_2 / r_1)$
Power	Varies with cube of speed ratio: $HP_2 = HP_1\ (RPM_2 / RPM_1)^3$	Varies directly with density ratio: $HP_2 = HP_1\ (r_2 / r_1)$
Noise	$N_2 = N_1 + 50 \log_{10}(RPM_2 / RPM_1)$	$N_2 = N_1 + 20 \log_{10}(r_2 / r_1)$

As an example of the interaction of the fan laws, assume we want to increase airflow out of a fan by 10%. By increasing the fan speed 10%, we will achieve the increased airflow.

However, this will require 33% more horsepower from the fan motor. Usually, the fan motor is being fully used and has no extra horsepower capability.

Other solutions will have to be considered. The fan laws can be extremely useful in predicting the effect on fan performance and specification when certain operating parameters are changed.

7. Density Effects on Fan Performance

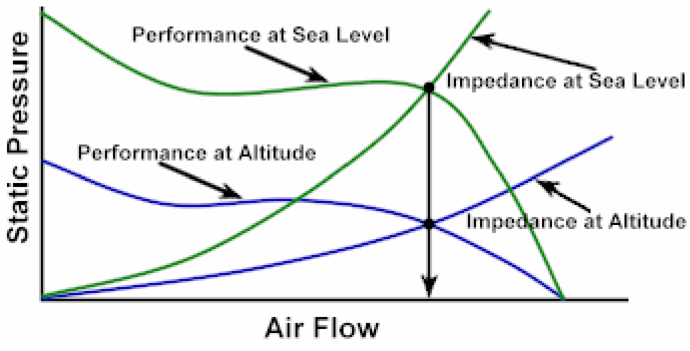

Figure 2.20 Density Effect on Fan Performance (Comair Rotron, n.d)

Since a fan is a constant volume machine, it will move the same CFM of air no matter what density of the air as seen in figure 2.11. However, a fan is not a constant mass flow machine.

Therefore, mass flow changes as the density changes. This becomes important when equipment must operate at various altitudes. The mass flow is directly proportional to density change, while the volume flow (CFM) remains constant.

As air density decreased, mass flow decreases and the effective cooling will diminish proportionately.

Therefore, equivalent mass flow is needed for equivalent cooling, or the volume flow (CFM) required at altitude (low density) will be greater than what required at sea level to obtain equivalent heat dissipation.

2.4 Precision Centigrade Temperature Sensor

The temperature sensor that we have chosen in performing all of the temperature monitoring is the LM35. It is a precision integrated-circuit temperature sensor whose output voltage is linearly proportional to the Centigrade (^{O}C) temperature.

The reason of determining LM35 to be implemented into the air cooling ventilation system is this sensor has an advantage over linear temperature that are calibrated beforehand in Kelvin (^{O}K) owing to the fact that the we don't need to subtract a constant voltage value from its output to obtain a Centigrade scaling to be sent to the PIC Microchip microcontroller (PIC 18F2550).

The LM35's low output impedance, linear output and precise inherent calibration makes the interfacing to readout or control circuitry easy. Besides, the LM35 has low self-heating which is 0.08^{O}C in still air because the LM35 only draws 60uA from the supply. Most importantly, the LM35 has a very low cost due to the calibration and trimming are done in the wafer stage. Thus, it is cost effective to be implemented practically into an intelligent temperature monitoring system (National Semiconductor, 2000).

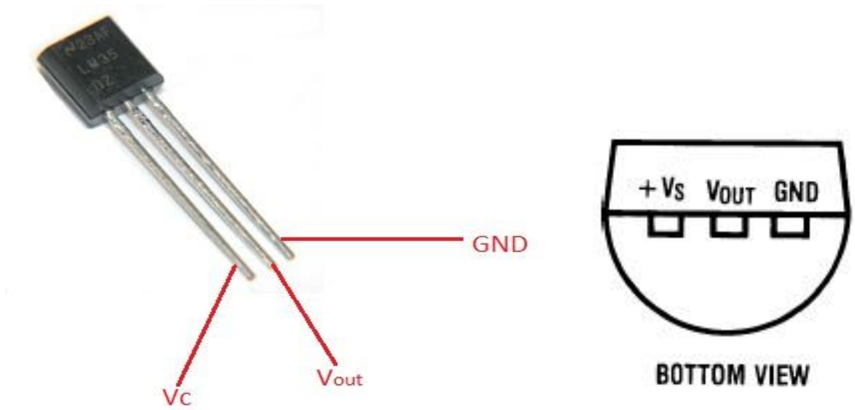

Figure 2.21.: LM35 (National Semiconductor, 2000)

The conversion between detected temperature and voltage is done by using the formula below:

$$^{O}C = V_{OUT} \text{ x } (100^{O}C/V)$$

Although the operating voltage, V_C ranges from 4V to 30V, the voltage applied into the LM35 of our intelligent electric vehicle monitoring system is the 5V which is tapped from Intel Atom Desktop Board (D510M0) power supply.

Furthermore, the response time of the LM35 is fast and very responsive as it can detect the certain temperature of the battery and reach 100% of the final value in 3 minutes. The profile of the response time is shown as below:

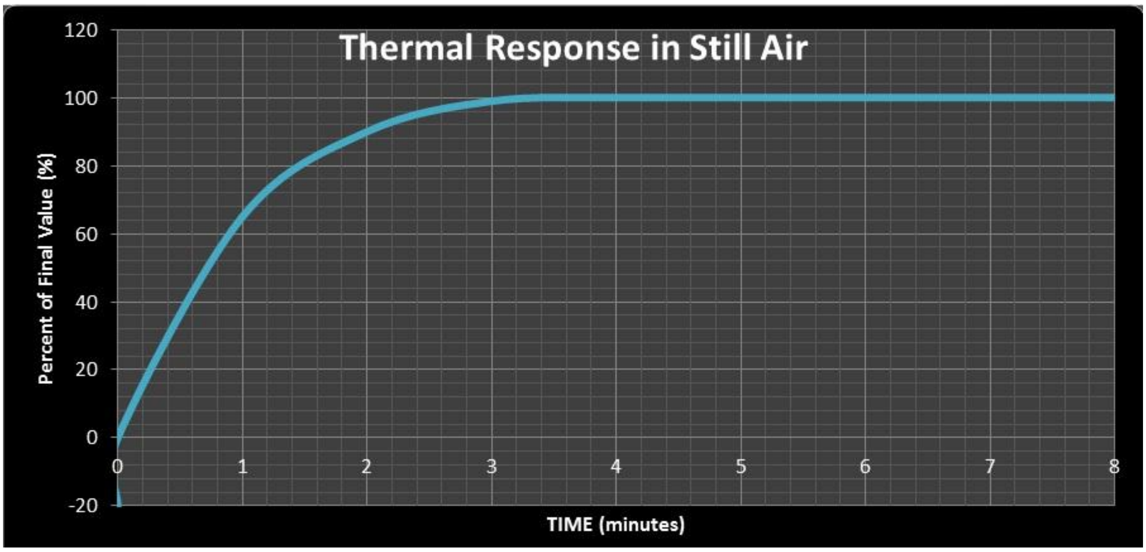

Figure 2.22: Thermal Response in Still Air (National Semiconductor, 2000)

Also, the LM35 is capable of delivering an output of 250mV in room temperature of 25Celcius. The conversion of detected temperature into output voltage is a factor of 10mV/^{O}C.

Hence, it has a linear temperature against output voltage profile as shown below:

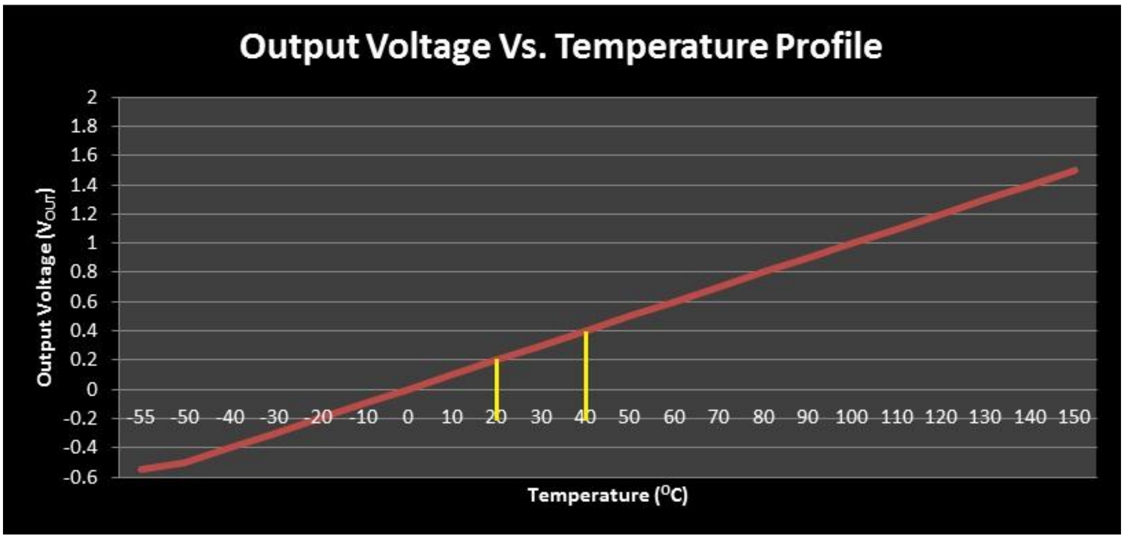

Figure 2.23: Output Voltage vs. Temperature Profile for LM35 (National Semiconductor, 2000)

As said previously, the safe operating area for the lead acid battery is between 20^{O}C and 40 ^{O}C. However, owing to the fact that the hot weather in Malaysia can easily heat up the battery packs, it is utmost imperative to develop a cooling ventilation system to extract the heat away from the battery packs and maintain it to be under 40^{O}C. Thus, the LM35 will detect for temperatures that is over 40^{O}C and trigger the PIC Microchip microcontroller (PIC 18F2550) to perform cooling ventilations.

2.5 Wireless Remote Desktop and Virtual Network Computing (VNC)

In computing, Virtual Network Computing (VNC) is a graphical desktop sharing system that uses the RFB protocol to remotely control another computer. It transmits the keyboard and mouse events from one computer to another, relaying the graphical screen updates back in the other direction, over a network.

VNC is platform-independent – a VNC viewer on one operating system may connect to a VNC server on the same or any other operating system. There are clients and servers for many GUI-based operating systems and for Java. Multiple clients may connect to a VNC server at the same time. Popular uses for this technology include remote technical support and accessing files on one's work computer from one's home computer, or vice versa.

A VNC system consists of:

- Client - the program that watches, controls, and interacts with the server. The client controls the server.

- Server - the program on the machine that shares its screen. The server passively allows the client to take control of it.

- Communication protocol (RFB) - a very simple protocol, based on one graphic primitive from server to client ("Put a rectangle of pixel data at the specified X,Y position") and event messages from client to server.

In the normal method of operation a viewer connects to a port on the server (default port 5900). Alternatively a browser can connect to the server (default port 5800). And a server can connect to a viewer in "listening mode" on port 5500.

One advantage of listening mode is that the server site does not have to configure its firewall to allow access on port 5900 (or 5800); the onus lies on the viewer, which is useful if the server site has no computer expertise, while the viewer user would be expected to be more knowledgeable.

The server sends small rectangles of the frame buffer to the client. In its simplest form, the VNC protocol can use a lot of bandwidth, so various methods have been devised to reduce the communication overhead. For example, there are various encodings (methods to determine the most efficient way to transfer these rectangles). The VNC protocol allows the client and server to negotiate which encoding will be used. The simplest encoding, which is supported by all clients and servers, is the raw encoding where pixel data is sent in left-to-right scan line order, and after the original full screen has been transmitted, only transfers rectangles that change.

This encoding works very well if only a small portion of the screen changes from one frame to the next (like a mouse pointer moving across a desktop, or text being written at the cursor), but bandwidth demands get very high if a lot of pixels change at the same time, such as when scrolling a window or viewing full-screen video.

VNC by default uses TCP (port number for communication end point) port 5900+N, where N is the display number (usually: 0 for a physical display). Several implementations also start a basic HTTP server on port 5800+N to provide a VNC viewer as a Java applet, allowing easy connection through any Java-enabled web browser. Different port assignments can be used as long as both client and server are configured accordingly.

Using VNC over the Internet works well if the user has a broadband connection at both ends. However, it may require advanced NAT, firewall and router configuration such as port forwarding in order for the connection to go through.

Some users may choose to use instant private networking applications such as Virtual Private Network (VPN) applications such as Hamachi to make usage over the Internet much easier. Alternatively, a VNC connection can be established as a LAN connection if VPN is utilized as a proxy.

Note that the machine the VNC server is running on does not require to have a physical display. Xvnc is the Unix VNC server, which is based on a standard X server. To applications Xvnc is an X "server" (ie displays client windows), and to remote VNC users it is a VNC server. Applications can display themselves on Xvnc as if it was a normal X display, but they will appear on any connected VNC viewers rather than on a physical screen.

Alternatively a machine (which may be a workstation or a network server) with screen, keyboard, and mouse can be set up to boot and run the VNC server as a service or daemon, then the screen, keyboard, and mouse can be removed and the machine stored in an out-of-the way location.

In addition, the display that is served by VNC is not necessarily the same display seen by a user on the server. On Unix/Linux computers that support multiple simultaneous X11 sessions, VNC may be set to serve a particular existing X11 session, or to start one of its own. It is also possible to run multiple VNC sessions from the same computer. On Microsoft Windows the VNC session served is always the current user session.

VNC is commonly used as a cross-platform remote desktop system. For example, Apple Remote Desktop for Mac OS X (and more recently, "Back to My Mac" in 'Leopard' - Mac OS X 10.5) interoperates with VNC and will connect to a Linux user's current desktop if it is served with x11vnc, or to a separate X11 session if one is served with TightVNC. From Linux, TightVNC will connect to a Mac OS X session served by Apple Remote Desktop if the VNC option is enabled, or to a VNC server running on Microsoft Windows.

CHAPTER 3

METHODOLOGY

3.1 Introduction

Basically, the EVICS is divided into six MAIN modules:

1. Battery Voltage Monitoring Module
2. Battery Current Monitoring Module
3. Battery Temperature Monitoring Module
4. Vehicle Speed Monitoring Module
5. Protection and Circuit Isolation Module
6. Wireless Remote Desktop Control Module

However, in this project report about EVICS, we will discuss about the Battery Temperature Monitoring Module, Vehicle Speed Monitoring Module and Wireless Remote Desktop Control Module. And, lastly we will discussed about the Reverse Parking Sensor Module.

3.1.1 General Idea of EVICS

Basically, the EVICS project can divide into several topics as below:

1. Voltage Measurement
2. Current Measurement
3. Temperature Measurement
4. Speed Measurement
5. Protection and Isolation Circuit
6. RPM-Voltage Motor Testing
7. Air Cooling Ventilation System for Battery Compartment
8. Programming (Bash script, Action Script 3.0, C Programming, Shell Script, CGI Script and etc)
9. Backup Recovery System
10. Independent Voltage Indicator
11. Independent Speed Measurement Circuit
12. The Intel® Desktop Board D510MO
13. Virtual Network Computing (VNC) and SSH File Transfer Protocol
14. Temperature Sensor Watchdog System
15. Automatic Intelligent Lighting System
16. Power Inverter DC/AC Converter
17. Reverse Parking Sensor

Below is figure 3.1 showing the overall components that are in the EVICS:

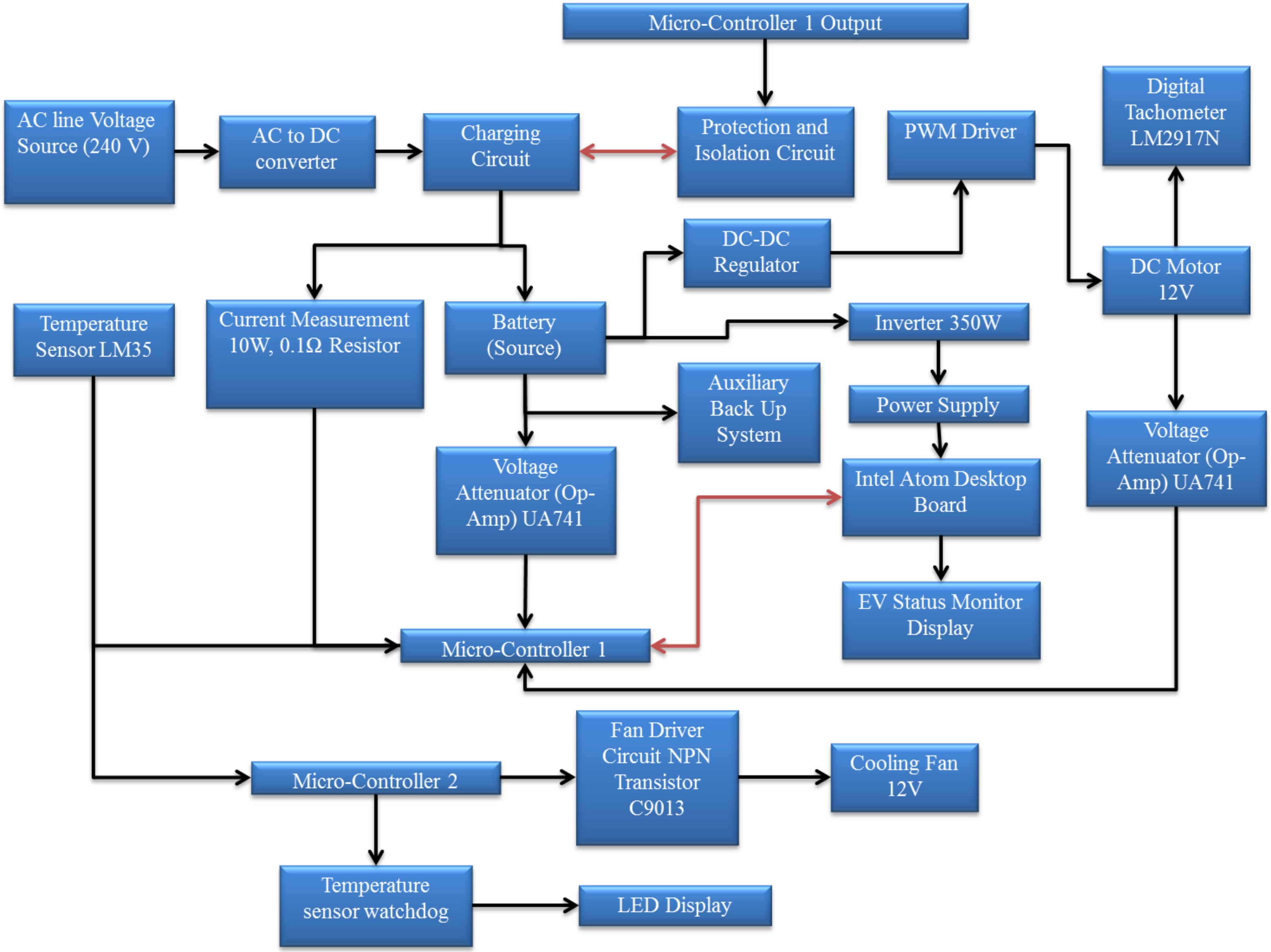

Figure 3.1 Overall Functions of EVICS

3.2 Project Management

Project management is the discipline of planning, organizing, securing and managing resources to bring about the successful completion of specific project goals and objectives.

Therefore, time and hard work have been spent to plan and organize this project before implementation of engineering methods in designing and solving problems. Below figure shows our project's planning, implementation, integration and until the end which is documentation.

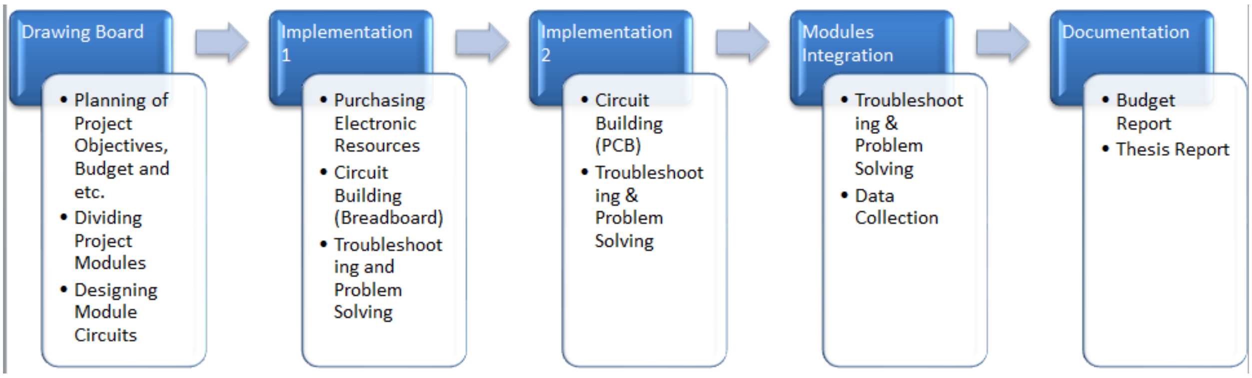

Figure 3.2 Overall Process Flow of Project

3.3 Temperature Monitoring Module

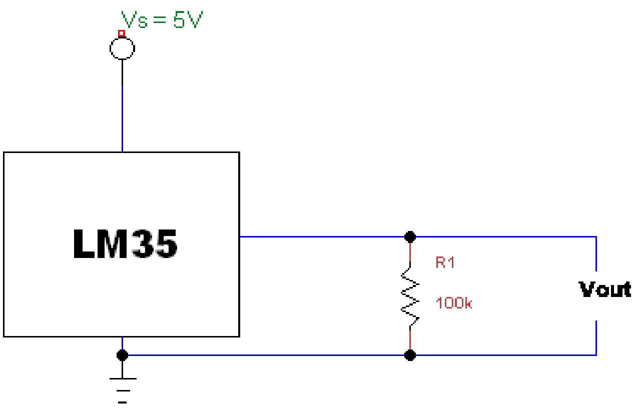

Figure 3.3 LM35 Temperature Sensor Circuit

Basically, the main component in this temperature module is the temperature sensor, LM35. The LM35 is chosen as the choice of temperature sensor due to the fact that the easy implementation of the sensor in circuit, the low voltage output from it and the accuracy of the sensor.

The designed circuit shown in figure 3.3 consists of the LM35 which is temperature sensor that is designed to detect the changes in temperature and convert it into corresponding voltage value. The varying output voltage will then be feed into the analogue input of the PIC Microchip microcontroller directly to perform the ADC (Analogue-to-Digital Conversion) programming required to transmit data into the Intel Atom Desktop Board (D510M0) and also to trigger the air cooling ventilation system.

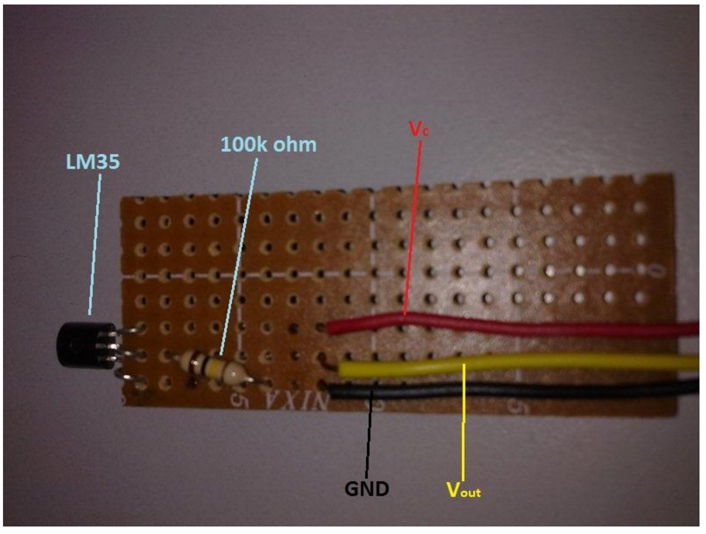

Figure 3.4 Outcome of the LM35 Temperature Sensor Circuit

The figure above shows the outcome circuit that is ready to be implemented not only into the EVICS's battery temperature monitoring system but also to any system that requires precise and sensitive temperature detection.

3.3.1 Air Cooling Ventilation System of Battery Compartment

The main circuits that are used in this module are:

- LM35 Temperature Circuit
- PIC Microchip microcontroller (PIC 18F2550)
- Fan Driver Circuit
- Two 12V Fans (0.15A) – Cool Air Inlet Fan
- One 12V Fan (0.45A) – Hot Air Extractor Fan
- One 5V Fan (0.15A) – Air Circulator Fan

Moreover, the LM35 temperature circuit is used in combining the detection circuit to the PIC Microchip microcontroller (PIC 18F2550), we can automatically trigger the cooling fans to turn on and off using programming whenever the battery compartment temperature increases above 25^{O}C. The temperature is set at this particular threshold according to the research done in the literature review.

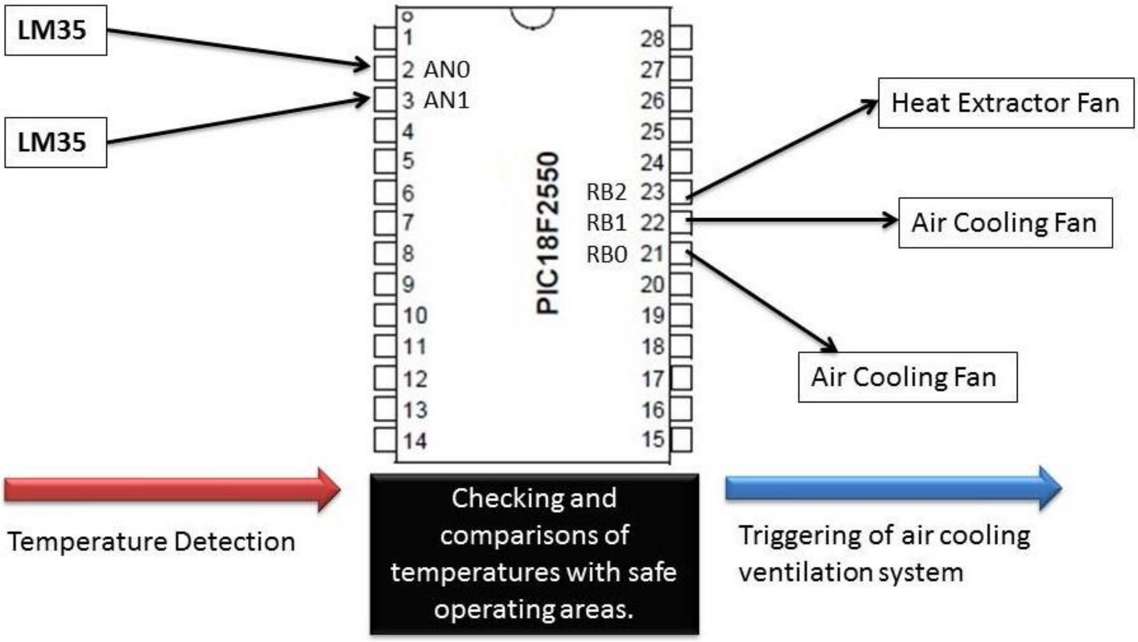

Figure 3.5 Process Flow between LM35 with PIC18F2550

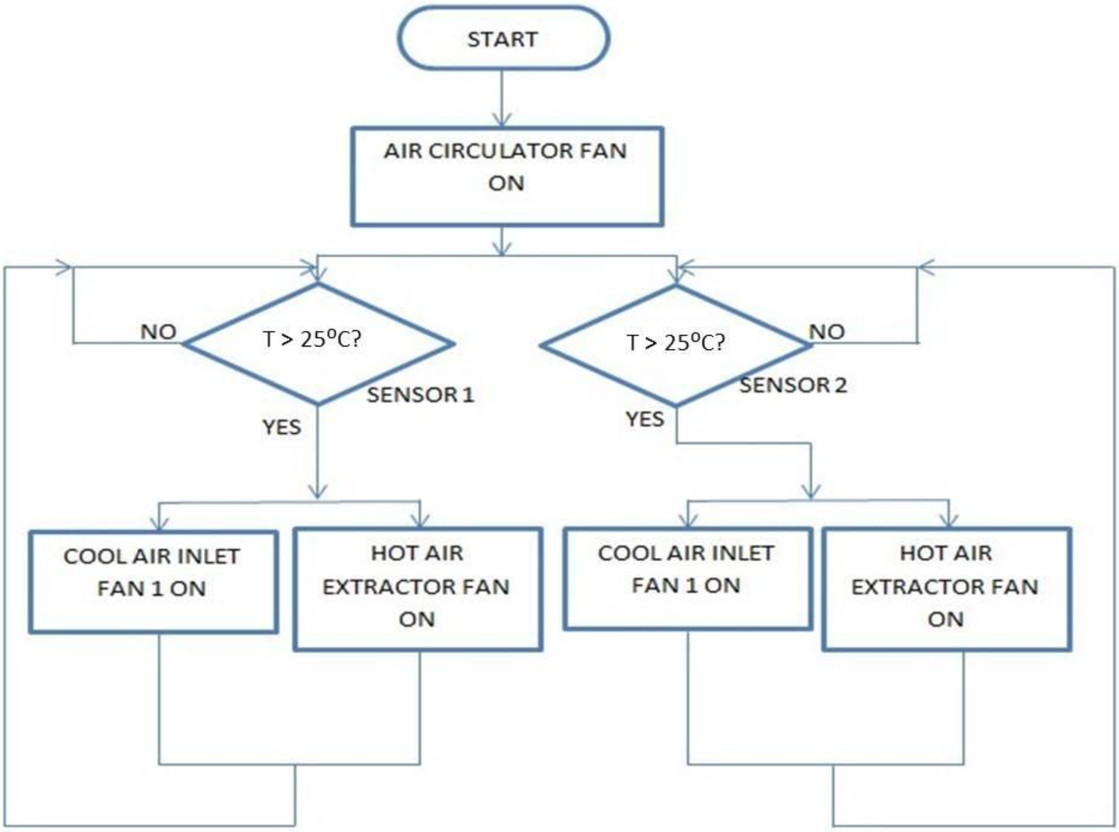

Figure 3.6 Flow Chart of the Air Cooling Ventilation System

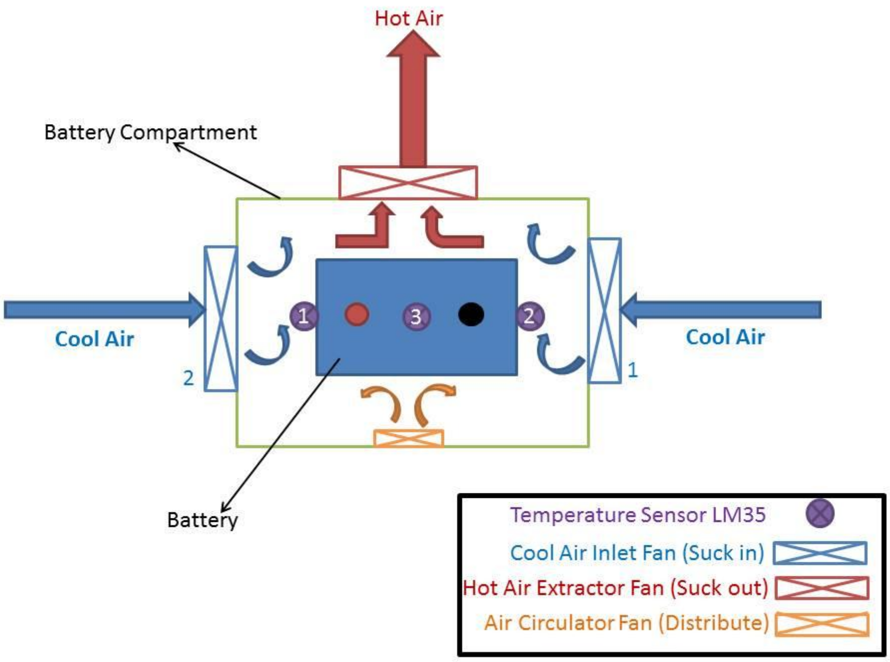

Figure 3.7 Overall Operation of the Air Cooling Ventilation System

Above figure 3.7 is the overall operation of the air cooling ventilation system that is implemented to cool the battery and maintain the battery temperature in an optimum temperature which is 25^{O}C while the figure 3.6 describes the programming flow chart of the whole Air Cooling Ventilation System.

First and foremost, the air circulator fan is always turned on to circulate the air flow and distribute the internal air temperature so that the temperature sensors are able to detect a more precise and average temperature value. The air circulator fan runs on a very low power consumption which is 0.75W as it is running on 5V, 0.15A.

However, the two Cool Air Inlet fans are running on 1.8W which is 12V, 0.15A. The two cool air inlet fans are used to suck in cool air from the outside and into the battery compartment to cool the battery while the hot air extractor fan is used to suck out the warm air from the battery. As far as it is concerned, the hot air extractor fan is running on 5.4W which is a rating of 12V and 0.45A. Thus, this Air Cooling Ventilation System is able to maintain a quintessential temperature for the battery to operate.

Basically, there are three sensors implemented in this battery temperature monitoring module. Sensor 1 and 2 are implemented to trigger the air cooling ventilation system when either one of the two sensors (sensor 1 or 2) detects at hotspot on either side of the battery pack. In addition, sensor 3 is used as a temperature data collector for the data to be sent to the Atom board serially through the PIC18F2550 Microchip microcontroller.

The hot air extractor fan and the cool air inlet fans are unable to be directly triggered and turned on by the output from PIC18F2550 Microchip microcontroller as the voltage (5V) and current is insufficient to power up the fan. Thus, a fan driver circuit is designed to trigger the fans to turn on whenever there is a HIGH output from the output ports of the microcontroller.

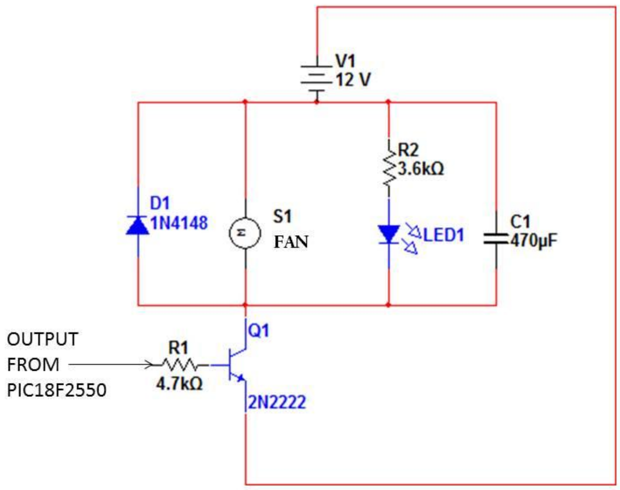

Figure 3.8 Fan Driver Circuit

As shown in figure above, each fan except for the Air Circulator fan are connected to this fan driver circuit. As you can see in the designed circuit, the fan is triggered using a NPN transistor. When microcontroller gave an output of high to the base of the transistor, the fan and the WHITE LED indicator will turn on. The WHITE LED is used to indicate that the fan is turned on to notify users as the air cooling ventilation system is turned on to cool down the battery pack. The 1N4148 diode is to offer a protection purpose for the NPN transistor to avoid burning the transistor in case of a surge of current from the supply.

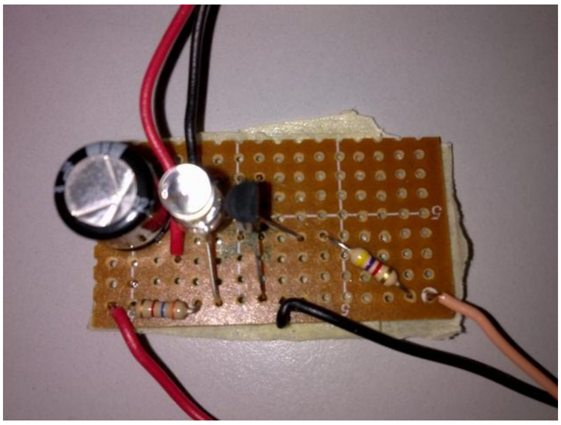

Figure 3.9 Outcome Circuit of the Fan Driver

Below is the coding of the battery heat ventilation system:

```
//############################## Temperature Module ##############################
/********************** Battery Heat Ventilation System ************************/


        ADCON0=0b00000001;                  //AN0
        ADCON0bits.GO_DONE = 1;             //Start A/D Conversion
        while(ADCON0bits.GO_DONE != 0);     //Loop here until A/D conversion completes
        if (ADRESL < 0x33 && ADRESH == 0b00){   //Check for temperature above 40 degrees to turn on fan

                PORTBbits.RB0=0x00;         //SOA Fan Inlet 1 remains off
                PORTBbits.RB2=0x00;         //SOA Fan Outlet 3 remains off

                if (ADRESL == 0x00){
                    PORTBbits.RB3=0xFF;     //RB3 RED ON
                    PORTBbits.RB5=0x00;     //RB5 GREEN OFF
                    }

                else{
                    PORTBbits.RB3=0x00;     //RB3 RED OFF
                    PORTBbits.RB5=0xFF;     //RB5 GREEN ON
                    }
        }
        else{
            PORTBbits.RB0=0xFF;             //Critical Fans (1&3) turn on
            PORTBbits.RB2=0xFF;
        }

        ADCON0=0b00000101;                  //AN1
        ADCON0bits.GO_DONE = 1;             //Start A/D Conversion
        while(ADCON0bits.GO_DONE != 0);     //Loop here until A/D conversion completes
        if (ADRESL < 0x33 && ADRESH == 0b00){

                PORTBbits.RB1=0x00;         //SOA Fan Inlet 2 remains off
                PORTBbits.RB2=0x00;         //SOA Fan Outlet 3 remains off

                if (ADRESL == 0x00){
                    PORTBbits.RB4=0xFF;     //RB4 RED ON
                    PORTBbits.RB6=0x00;     //RB6 GREEN OFF
                }
                else{
                    PORTBbits.RB4=0x00;     //RB4 RED OFF
                    PORTBbits.RB6=0xFF;     //RB6 GREEN ON
                    }
        }

        else{
            PORTBbits.RB1=0xFF;             //Critical Fans (2&3) turn on
            PORTBbits.RB2=0xFF;
        }

        ADCON0=0b00001001;                  //AN2
        ADCON0bits.GO_DONE = 1;             //Start A/D Conversion
        while(ADCON0bits.GO_DONE != 0);     //Loop here until A/D conversion completes
        if (ADRESL == 0x00 && ADRESH == 0b00){
            PORTBbits.RB7=0xFF;             //RB7 RED ON
            PORTCbits.RC0=0x00;             //RC0 GREEN OFF
        }
        else{
            PORTBbits.RB7=0x00;             //RB7 RED OFF
            PORTCbits.RC0=0xFF;             //RC0 GREEN ON
        }

/********************** Battery Heat Ventilation System ************************/
//############################## Temperature Module ##############################
```

The PIC18F2550 is programmed using PIC KIT 2 and MPLAB IDE software which both are from Microchip. As you can see in my if-else function, the condition is set to turn on the fans only when the detected temperature from the analogue input (AN0 and AN1) is above 25^{O}C. However, the value of 25^{O}C is supposed to generate a voltage amount of 0.25V after the temperature is converted into voltage by the LM35 temperature sensor.

The LM35 temperature-to-voltage formula is as below:

$$V_{OUT} = {}^{O}C / (100^{O}C/V)$$

Due to the fact that the ADC programming of the PIC takes in varying analogue input, thus it is very convenient and safe in applying the output of the LM35 circuit directly into the PIC as the voltage is only in the range of millivolt. By knowing that 25^{O}C is equivalent to 0.25V. Thus, the threshold for the if-else condition mentioned above can be calculated using the formula below:

Translated decimal value, n_D $= (V_{ANALOGUE\ INPUT}/5) * 1024$

Translated Hexadecimal value, n_H = (Hexadecimal)

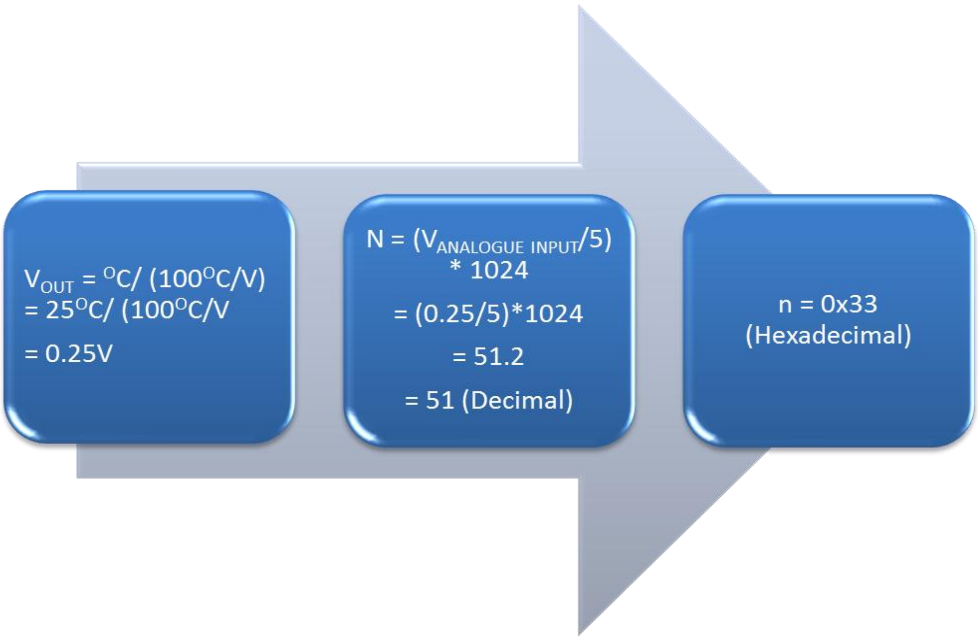

Figure 3.10 Determining the Threshold Value

(Note: $V_{OUT} = V_{ANALOGUE\ INPUT}$)

3.4 Interfacing the Temperature Data into the Intel Atom Desktop Board

The LM35 temperature circuit can detect the real-time temperature and send corresponding characters to the Intel Atom Desktop Board (D510M0) by using the serial communication between PIC18F2550 and the Intel Atom Desktop Board. By doing this, the Atom board will then decode the characters and display the real-time temperature to the users through the usage of bash script (Serial.sh).

Below is the coding of the temperature data interfacing coding:

```
/**********************************************************
MODULE : TEMPERATURE MONITORING SYSTEM
CTRL : AN2 [INPUT] RB2 [OUT]
**********************************************************/
        ADCON0=0b00001001;  //AN2
        ADCON0bits.GO_DONE = 1;
        while(ADCON0bits.GO_DONE != 0);//Loop here until A/D conversion completes
        if ( ADRESL < 0x54 && ADRESH==0b00){
            //PORTBbits.RB2=0x00;
            k=0;
            if (ADRESL >= 0 && ADRESL < 41)
            temp='s';
            else if (ADRESL >= 41 && ADRESL < 51)
            temp='t';
            else if (ADRESL >= 51 && ADRESL < 61)
            temp='u';
            else if (ADRESL >= 61 && ADRESL < 72)
            temp='v';
            else if (ADRESL >= 72 && ADRESL < 82)
            temp='w';
            else
            temp='x';
        }
        else {
        temp='y';
        k=1;
        //PORTBbits.RB2=0xFF;
        }
```

The code above is programmed into the PIC18F2550. It shows the corresponding characters that will be sent to the Intel Atom Desktop Board through serial communication. These characters are sent at a time in a real-time manner, thus whenever the temperature is in that programmed range of temperatures, and then the PIC microcontroller will send the corresponding characters.

Table 3.1 Temperature-Character Table

TEMPERATURE RANGE, T (^{O}C)	CHARACTER
0 <= T < 20	s
20 <= T < 25	t
25 <= T < 29	u
29 <= T < 35	v
35 <= T < 40	w
40 <= T < 41	x
T > 41	y

3.5 Temperature Sensor Watchdog Module

By using programming of the PIC18F2550, it is possible to trigger an array of corresponding LEDs to show that the temperature sensor is either working or malfunction.

If the temperature sensor 1 is working properly, thus there will be an output from the PIC to light up a green LED in terms of sensor 1. If the temperature sensor 1 is malfunction, hence it is unable to convert any temperature into voltage for the input of PIC, and then the PIC will give an output to light up a red LED while turning off the green LED.

Altogether we have three LM35 temperature sensor circuits, thus we need three sets of red and green LED indicators for this module.

The reason for this module is notify the users about the status of the temperature sensors. And, it will be very convenient for engineers to troubleshoot the problem if something had happened to the temperature sensors. Thus, this module will make the EVICS even more innovative and intelligent as it can detect the fault on its own and display it out to the users. Moreover, this module can be implemented with the Intel Atom board to display sensor status on the GUI.

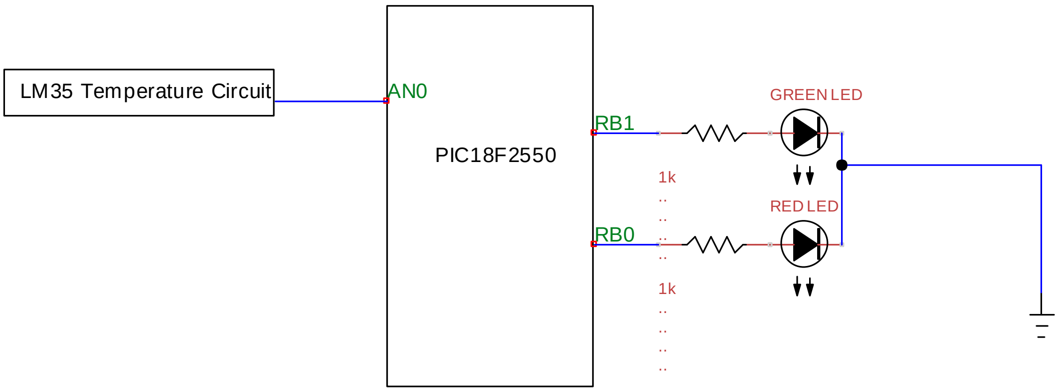

Figure 3.11 Temperature Sensor Watchdog Circuit

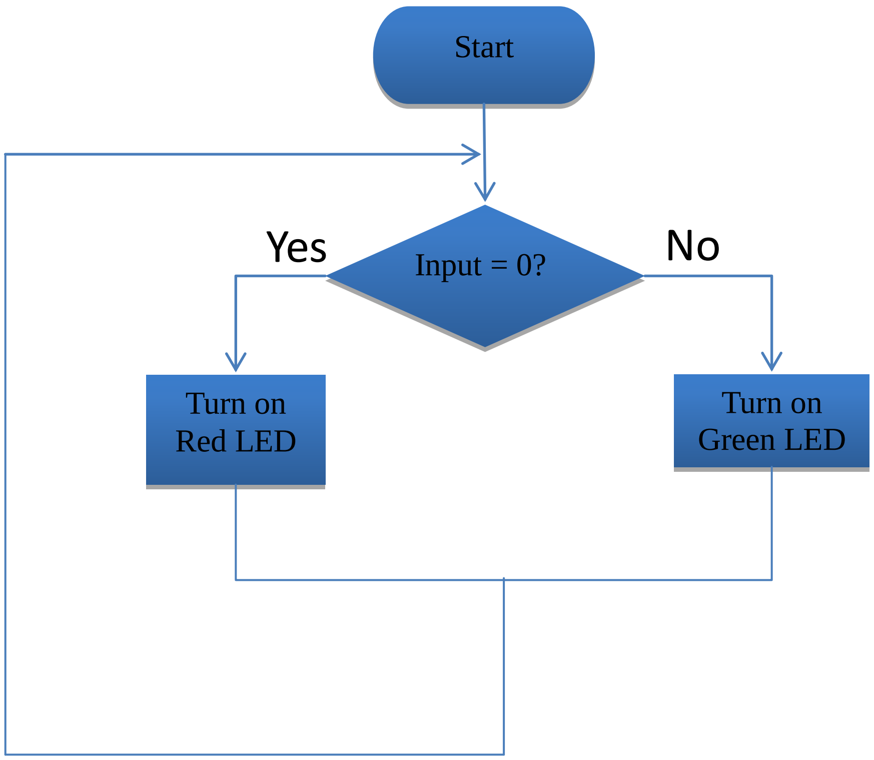

Figure 3.12 Flow chart of the Temperature Sensor Watchdog Module

Below is the code used to program the PIC18F2550 for the watchdog purpose:

```
ADCON0=0b00000001;                      //AN0
ADCON0bits.GO_DONE = 1;                 //Start A/D Conversion
while(ADCON0bits.GO_DONE != 0);         //Loop here until A/D conversion completes
if (ADRESL == 0x00 && ADRESH == 0b00){  //Check for temperature above 40 degrees to turn on fan

            PORTBbits.RB0=0xFF;         //RB0 red on
            PORTBbits.RB1=0x00;         //RB1 green off
}

else{
            PORTBbits.RB0=0x00;         //RB0 red off
            PORTBbits.RB1=0xFF;         //RB green on
            }



ADCON0=0b00000101;                      //AN1
ADCON0bits.GO_DONE = 1;                 //Start A/D Conversion
while(ADCON0bits.GO_DONE != 0);         //Loop here until A/D conversion completes
if (ADRESL == 0x00 && ADRESH == 0b00){

            PORTBbits.RB2=0xFF;         //RB2 red on
            PORTBbits.RB3=0x00;         //RB3 green off
        }
else{
            PORTBbits.RB2=0x00;         //RB2 red off
            PORTBbits.RB3=0xFF;         //RB3 green on
            }
ADCON0=0b00001001;                      //AN2
ADCON0bits.GO_DONE = 1;                 //Start A/D Conversion
while(ADCON0bits.GO_DONE != 0);         //Loop here until A/D conversion completes
if (ADRESL == 0x00 && ADRESH == 0b00){
    PORTBbits.RB7=0xFF;                 //RB7 red on
    PORTBbits.RB6=0x00;                 //RB6 green off
}
else{
    PORTBbits.RB7=0x00;                 //RB7 red off
    PORTBbits.RB6=0xFF;                 //RB6 greeb on
}
```

3.6 Vehicle Speed Monitoring Module

Speed measurement and display is utmost important for users to determine whether they are driving under the speed limit and being able to maintain road safety.

Therefore, one of the advantages of EVICS is that we are able to measure the speed of the motor and display the motor RPM and kilometre per hour (km/h) in an innovative and ingenious way. Unlike the internal combustion engine, electric motor draws current from the power source which is the lead acid battery. Hence, the method to measure the motor RPM is to measure the voltage across the motor. This is because the rpm of the dc motor is proportional to the voltage across it.

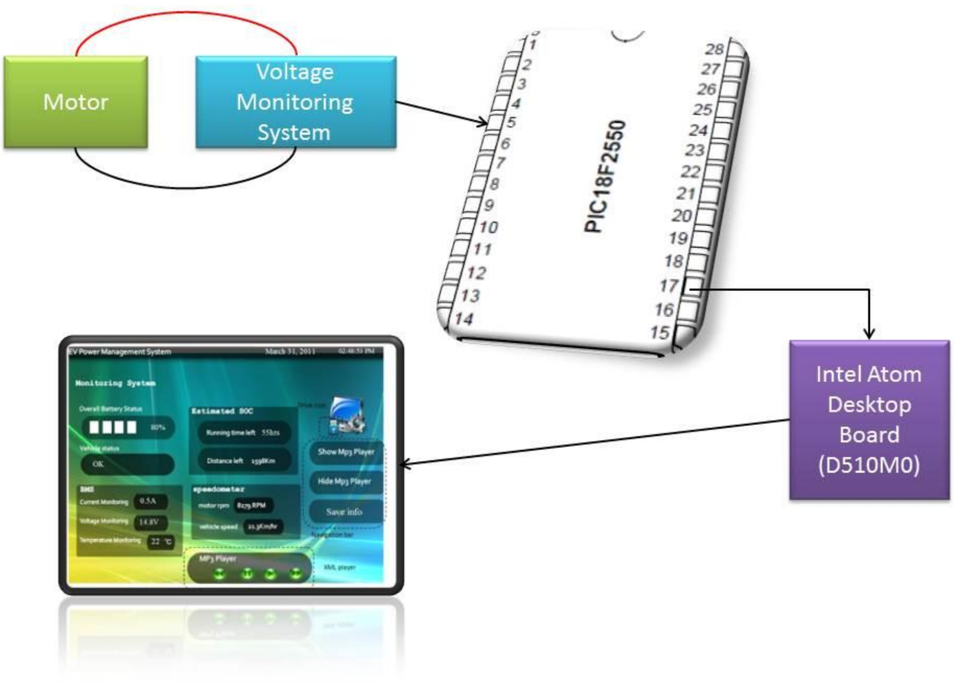

Figure 3.13 Overall Voltage-Speed Measurement Modules

As you can see from the figure above, the voltage from the electric motor is being attenuated by the utilization of operational amplifiers (UA741) which is a circuit used in a part of the Voltage Monitoring Module. The attenuation is approximately 0.068. Thus, for a maximum voltage value of 12V across the motor, the attenuated output from the op-amp will be 0.816V. It is truly a cost effective way to measure the speed of the motor by implementing the attenuation op-amp circuit from the voltage monitoring module.

Other than avoiding high voltage flowing into the PIC (12V input will damage it), it is also because if the voltage applied into the analogue input of PIC18F2550 is more than 1.25V, it will have its most significant input bits (ADRESH) to not be 0b00 and thus it will then have another new set of 10bits. This will confuse the Intel Atom Board as the PIC will tend to send the same data/character even though there are two same input voltages.

It is done this way is due to the experience of using the PIC and as long as the input voltage is kept below 1.25V, the voltage detected across the motor will not cross over to the new set of 10bits (ADRESH = 0b01,0b10, 0b11).

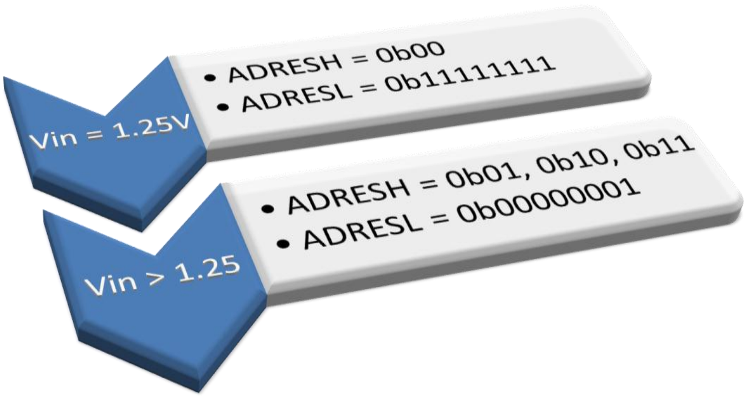

Figure 3.14 ADRESH-ADRESL (10bits) of input of the PIC18F2550

Additionally, just like the temperature module, the value of voltage across the motor after attenuation also can be feed into the PIC, so that corresponding characters can be sent to Intel Atom Board through serial communication and the characters will be decoded into corresponding rpm and km/h.

Below is the table used to determine the corresponding characters and corresponding attenuated voltage range across the motor:

Table 3.2 Motor Voltages – Character Table

MOTOR VOLTAGE RANGE, V	CHARACTERS
0 – 0.718	K
0.718 – 1	L
1 – 2	M
2 – 3	N
3 – 4	O
4 – 5	P
5 – 6	Q
6 – 7	R
7 – 8	S
8 – 9	T
9 – 10	U
10 – 11	V
11 – 12	W
> 12	X

The coding below is programmed into the PIC and hence when the voltage falls in that particular range, the PIC will automatically send the corresponding character to the Intel Atom Board and from there some heavy programming will be done so that the users can see the display of speed of the motor and vehicle.

Thus, below is the coding of the motor data interfacing coding:

```
ADCON0=0b00001101;                        //AN3
ADCON0bits.GO_DONE = 1;                   //Start A/D Conversion
while(ADCON0bits.GO_DONE != 0);           //Loop here until A/D conversion completes

if (ADRESL < 0xCD && ADRESH == 0b00){    // Less than 14.72V

    if (ADRESL >= 0 && ADRESL < 10)           // 0V-0.718V
        motor_rpm='K';                    //0 RPM
    else if (ADRESL >= 10 && ADRESL < 14)    // 0.718V-1V
        motor_rpm='L';                    //1030 RPM
    else if (ADRESL >= 14 && ADRESL < 28)    // 1V-2V
        motor_rpm='M';                    //3284 RPM
    else if (ADRESL >= 28 && ADRESL < 42)    // 2V-3V
        motor_rpm='N';                    //5744 RPM
    else if (ADRESL >= 42 && ADRESL < 56)    // 3V-4V
        motor_rpm='O';                    //8279 RPM
    else if (ADRESL >= 56 && ADRESL < 70)    // 4V-5V
        motor_rpm='P';                    //10915 RPM
    else if (ADRESL >= 70 && ADRESL < 84)    // 5V-6V
        motor_rpm='Q';                    //13427 RPM
    else if (ADRESL >= 84 && ADRESL < 98)    //6V-7V
        motor_rpm='R';                    //15920 RPM
    else if (ADRESL >= 98 && ADRESL < 111)   //7V-8V
        motor_rpm='S';                    //18516 RPM
    else if (ADRESL >= 111 && ADRESL < 125) //8V-9V
        motor_rpm='T';                    //21213 RPM
    else if (ADRESL >=125 && ADRESL < 139)   //9V-10V
        motor_rpm='U';                    //23942 RPM
    else if (ADRESL >=139 && ADRESL < 153)   //10V-11V
        motor_rpm='V';                    //26614 RPM
    else if (ADRESL >= 153 && ADRESL < 168) //11V-12V
        motor_rpm='W';                    //29102 RPM
    else{
        motor_rpm='X';                    //31000 RPM MORE THAN 12V
    }
}
else{
        motor_rpm='Y';                    //Motor Overspeed
    }
```

The motor we used in this testing for the proportionality of motor RPM with voltage is a 12V, 2A dc motor.

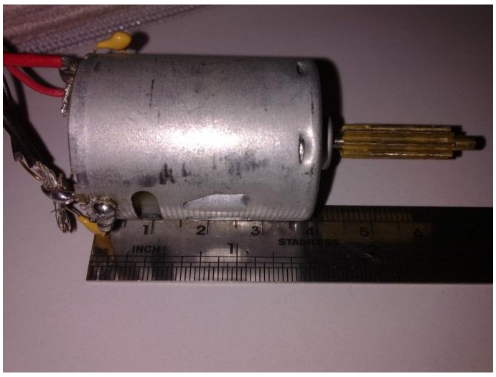

Figure 3.15 DC Electric Motor for Prototyping Purposes

The way we tested the theory of RPM being proportional with supply voltage is that we used a tachometer to measure the RPM of the motor as we increase the voltage across it from 0-12V as shown below:

Figure 3.16: DC Motor Testing for Voltage vs. RPM

As can be seen above, a small piece of white card is attached to the shaft of the dc motor and as the card cuts the light of the tachometer, it counts the revolutions that the motor takes per minute.

The reason we make a small piece of card and not a bigger piece because the motor will tend to vibrate during the application of a bigger load and this vibration will cause a loss of energy. This loss of energy will lead to an increase of torque needed by the motor to rotate and thus the current flowing into the motor will increase while the voltage will drop.

Even though we keep increasing the motor voltage, the increase of current causes the voltage across the motor to not increase and thus making the motor turn slower. Therefore, a platform is built to house the motor and gears are paired to the shaft of the dc motor for the experiment to be done conveniently.

The reason we use gears is that the gears we paired with the motor are speed reducers but it will increase the torque of the motor, thus making it able to handle bigger load, so we can mount a bigger white card in order to cut the light of the tachometer.

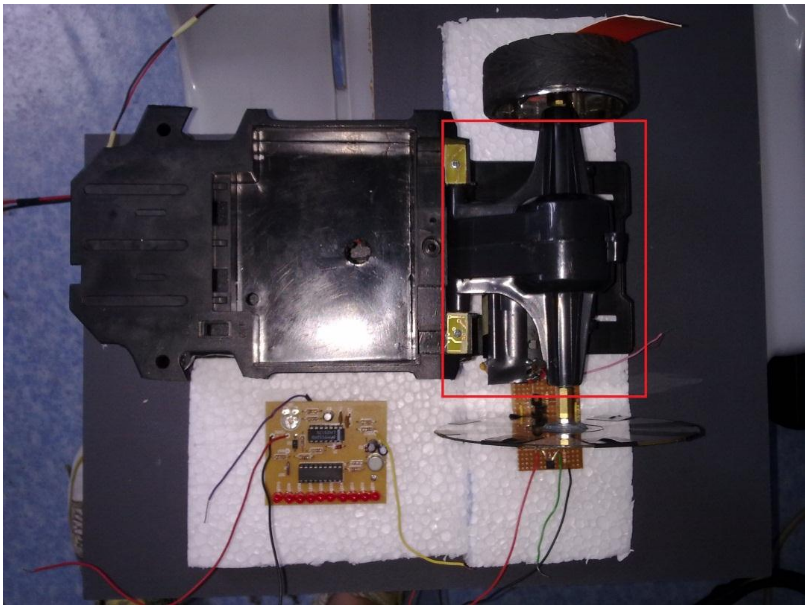

Figure 3.17 Housing for the DC motor

As can be seen above, the red box shows the housing for the gears that are paired with the motor.

However, it is imperative to calculate the velocity ratio and train value for the whole gear system.

Below shows the gear system that is attached to the dc motor:

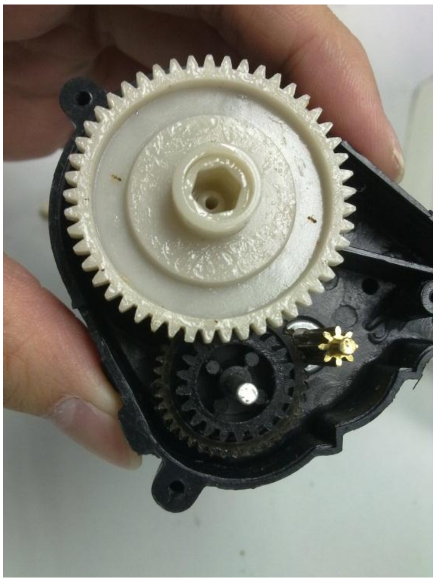

Figure 3.18: DC Motor Gears

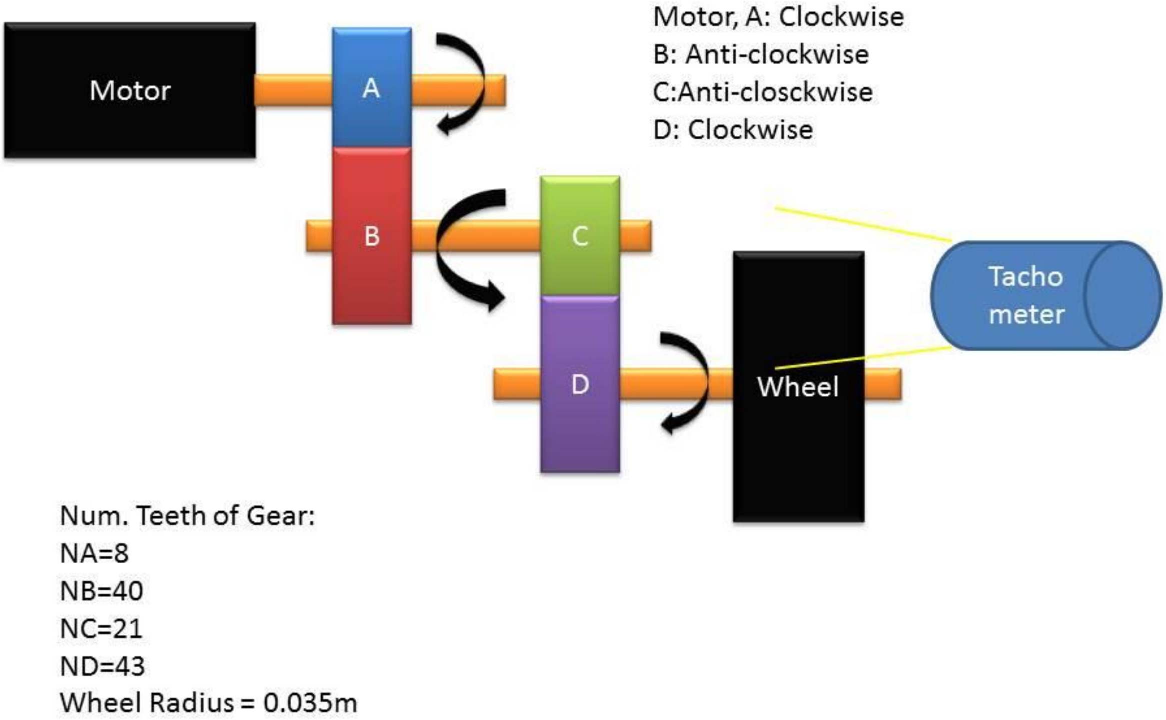

Figure 3.19: The Complete Gear System Layout

The formula used to calculate the corresponding raw motor speed given that we measure the value of the speed of the wheel (Norton, 2008):

- $N_B/N_A = n_A/n_B$;$n_{A,}$ n_B : gear speed
- $N_D/N_C = n_C/n_D$;n_C, n_B : gear speed

- Velocity Ratio, $VR_1 = N_B/N_A$
- Velocity Ratio, $VR_2 = N_D/N_C$

- Train Value, TV $= (N_B/N_A)*(N_D/N_C)$
  $= (VR_1)*(VR_2)$
  $= (40/8) * (43/21)$
  $= 10.23809524$

- $n_A = n_D * 10.23809524$; n_A :Speed of Motor & n_D:Speed of Wheel

- Speed of the car, km/h= (2*π*radius of wheel*rpm of wheel*60)/1000

- Rotational speed, $S = (f_{in}/8)*60$ rpm

f_{in} is the input frequency that is generated by the photo-interrupter circuit when it is being cut by the flywheel which will be shown on the next topic.

3.7 Backup Speedometer System

There's always a possibility that the Intel Atom Desktop Board may fail and thus the GUI (Graphic User Interface) will not be able to display speed that is required by the users. For road safety purposes, a backup speedometer system is designed to assist users in monitoring their speed while driving the electric vehicle before sending the electric vehicle to engineers for troubleshooting.

The circuit is implemented with the integration of the photo-interrupter circuit with the tachometer circuit.

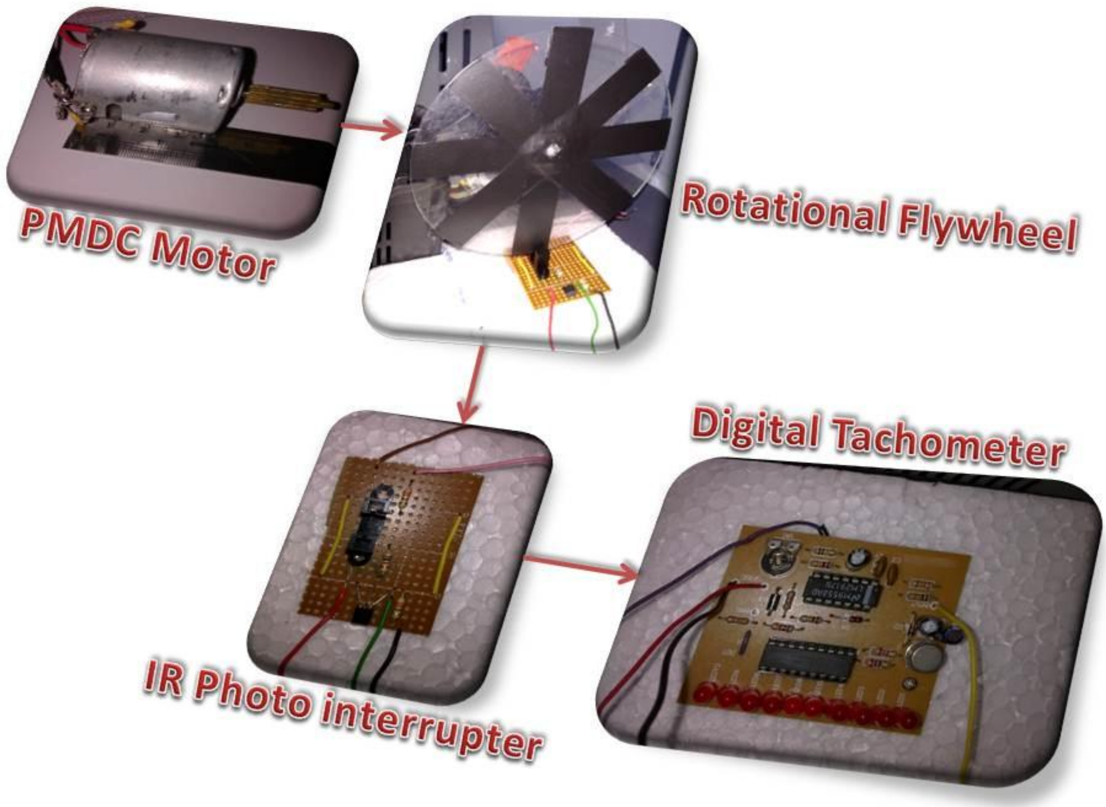

Figure 3.20 Flow chart of the back-up speedometer system.

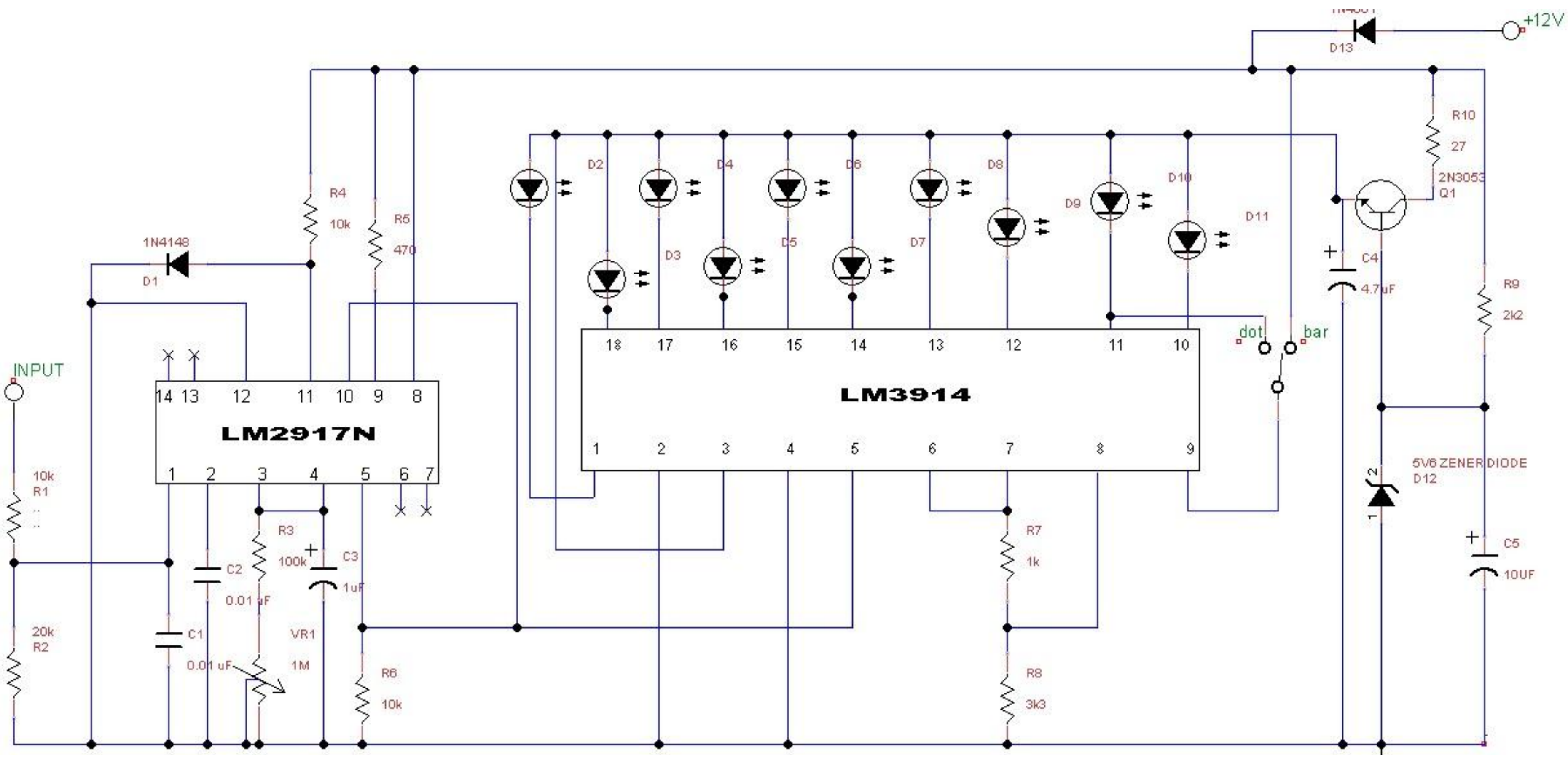

Figure 3.21 the Digital Tachometer Circuit

An easy way of measuring RPM is to convert the frequency of a sensor attached to the motor into a proportional voltage by using the frequency-to-voltage converter, LM2917N. And, by implementing the LM3914, it is easy to display to the user the varying rpm corresponding with the changes of red LEDs. The LM3914 is a monolithic integrated circuit that senses analogue voltage levels and drives 10 LEDs, providing a linear analogue display.

When the wheel moves from slow to fast, the frequency will also gradually increase as the number of interrupts for the photo-interrupter increases. An increase of frequency can only means that the voltage output from LM2917N to LM3914 will increase. Therefore, the LEDs will light one by one from LED1 to LED11. Meanwhile, the LEDs light up one by one because the dot function (see figure 3.21) have been set. When in the dot mode, there is a small amount of overlap or "fade" (about 1 mV) between segments. This assures that at no time will all LEDs be "OFF", and thus any ambiguous display is avoided.

Besides, LM2917N is a monolithic frequency to voltage converters with a high gain op amp and comparator. The advantages for using the LM2917N is that it has an output that swings to ground for zero input frequency and it is extremely easy to use as it has an easy formula of calculating the output voltage of LM2917 which is:

$$V_{OUT} = f_{in} \times V_{CC} \times R_1 \times C_1$$

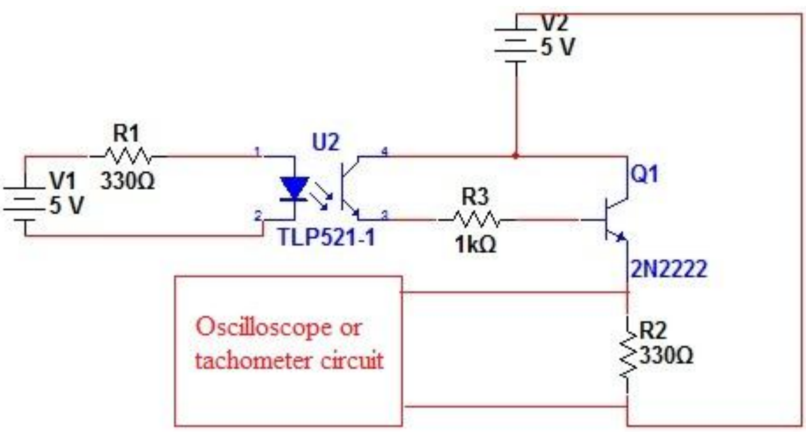

Figure 3.22 Photointerupter Circuit

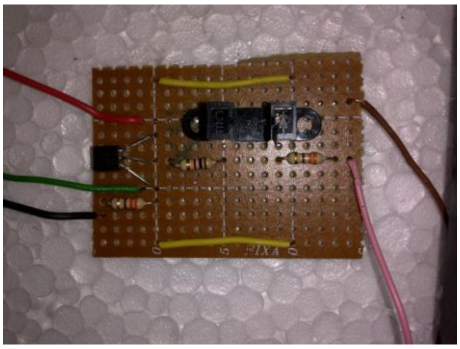

Figure 3.23: Photo Interupter

Meanwhile, the photo interrupter circuit is designed to take the rotation of the wheel of the electric car by attaching a flywheel to it. When the photo interrupter is covered by the black side of the flywheel, the output signal will be low and the base of the photo transistor will not be triggered and the current will not flow through the R3 to trigger the NPN transistor, thus when we use an oscilloscope to measure across R2, there will be no signal.

However, when the photo interrupter is uncovered and it allows the infrared wave to transmit from the transmitter to the receiver, the base of the photo transistor will be triggered and thus the power supply will allow the current to flow through R3 to trigger the NPN transistor and thus completing the circuit, so that when we measure across R2, there will be high signal.

Hence, when this sequence of covered and uncovered is happening at a very fast rate, it will consequently generate a square wave that has amplitude of 5V and the frequency generated is depending of the rotation speed of the motor. The speed of the motor in turn proportional to the voltage supplied to it.

In addition, the frequency generated can be feed into the tachometer circuit to convert frequency into voltage using the LM2917N and thus indicating the speed of the motor to the users even if there is no GUI.

In addition, the voltage at Pin5 of the LM2917N varies when the input frequency varies. Thus, at pin 5, we can get the corresponding voltage with frequency that is being fed into the LM3914 for it to display the speed of the wheel using the 10 LEDs. The frequency increase when the wheel moves faster due to more voltage being supplied to the motor, thus when frequency increase, the voltage at pin 5 will also increase.

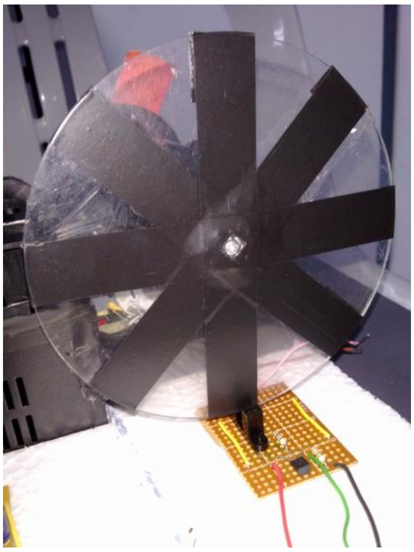

Figure 3.24 Prototyping with a flywheel and the Photo interrupter

3.8 Virtual Network Computing

In this part of the project, there are three software that are specifically implemented into EVICS as an innovative step to troubleshoot the firmware of EVICS wirelessly without the need to approach the hardware and plug in external input devices (keyboard and mouse) to fix the problem.

The software mentioned to perform Virtual Network Computing and Wireless Remote Desktop Control are as below:

1. FileZilla
    - It is a FTP (File Transfer Protocol) application installed on Windows that allows users to transfer file from client side to the server side. Here, the EVICS will be the server side while the engineer's laptop will be the client.
2. VNC Viewer 4
    - It is a VNC application that allows client to graphically view the server screen and control it remotely.

3. Android VNC
    - It is the same function as a VNC Viewer 4 but it can be installed into any Android-based mobile phone.

3.9 Reverse Parking Sensor Circuit

The reverse parking sensor here uses the technology of the infrared receiver and transmitter.

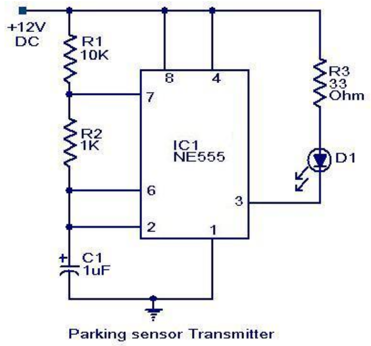

Figure 3.25 Parking Sensor Transmitter

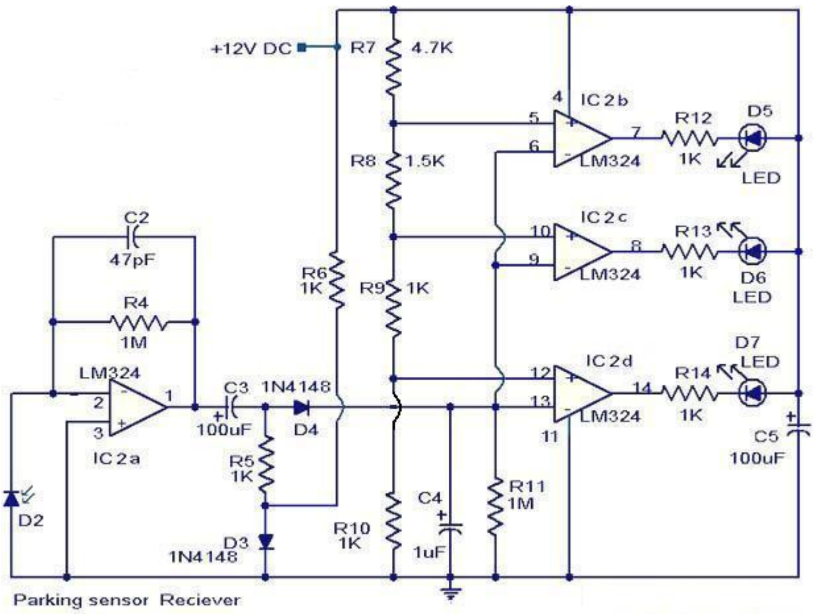

Figure 3.26 Parking Sensor Receiver

This simple circuit can be used as an aid for sensing the distance between the rear bumper of the car and any obstacle behind the car. The distance can be understood from the combination of the LEDs (D5 to D7) glowing. At 25cm D7 will glow, at 20 cm D7&D6 will glow and at 5cm D7, D6 and D5 will glow. When the obstacle is beyond 25 cm none of the above LEDs will glow.

Two ICs are used in the circuit. The IC1 (NE555) is wired as an astable multivibrator for driving the IR Diode D1 to emit IR pulses. The operating frequency of the transmitter is set to be 120Hz.

The IR pulses transmitted by D1 will be reflected by the obstacle and received by the D2 (IR photo diode).The received signal will be amplified by IC2a.The peak of the amplified signal will be detected by the diode D4 and capacitor C4.R5 and R6 compensates the forward voltage drop of D4.The output voltage of the peak detector will be proportional to the distance between car's bumper and obstacle. The output of peak detector is given to the inputs of the other three comparators IC2b, IC2c and IC2d inside the IC2 (LM324).The comparators switch the status LEDs according to the input voltage their inverting inputs and reference voltages at their non-inverting inputs. Resistances R7 to R10 are used to set the reference voltages for the comparators.

Moreover, there is also a simpler back-up circuit designed as an alternative in case the circuit above has not a strong signal to be transmitted to the receiver which is shown below:

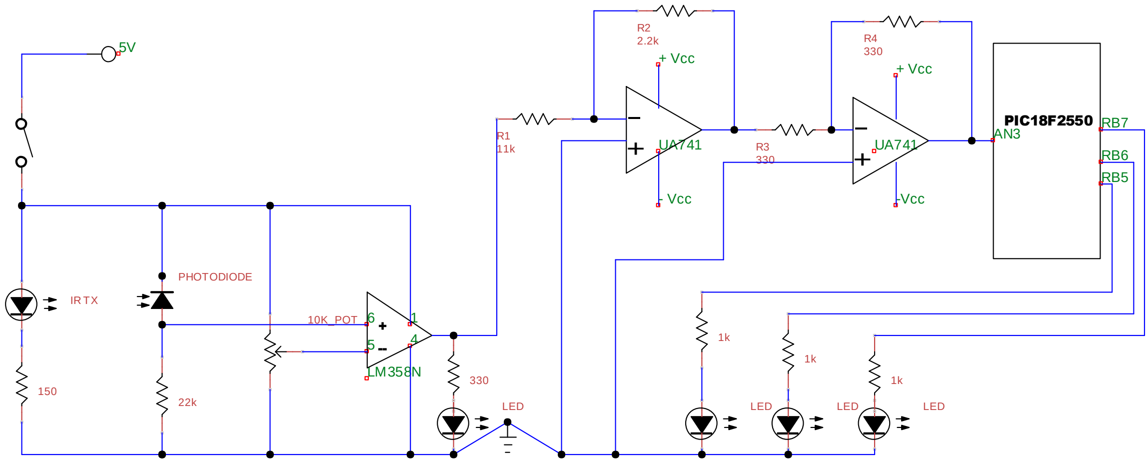

Figure 3.27 Reverse Parking Sensor

CHAPTER 4

RESULTS AND DISCUSSIONS

4.1 LM35 Temperature Sensor

4.1.1 Accuracy

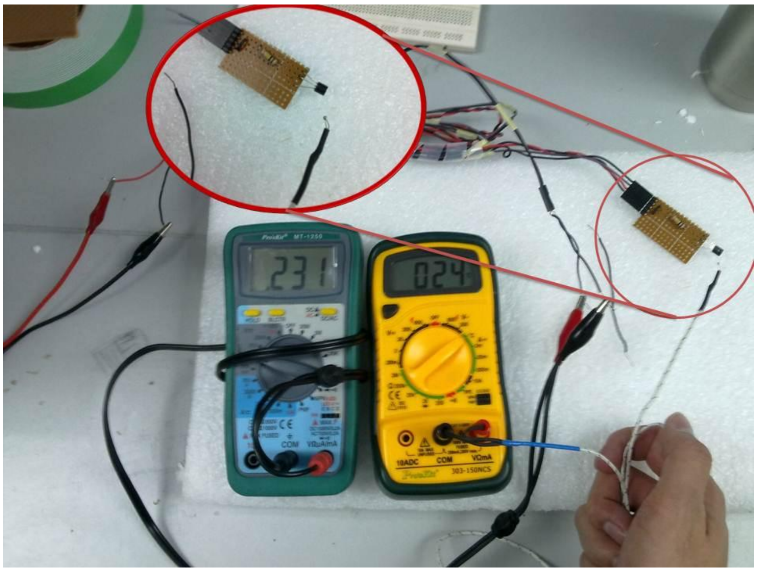

Figure 4.1 Temperature Sensor LM35 Circuit with Digital Thermometer

As seen in the figure 4.1 above, the temperature sensor LM35 is used side by side with a digital thermometer. The digital thermometer will tell the exact temperature of the environment while the LM35 circuit will generate the appropriate voltage that matches the temperature of the thermometer after dividing it by 10mV/^{O}C.

Figure 4.2 Room Temperature

From the figure 4.2 above, the temperatures are:

- Thermometer Temperature, Tt = 23^{O}C
- LM35 Sensor Temperature, Ts = 0.231V*(100^{O}C/V)

  = 23.1^{O}C

Thus, a thermos flask is used to preserve a controlled temperature environment for data collection and experiment purposes. Note: both the temperature sensor LM35 and thermometer are place above the water level within the thermos. As seen in figure 4.3, hot water is filled into it, so that it can be easily cooled when cool water is poured into it.

Figure 4.3 Digital Thermometer inside the Thermos to monitor the Temperature

Figure 4.4 The LM35 Sensor and the Thermometer inside the Thermos

By adding in a small amount cold water into the thermos after each reading is taken, we can have various temperature levels inside the thermos.

Table 4.1 Relationship between Voltage and Various Temperature

Voltage Output from LM35, V	**Temperature from LM35, ^{O}C**	**Temperature inside the Thermos, ^{O}C**
0.685	68.5	67
0.571	57.1	59
0.444	44.4	43
0.347	34.7	36
0.280	28	29
0.260	26	27
0.235	23.5	26
0.215	21.5	23

From the above results, the average temperature detected by the thermometer is:

(67+59+43+36+29+27+26+23)/8 = (310/8) ^{O}C

= 38.75^{O}C

The average temperature detected by the LM35 sensor is:

(68.5+57.1+44.4+34.7+28+26+23.5+21.5)/8 = (303.7/8) ^{O}C

= 37.9625 ^{O}C

Percentage Difference between two average values is:

([38.75-37.9625]/38.75)*100% = **2.03%**

Hence, the LM35 sensor possesses good accuracy in measuring temperature with just a 2.03% difference compared to the real temperature.

4.1.2 Response Time

Next, it is important to investigate the response time of the temperature sensor as we are dealing with real-time communication with PIC and the Intel Atom Desktop Board.

A target temperature has already been set for the LM35 sensor to hit which is $75^{O}C$. The value of voltage is taken every second while the LM35 detects a gradual increase of temperature until a certain point it reaches steady state. This data collecting can only be done by using a video camera as taking reading every second is too fast.

The table that shows the output voltage and eventual temperature from the LM35 every second can be found in the appendix (200 samples) while the response time curve of the LM35 is plotted as follows:

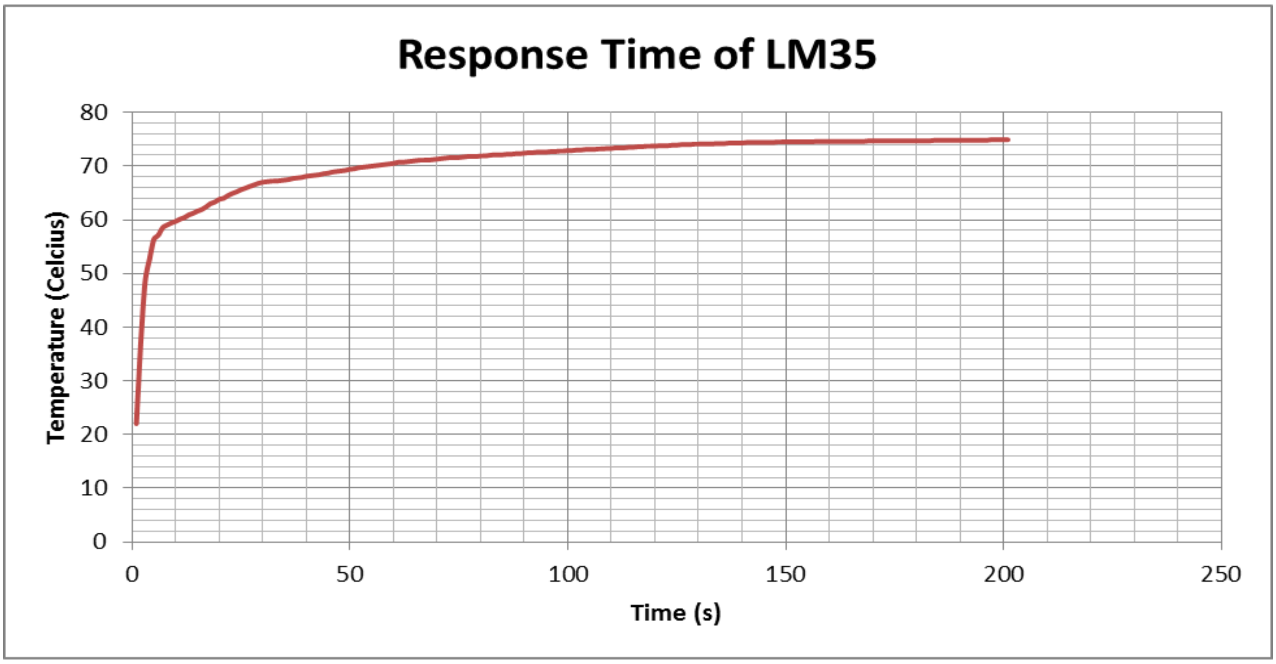

Figure 4.5 Response Time of LM35

The response time from this experiment matches with response time given by LM35 datasheet, which is approximately 200s, equivalent to three minutes for it to reach the 100% of the final value which is in this case, $75^{O}C$.

4.2 Fan Driver Circuit and Air Cooling Ventilation System

Figure 4.6 Fan Driver Circuit

In this part of the result and discussion, we are going to talk about the various resistors that are tested to determine the perfect base resistance of the NPN C9013 transistor.

First and foremost, the reason that a specific resistance needed to be at the base of the transistor because it is found out that during the process of this project, the PIC18F2550 will give a small voltage of maximum 1V at the output port even though that particular port is not trigger to be HIGH. For instance, the temperature has not reached critical level, so the PIC would not trigger the fan driver circuit, however if the resistor at the base of the transistor is not sufficient, it will trigger even the output is set to LOW as the transistor base voltage is only 0.741V, hence the fans will be always turned on if the base resistance is not high enough.

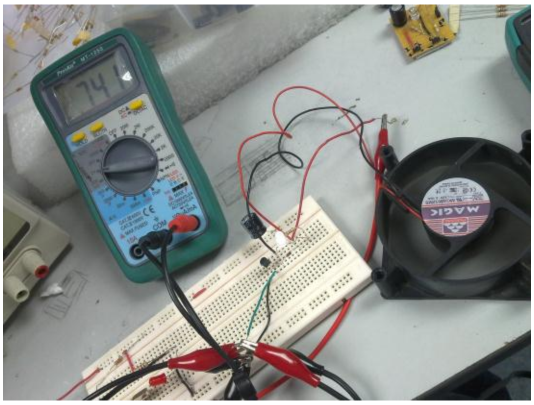

Figure 4.7: Transistor Base Voltage, 0.741

Here, various resistors are used to find the correct one. In the first part, we are to find the triggering voltage according to the resistant given. That means supply the voltage until it is just turned on, then record down the voltage values. The higher the resistance of the base resistor, the higher it will be for the triggering voltage. The triggering voltage must not be too low while in the meantime still being able to maintain enough current flow to turn the fan.

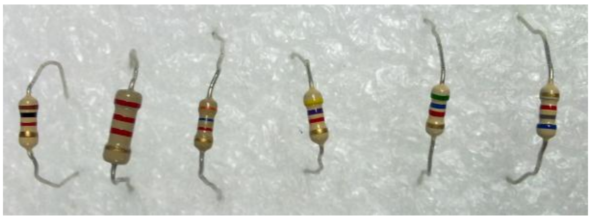

Figure 4.8 Resistors (from left: 1k, 2.2k, 3.6k, 4.7k, 5.6k, and 6.8k)

Table 4.2 The Relationship between Base Resistance and triggering voltage

Base Resistance, R_B (Ω)	**Trigger Voltage, V_{IN} (V)**	**Voltage Across Resistor, V_{RB}(V)**
1k	0.8	0.12
2.2k	0.94	0.59
3.6k	1.29	1.03
4.7k	1.33	1.23
5.6k	1.43	1.46
6.8k	1.66	1.56

Due to the undesired voltage from the PIC, the voltage is set constant at 1V to see which resistor will not trigger the LED to turn on as the LED is an indication that there is voltage supplied to the fan, but the fan does not turn in this case because the base voltage is not high enough to allow more current to flow to the fan. The aim is to choose a resistor value that limits the unwanted voltage as much as possible while still be able to turn the fan efficiently.

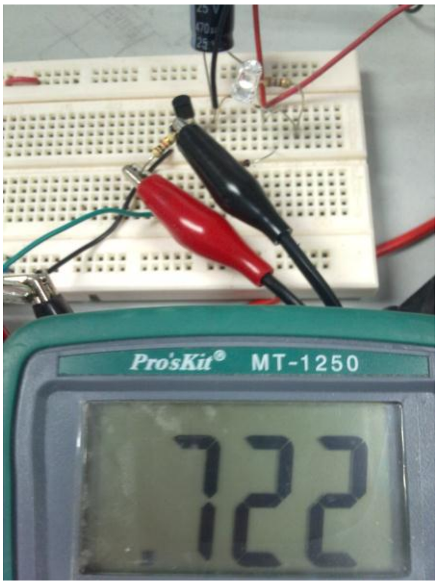

Figure 4.9 1kΩ - LED still ON

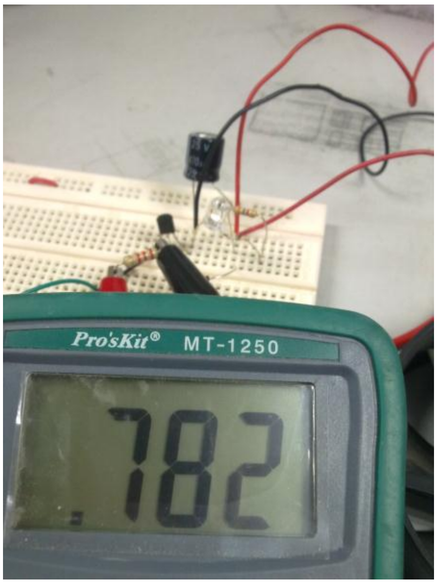

Figure 4.10 2.2kΩ - LED still ON

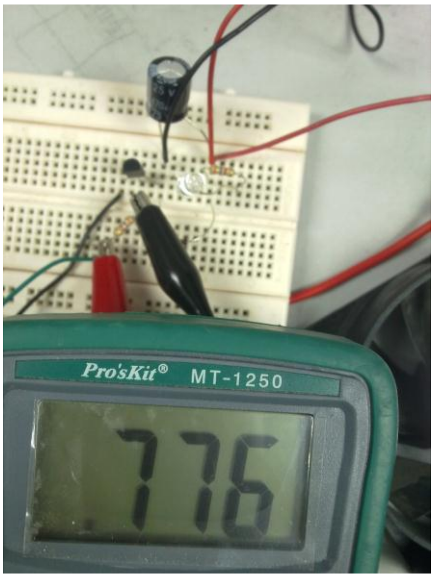

Figure 4.11 3.6kΩ - LED still ON

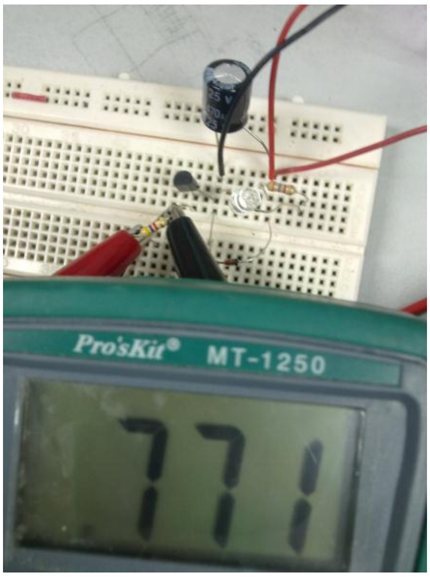

Figure 4.12 4.7kΩ - LED slightly ON

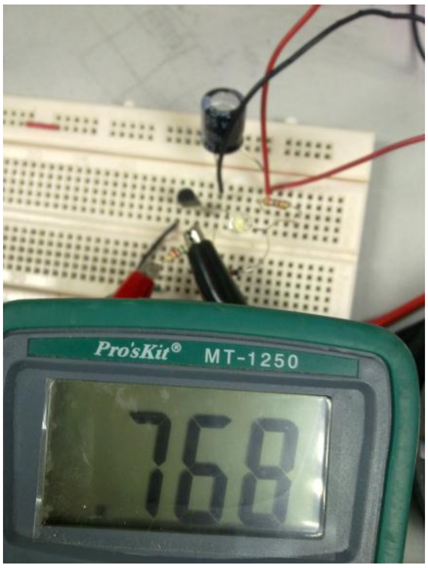

Figure 4.13 5.6kΩ - LED OFF

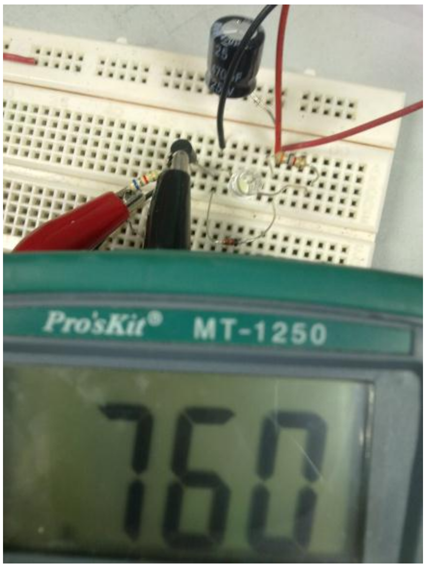

Figure 4.14 6.8kΩ - LED OFF

In conclusion, the selected resistor is 4.7kΩ because the triggering voltage of it is 1.33V which is slightly above the undesired voltage of 1V. Besides, choosing 5.6kΩ and 6.8kΩ for the fan driver circuit tends cause the fan to turn slow and not as fast as implementing 4.7kΩ into the fan driver circuit.

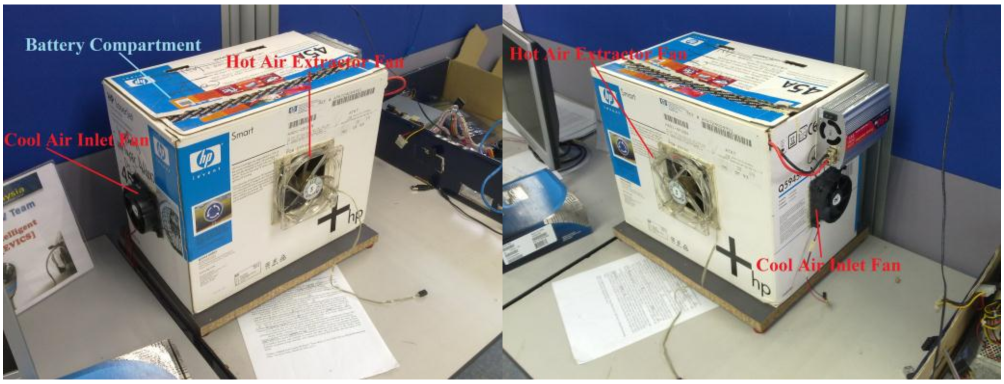

Figure 4.15 Battery Compartment with Complete Air Cooling Ventilation System

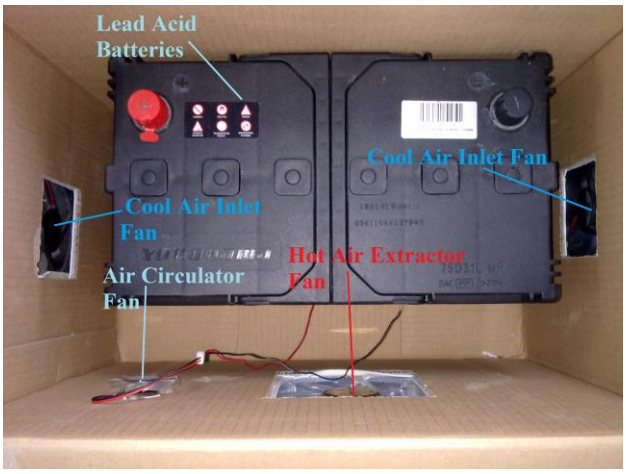

Figure 4.16 Battery Compartment (inside)

The figures below show that the fans in action when they are being triggered once the temperature increase above 25^{O}C.

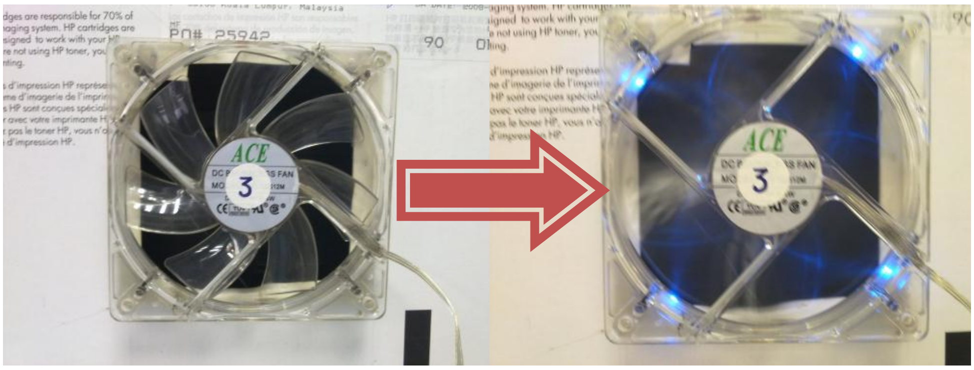

Figure 4.17 The Hot Air Extractor Fan in Action

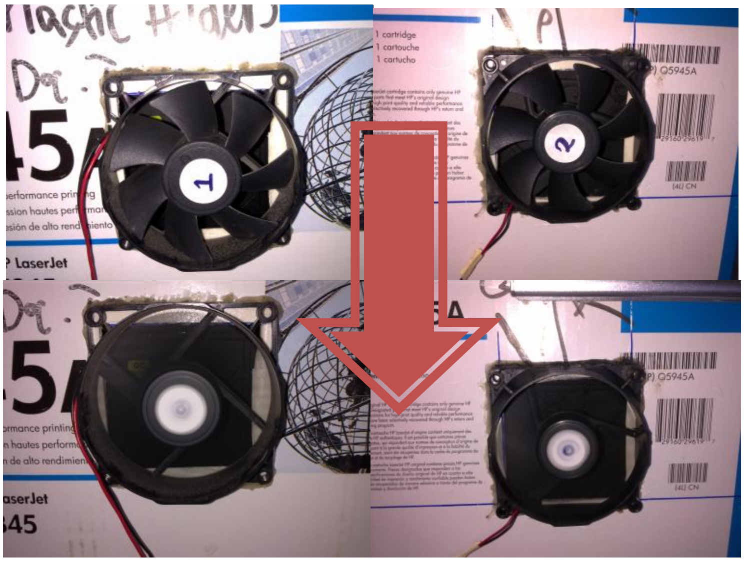

Figure 4.18 Both of the Cool Air Inlet Fan in Action

4.3 Temperature Sensor Watchdog Module

In EVICS, the temperature sensors can be monitored automatically by using a technique called watchdog. Basically, it is like having a "watchdog", watching over the temperature sensors to avoid any fault to happen without the notice of the users. This makes it easier for users to know whether their temperature sensor is functioning properly.

The watchdog here is mainly utilizing the ADC programming to compare with a reference level which is 0V in this case as a damaged LM35 will not output any voltage.

The figures below show the simulation of experiment and result that have been achieved:

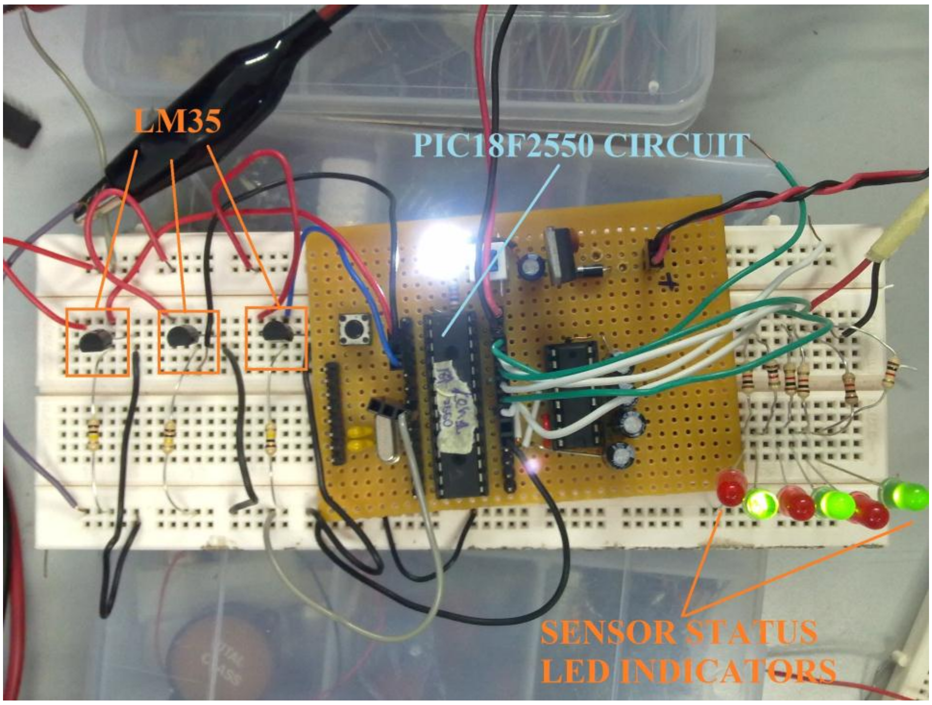

Figure 4.19 All Three LM35 Sensors working properly with all of the green LEDs ON

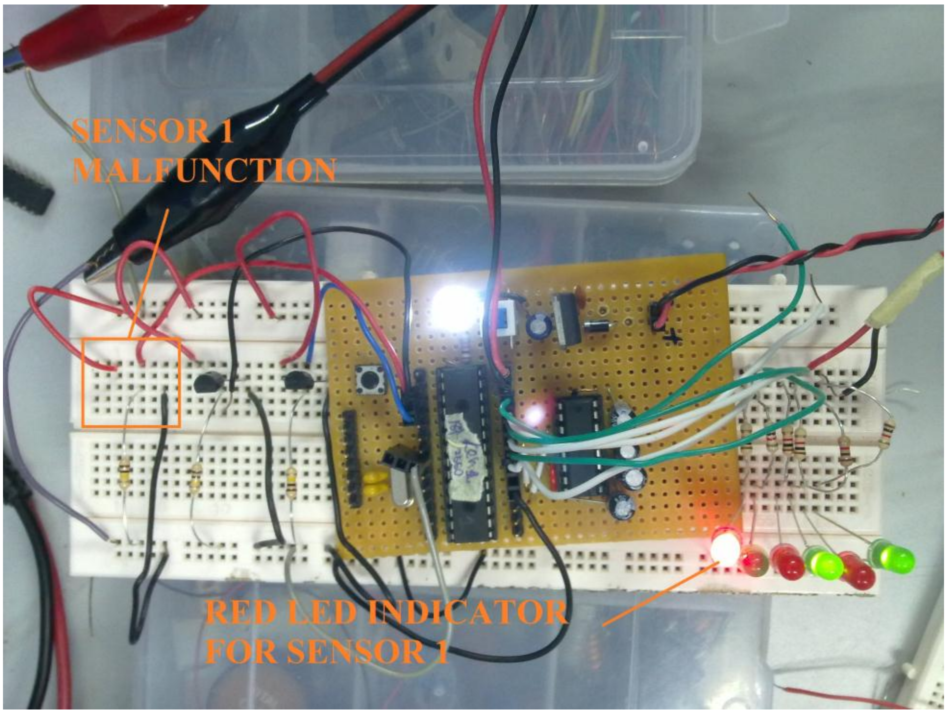

Figure 4.20 Sensor 1 Malfunctions, Red LED.1 ON

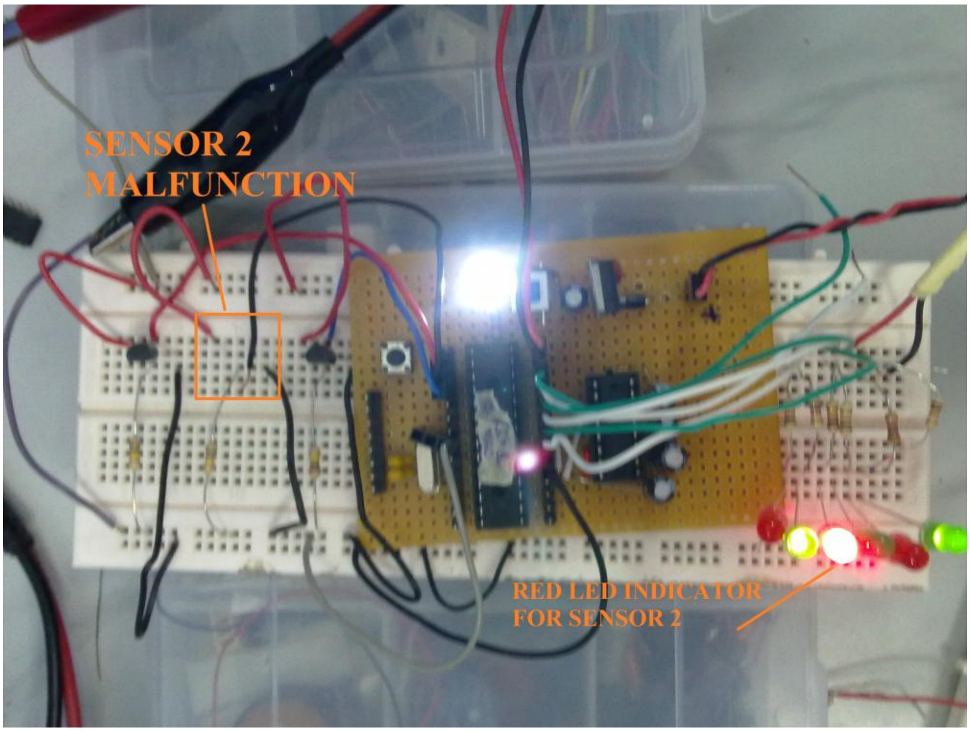

Figure 4.21 Sensor 2 Malfunctions, Red LED.2 ON

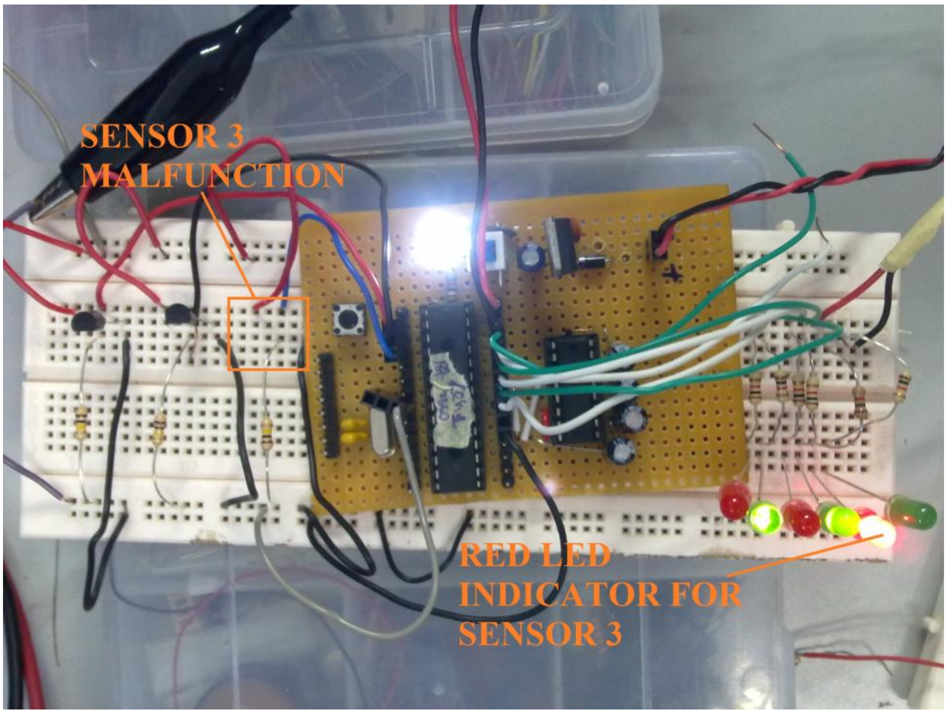

Figure 4.22 Sensor 3 Malfunctions, Red LED.3 ON

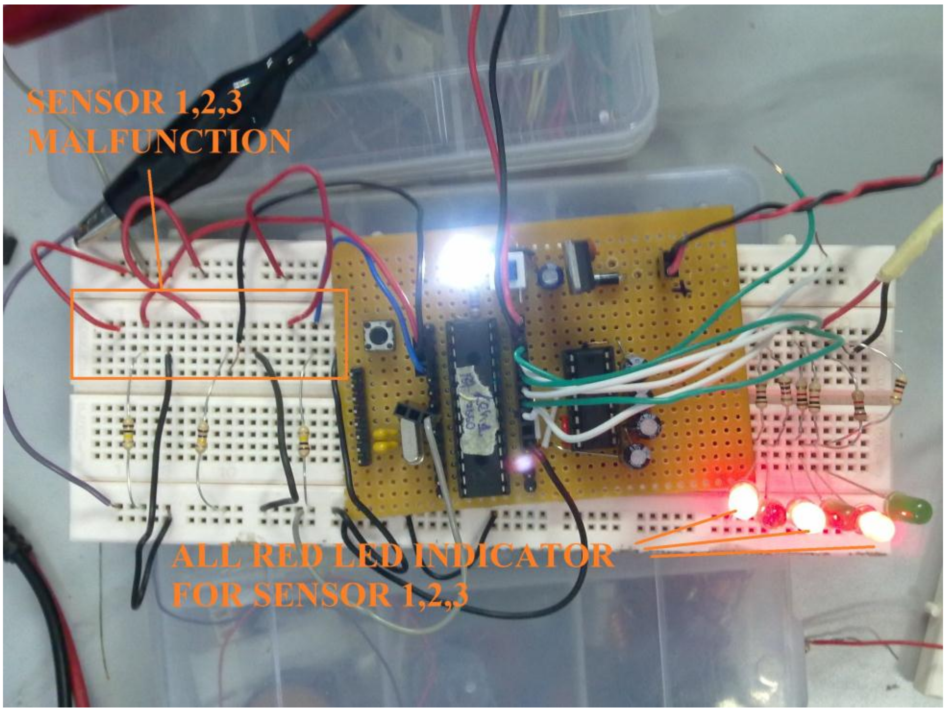

Figure 4.23 All Three LM35 Sensors malfunction with all of the red LED ON

4.4 Calculating the Raw Motor Speed and km/h

As we all know the increase in voltage will cause an increase of rpm of the motor. Here, we measured the wheel's rpm and thus are able to calculate the km/h and using reverse calculation, we can get the raw motor rpm as well.

The formulas in doing so are mentioned earlier:

- $n_A = n_D$ *10.23809524 ; n_A :Speed of Motor & n_D:Speed of Wheel
- Speed of the car, km/h= (2*π*radius of wheel*rpm of wheel*60)/1000

Table 4.3 Results from Calculations for motor and wheel rpm and the km/h of the prototype car.

Voltage, V	Measured Wheel RPM, rpm	Calculated Motor Raw RPM, rpm	Kilometer per Hour according to Wheel RPM, km/h
0	0	0	0
1	201.3	2060.928572	2.656090925
2	440.2	4506.809525	5.808302162
3	681.9	6981.357144	8.997458529
4	935.3	9575.690478	12.34099276
5	1197	12255	15.79404291
6	1426	14599.52381	18.81562672
7	1684	17240.95238	22.21985652
8	1933	19790.2381	25.50533412
9	2211	22636.42858	29.1734577
10	2466	25247.14286	32.53810344
11	2733	27980.71429	36.06108544
12	2952	30222.85715	38.95072236

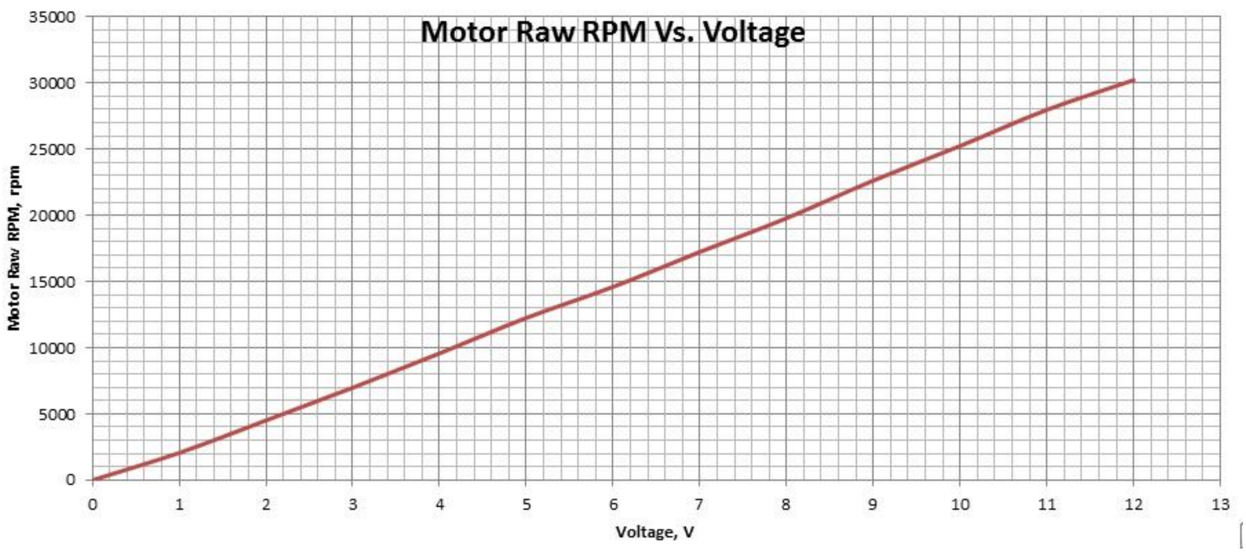

Figure 4.24 Motor Raw RPM vs. Voltage

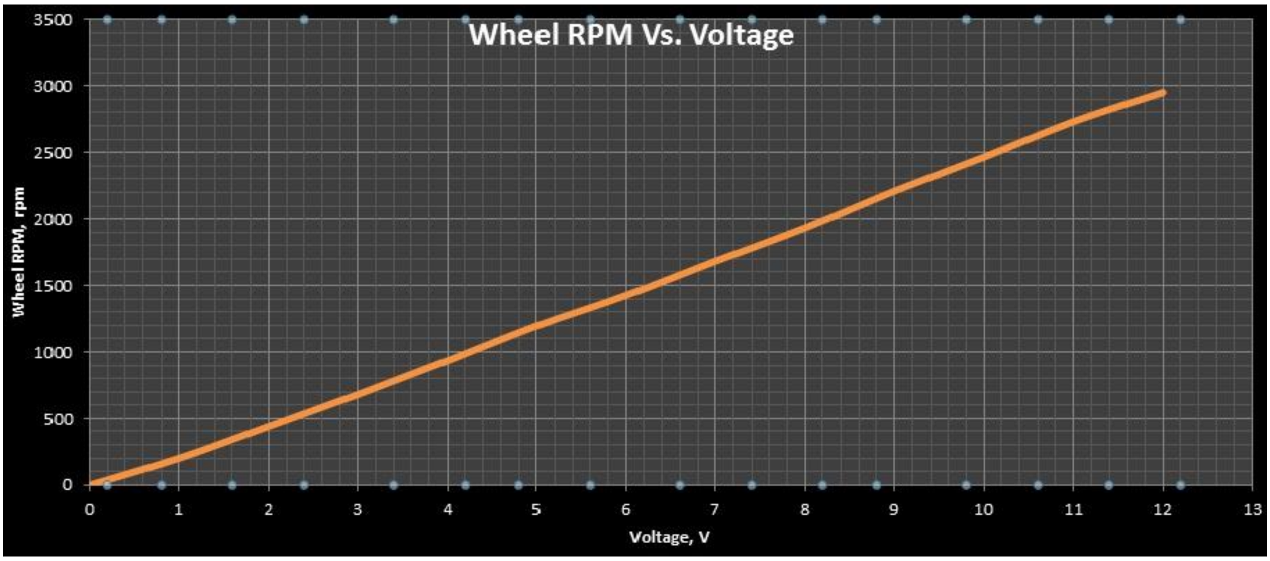

Figure 4.25 Wheel RPM vs. Voltage

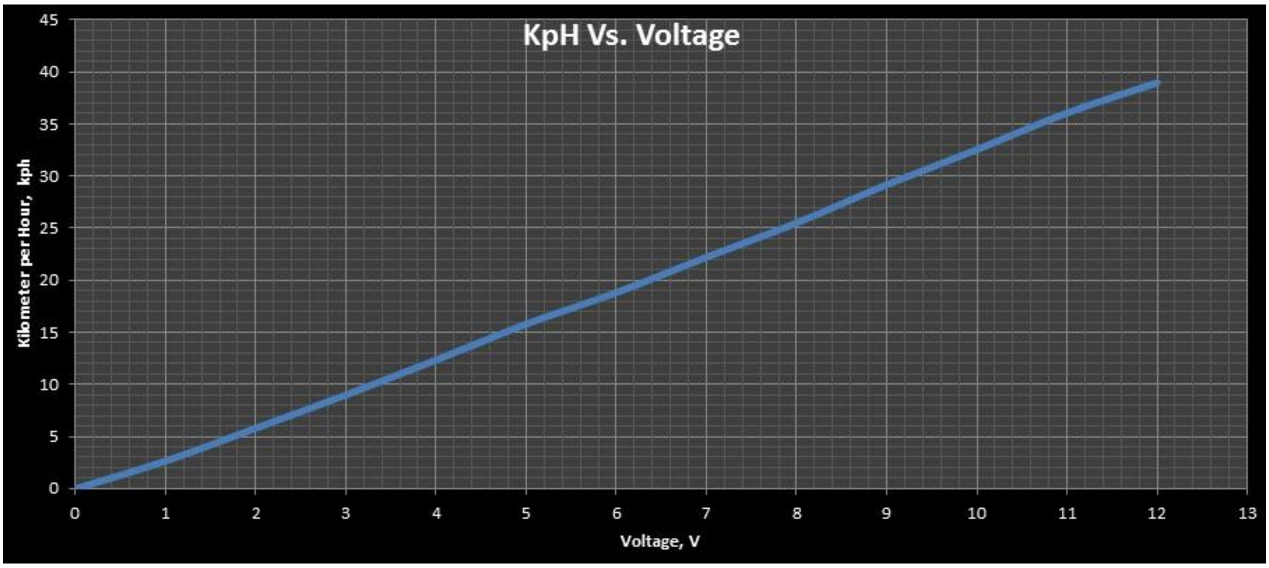

Figure 4.26 Kilometre per Hour vs. Voltage

As can be seen from the graphs above, the relationship between the motor rpm, wheel rpm and vehicle speed is related. Thus, the voltage supplied to the motor is always proportional to the rpms (motor & wheel) and the vehicle speed. And, this is one of EVICS's innovations as this way in measuring and monitoring speed is cost-effective and easy, there's no need for measurement devices coupled to the wheel, sensors, or any variable magnetic reluctance pick-ups.

Table4.4 Corresponding Characters Sent from PIC-to-Intel Atom Board

Voltage Range	Average Motor RPM	Average Wheel RPM	Average Kph	Characters Sent
0 to 0.718	0	0	0	K
0.718 to 1	1030	100.6046511	1.327447099	L
1 to 2	3284	320.7627906	4.232365312	M
2 to 3	5744	561.0418604	7.402772946	N
3 to 4	8279	808.6465115	10.66983935	O
4 to 5	10915	1066.116279	14.06707289	P
5 to 6	134729	13159.57674	173.6365244	Q
6 to 7	15920	1554.976744	20.51743477	R
7 to 8	18516	1808.539535	23.86311697	S
8 to 9	21213	2071.967441	27.33896631	T
9 to 10	23942	2338.52093	30.85605673	U
10 to 11	26614	2599.506976	34.29968649	V
11 to 12	29102	2842.52093	37.50618006	W

Unlike the temperature module, the voltage from the motor can't be feed into the PIC as it would damage the microcontroller and also caused confusion in character sending (ADRESH-ADRESL). Thus, the voltage is attenuated as can be seen in table 4.5 below by using operational amplifier.

Table 4.5 Attenuated Motor Voltage

Motor Voltage, V	Attenuated Voltage, V
0	0
1	0.068
2	0.136
3	0.204
4	0.272
5	0.34
6	0.408
7	0.476
8	0.544
9	0.612
10	0.68
11	0.748
12	0.816

4.5 Backup Speedometer Testing Results and Observations

It is utmost imperative for a control system to have a back-up system if the main core of the control system is unable to perform its operation. In this case, the Intel Atom Desktop Board is the main core in displaying the required information on motor speed (rpm), distance left to travel (km) and vehicle speed (km/h).

If the Intel Atom Desktop Board crashes or unable to operate, the display of the Graphic User Interface (GUI) will be gone. Therefore, a back-up system in EVICS will switch its power supply from the Intel Atom Desktop Board power supply directly to power source of the battery. From there, the backup speedometer will operate and display the speed of the vehicle in terms of LED display.

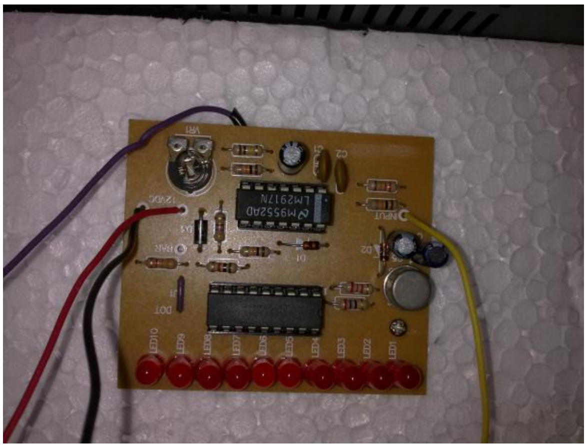

Figure 4.27 Outcome circuit of the Backup Speedometer

Here, we measure and get the corresponding values from:

- Voltage across motor
- Input Frequency from IR Photo-interrupter to Digital Tachometer
- Voltage output at pin 5 of LM2917N (Frequency-to-Voltage Converter)
- Corresponding LED that lid up
- Corresponding Wheel RPM
- Corresponding km/h of the vehicle

However, the rotational speed, S is calculated using the formula below:

$$\text{Rotational speed, } S = (f_{in}/8)*60 \text{ rpm}$$

Table 4.6 Backup speedometer Results and Corresponding LED and Speed

Motor Voltage, V_M (V)	Input Frequency, f_{IN} (Hz)	Rotational Speed, S (rpm)	Pin 5 Voltage, V_5 (V)	LED No.	Wheel RPM, n_{WHEEL} (rpm)	Vehicle Speed, v (km/h)
1	18	135	0.58	1	201.3	2.656090925
2	44	330	1.19	2	440.2	5.808302162
3	73	547.5	1.78	3	681.9	8.997458529
4	85	637.5	2.36	4	935.3	12.34099276
5	108	810	2.94	5	1197	15.79404291
6	125	937.5	3.46	6	1426	18.81562672
7	144	1080	4.00	7	1684	22.21985652
8	169	1267.5	4.74	8	1933	25.50533412
9	190	1425	5.32	9	2211	29.1734577
10	196	1470	5.89	9	2466	32.53810344
11	223	1672.5	6.03	10	2733	36.06108544
12	245	1837.5	6.27	10	2952	38.95072236

- Average value of Rotational Speed, S_{AVG} = 12150 rpm / 12
  = 1012.5 rpm
- Average value of Wheel RPM, $n_{WHEELAVG}$ = 18860.7 rpm/12
  = 1571.73 rpm

- The Difference Between Average value of Rotational Speed, S_{AVG} and Average value of Wheel RPM, $n_{WHEELAVG}$ = 1571.73 rpm - 1012.5 rpm

  = 559.23 rpm

- The Percentage Difference = (559.23 rpm/ 1571.73 rpm) * 100%

  = 35.5803%

As you can see from the results and calculations above, the percentage (%) is quite high. This is because the photo-interrupter circuit may not be fast enough in detecting the quick changes or cutting of the flywheel. This will then cause a great decrease in frequency, consequently, a decrease in calculated rotational speed.

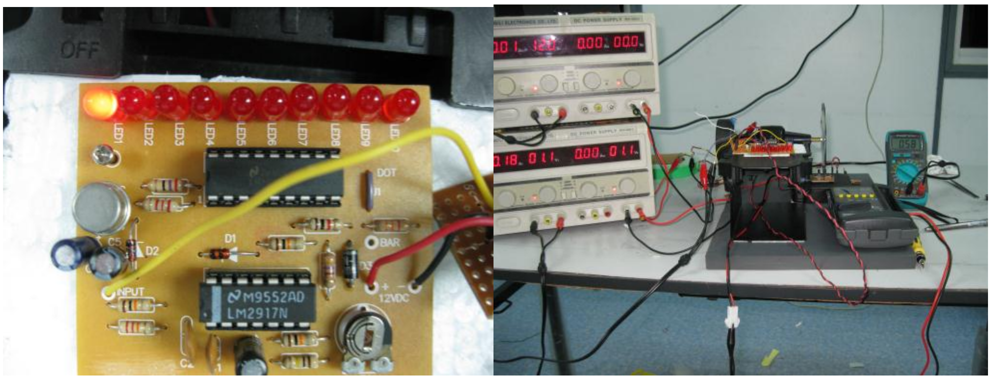

Figure 4.28 LED.1 with motor voltage 1V

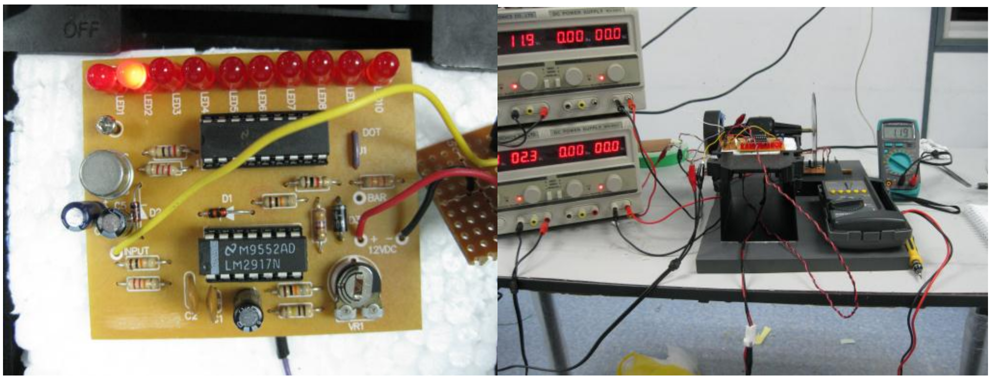

Figure 4.29 LED.2 with motor voltage 2V

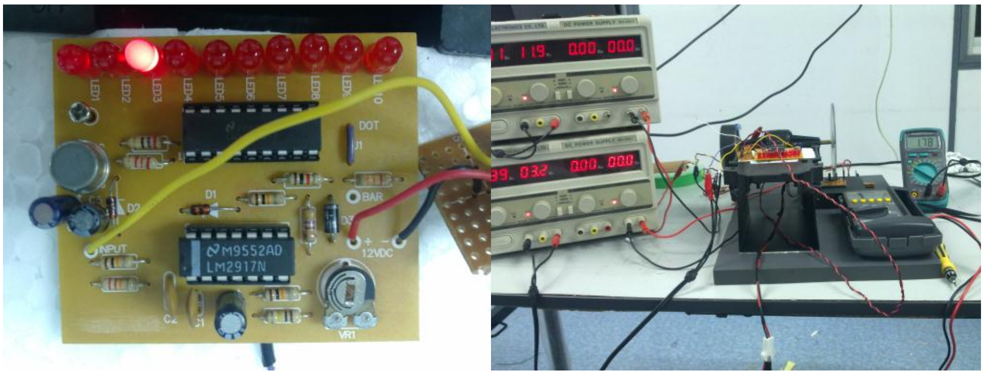

Figure 4.30 LED.3 with motor voltage 3V

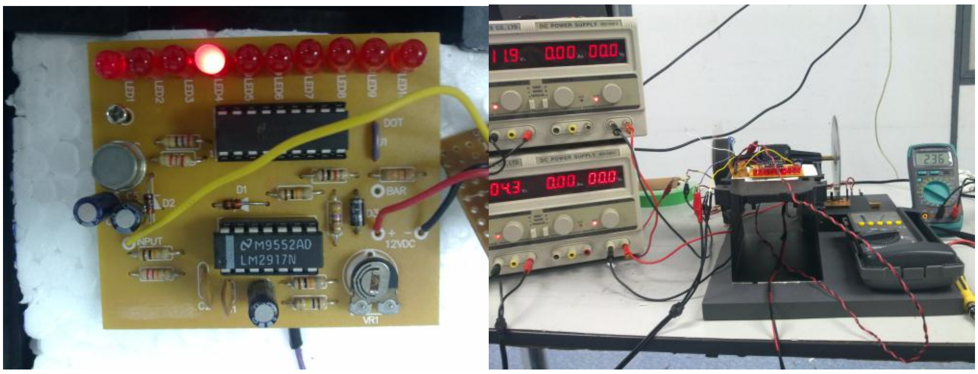

Figure 4.31 LED.4 with motor voltage 4V

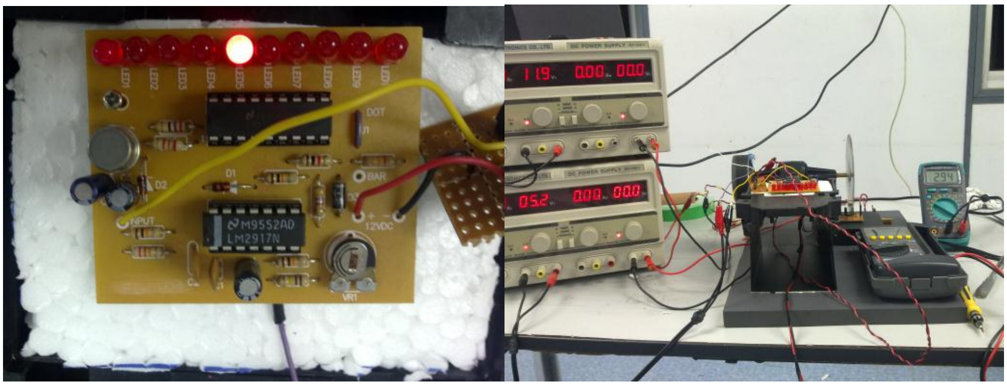

Figure 4.32 LED.5 with motor voltage 5V

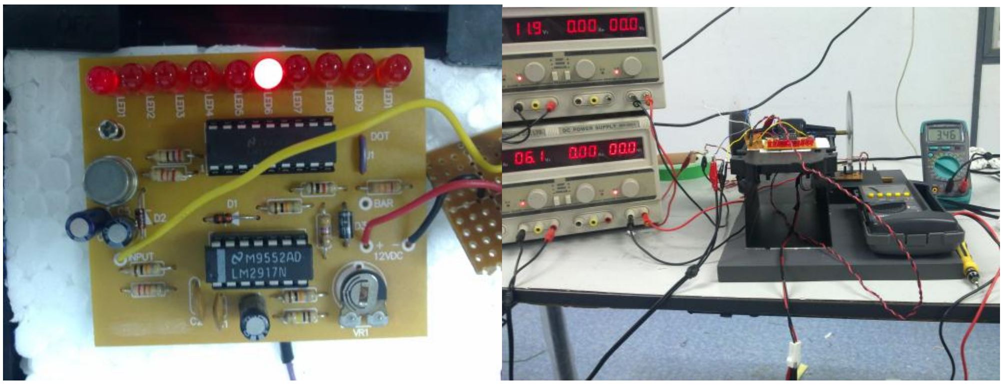

Figure 4.33 LED.6 with motor voltage 6V

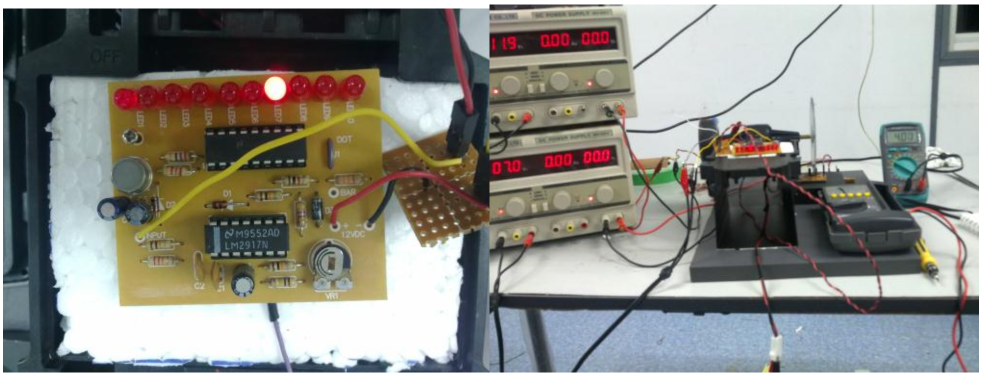

Figure 4.34 LED.7 with motor voltage 7V

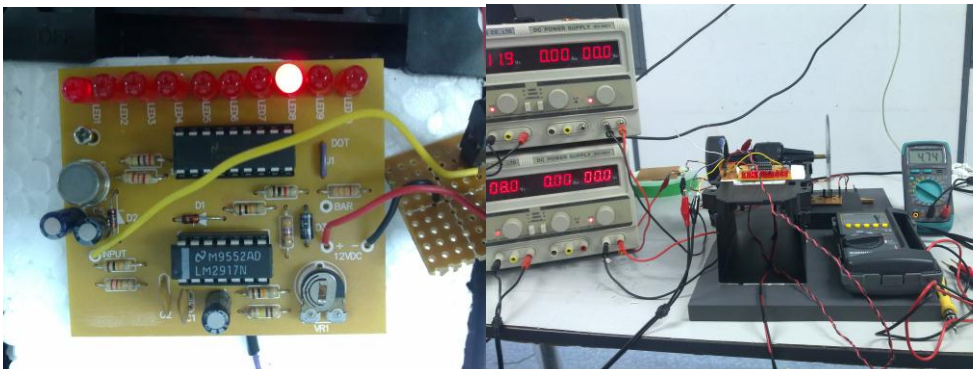

Figure 4.35 LED.8 with motor voltage 8V

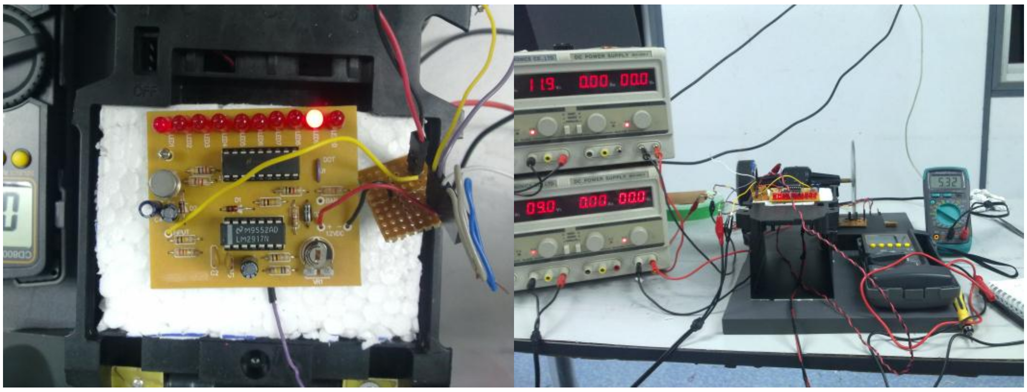

Figure 4.36 LED.9 with motor voltage 9V

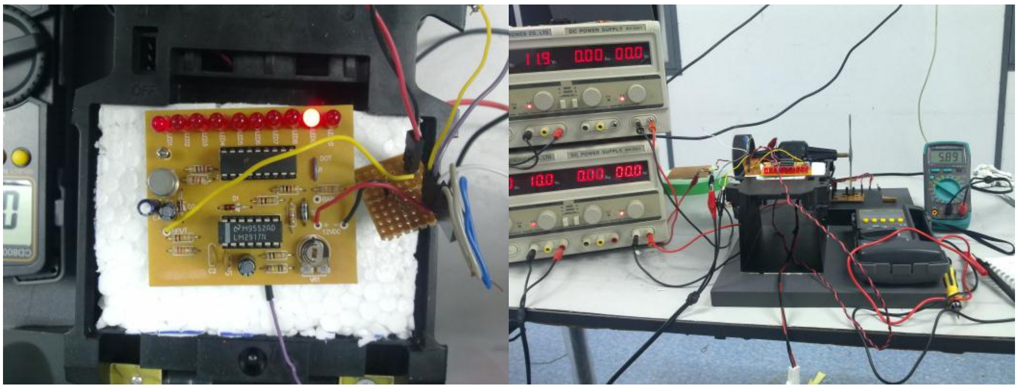

Figure 4.37 LED.9 with motor voltage 10V

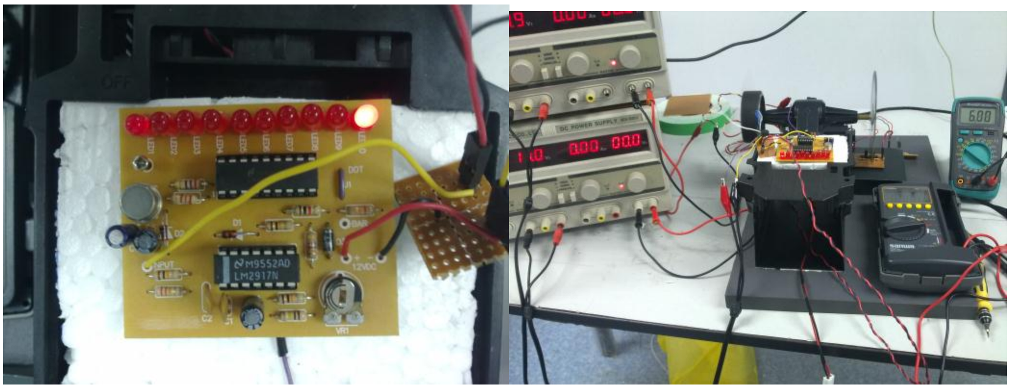

Figure 4.38 LED.10 with motor voltage 11V

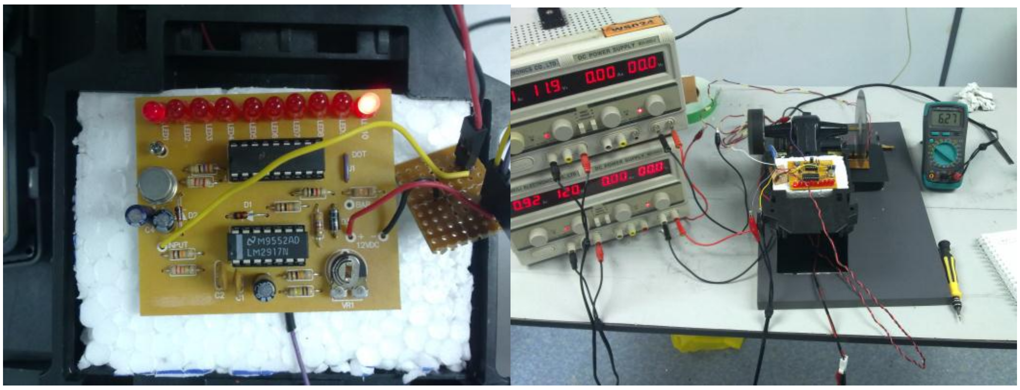

Figure 4.39 LED.10 with motor voltage 12V

4.6 Wireless Remote Desktop and Virtual Network Computing

This is one of the main innovations and most interesting modules in EVICS as it utilizes the Intel Atom Desktop Board as a server and engineers or even tech-savvy users can communicate wirelessly with EVICS. The main purpose of this module is do troubleshooting conveniently on EVICS without the hassle of approaching the EVICS hardware itself.

Let's say, the current monitoring system has malfunction, as engineer, he/she can look into the GUI remotely using his/her laptop or mobile phone and diagnose the problem and give instruction to technician to fix it. This will definitely be an advantage in car manufacturers and service centers if EVICS is implemented.

4.6.1 FileZilla

As we know, the FileZilla is a FTP (File Transfer Protocol) application that allows file transfer from the client to server and vice-versa. The advantage of this is we can remotely transfer updates and enhancement programs into EVICS main interface to improve the system stability and response time, making EVICS easily updatable and flexible for enhancements.

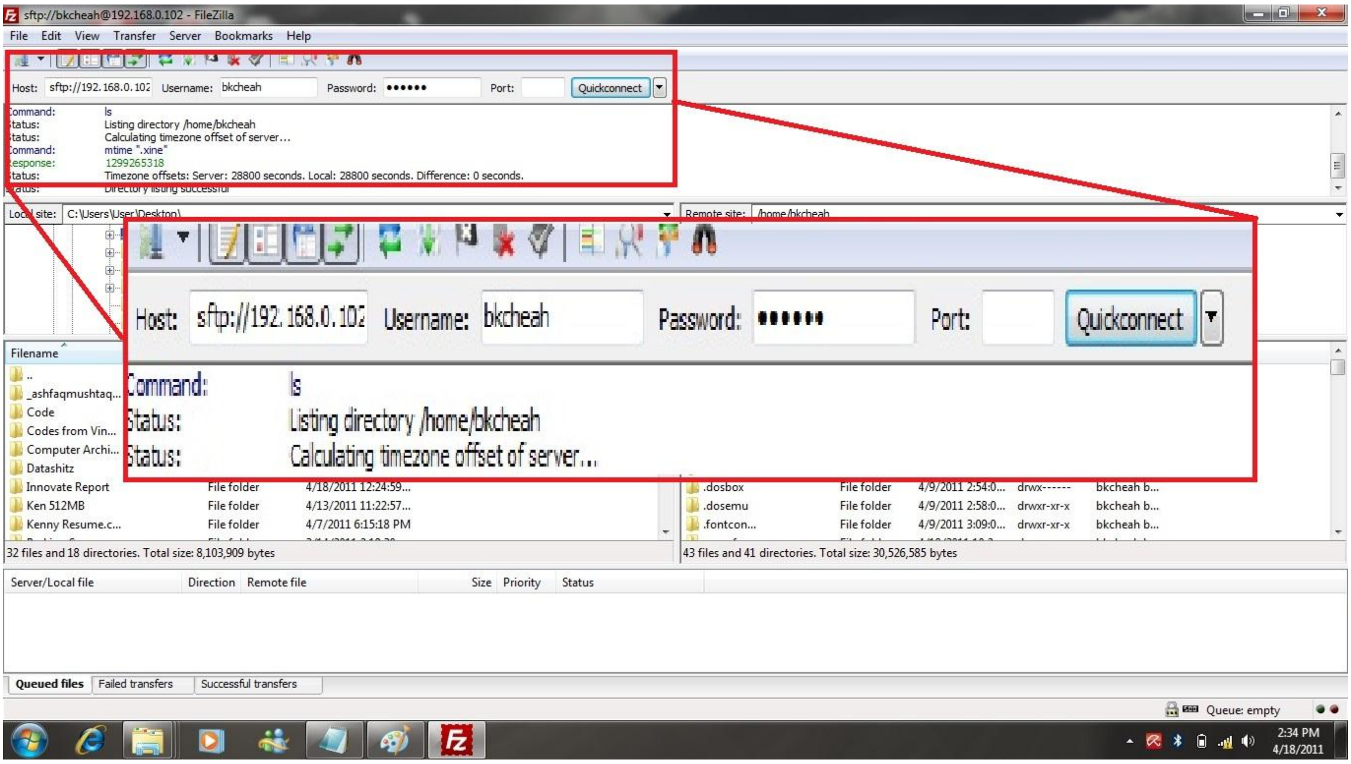

Figure 4.40 Main Interface of FileZilla

In figure 4.40, we first have to enter the server/host IP address, the username set by the server/host, the port number and lastly the password. After that, click on “Quickconnect” to make a connection with the server.

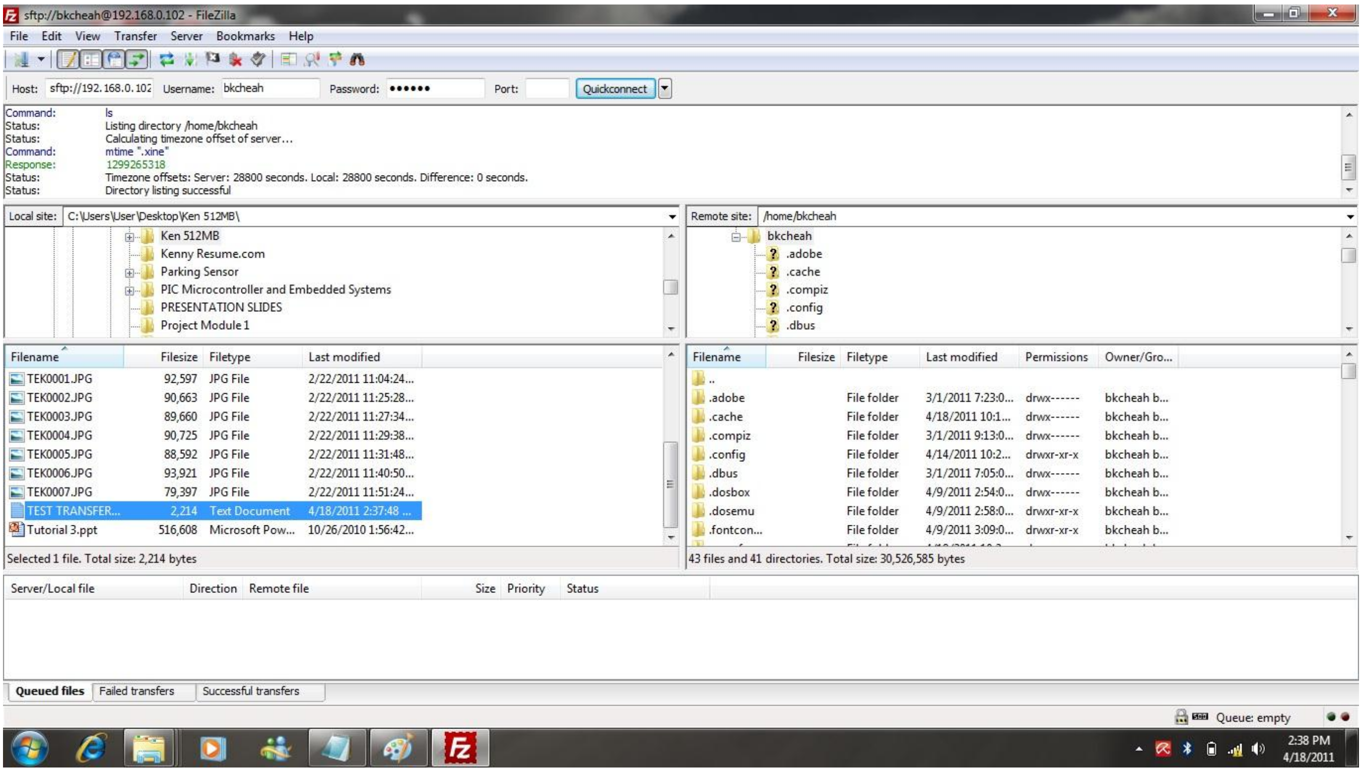

Figure 4.41 FileZilla Connection with EVICS Successful

If the connection is successful, the panel on the right (refer to figure 4.41) will be filled with file folders of the server/host and the status will show “ Directory Listing Successful”.

Now, the file that’s going to be transferred is a text document called “TEST TRANSFER.txt” as highlighted in figure 4.41.

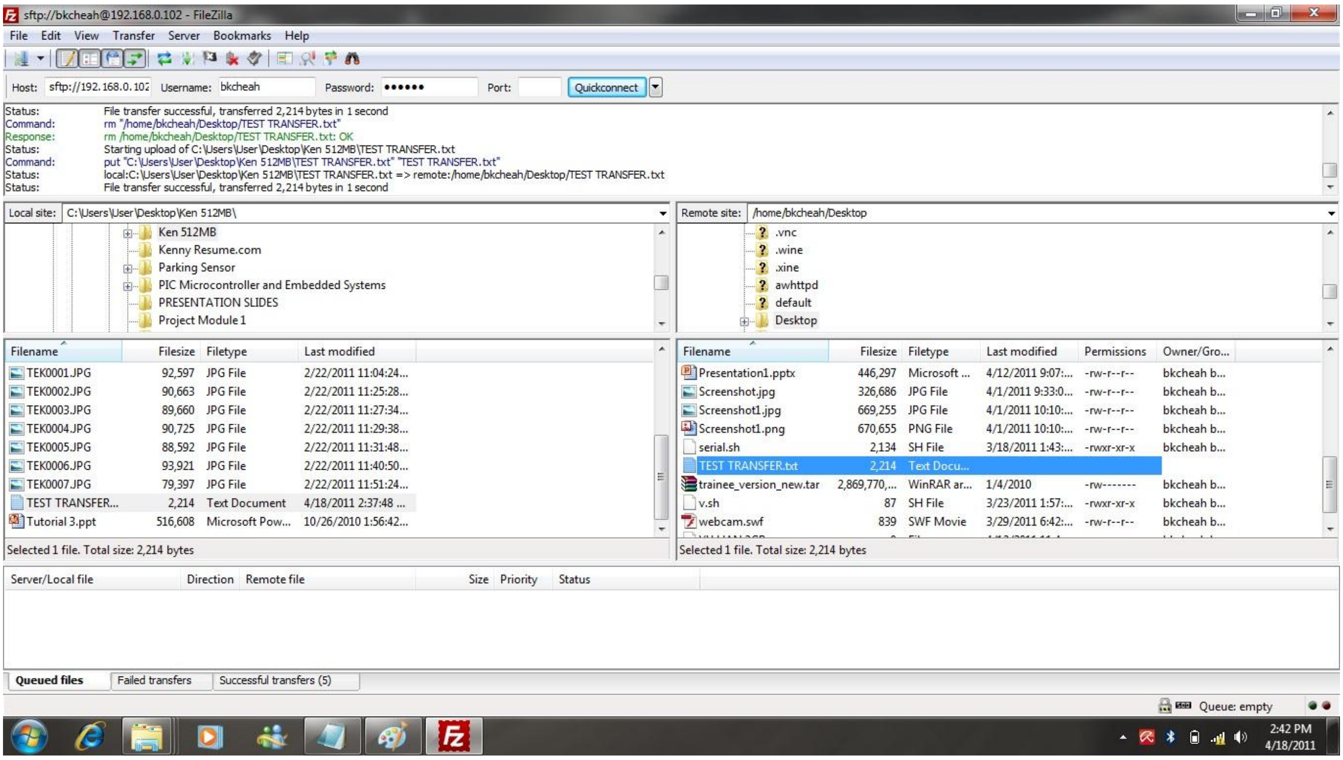

Figure 4.42 File Transfer of “TEST TRANSFER.txt” successful

If the file transfer is successful, you will see the file which is “TEST TRANSFER.txt” as highlighted in figure 4.42 also on the right panel. And, the status will notify users that the file is successfully transferred.

4.6.2 VNC Viewer 4

VNC Viewer 4 is GUI-based wireless remote desktop which allow real-time monitoring of the server side screen. The advantage of VNC Viewer 4 is it allows Windows based computers to connect to any server side computer with any operating system (Linux Ubuntu, Mac OS and etc.) Here, VNC Viewer is used to connect a Windows based laptop to the Intel Atom Board which runs on Linux Ubuntu and control it using Windows based computers in the comfort of your seat.

Figure 4.43 VNC Viewer 4 Start Up

Just like FileZilla, to start up the connection between client and server, it requires client side users to enter the host/server side IP address, the port numbers and the password set by the host.

Figure 4.44 the GUI of EVICS is shown on the screen of Windows based laptop

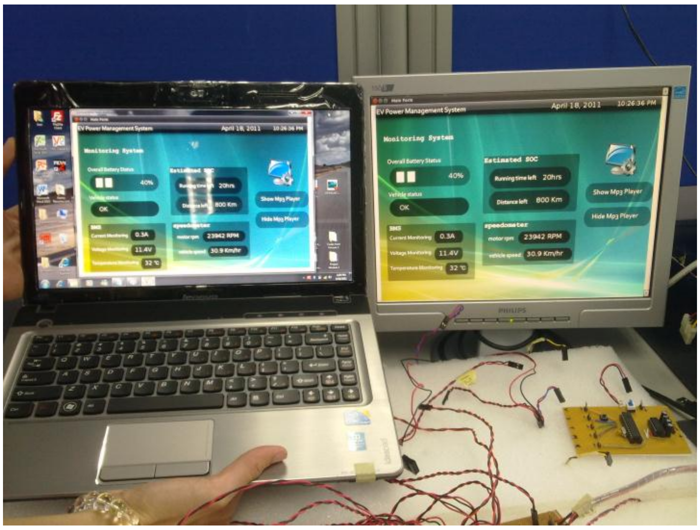

Figure 4.45 Wireless Remote Desktop

4.6.3 Android VNC

Figure 4.46 Android VNC on HTC Incredible S

Similar to VNC Viewer 4, Android VNC enables mobile phones with Android OS to be connected wirelessly to the Intel Atom Desktop Board. Thus, the user can check on the EVICS status or control the Intel Atom Desktop Board anywhere, anytime.

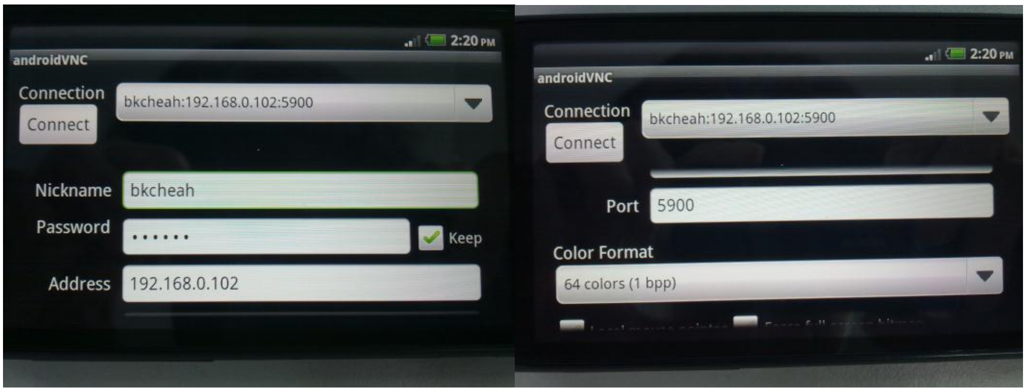

Figure 4.47 Connecting Using Android VNC

Similar to all of the software above, the required settings need to be entered in order to connect to the server/host. The only thing here that is different is the Port number has to be set 5900 because of the default settings in the server side.

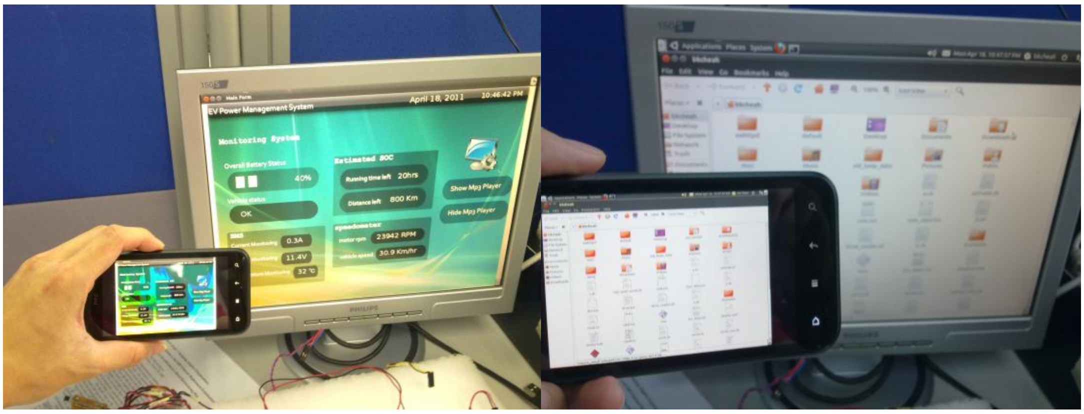

Figure 4.48 Android VNC Connections to EVICS GUI

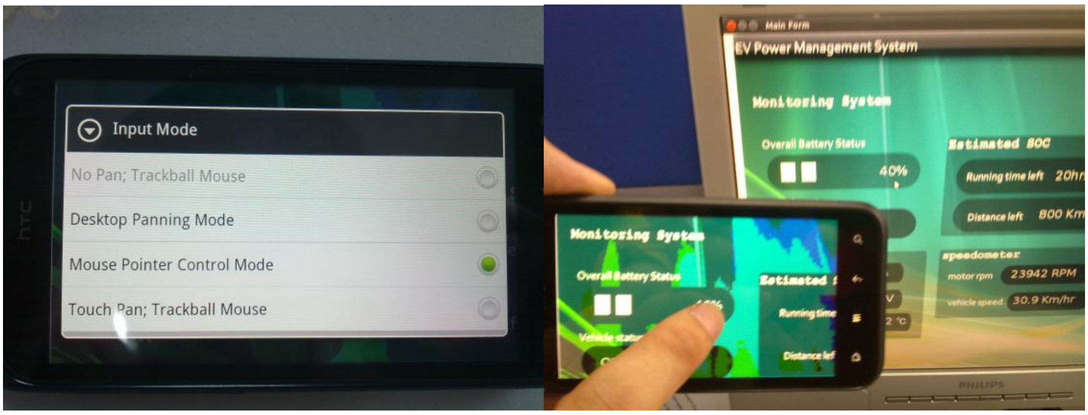

Figure 4.49 Able to control the mouse pointer of server side

4.7 Reverse Parking Sensor

Testing and troubleshooting have been done and there are a few advantages and disadvantages regarding the designed circuit.

The first circuit encounters a of not able to amplify the transmitted infrared signal at the receiver side. Thus, the range of reflected infrared wave from transmitter to obstacle and back to the receiver is extremely short.

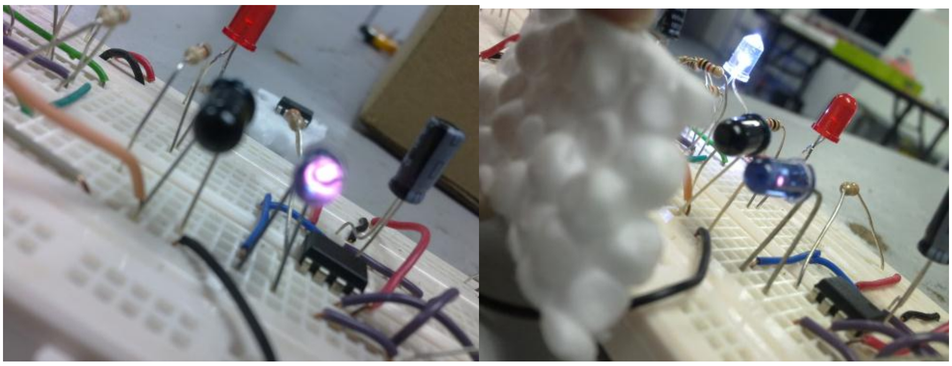

Figure 4.50 Transmitter Circuit Working Fine

As seen in figure 4.49, the transmitter circuit is working properly. However, the receiver circuit does not perform enough amplification of signal to boost the voltage across the other two LEDs, so that it will light up too.

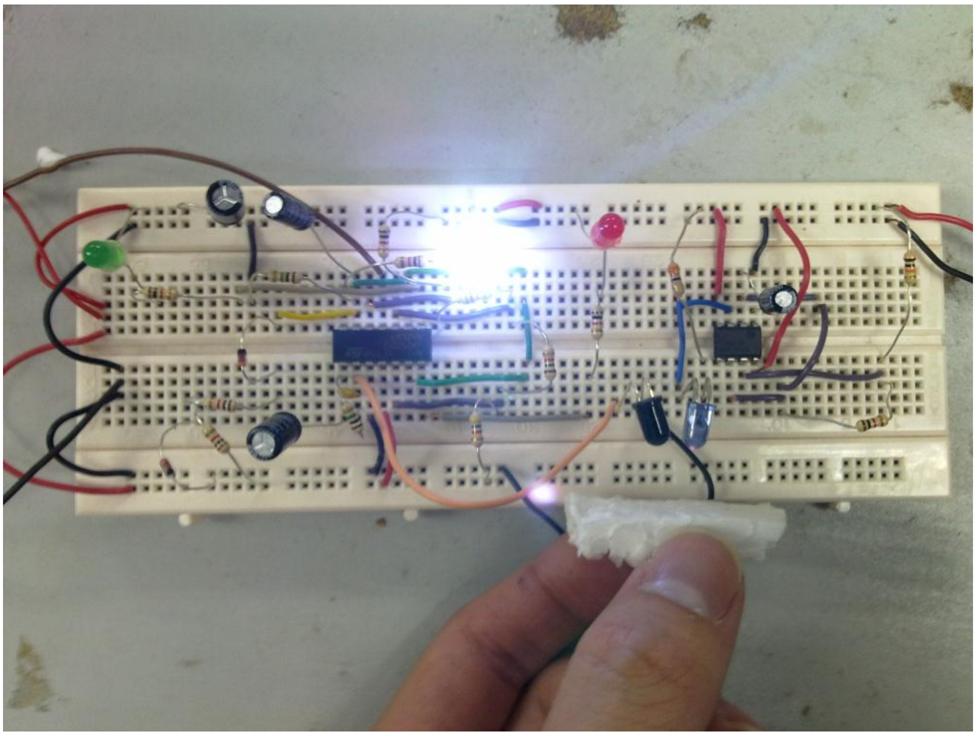

Figure 4.51 Circuit fail to amplify signal enough to light up the other two LEDs

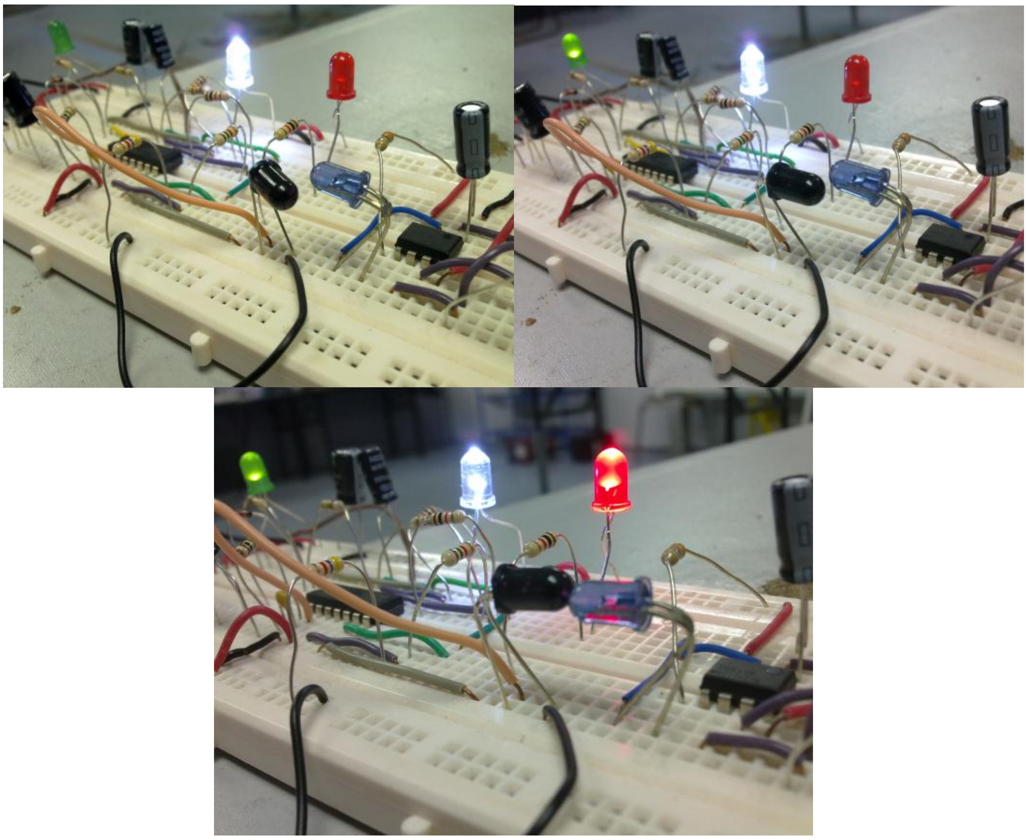

Figure 4.52 Reverse Parking Sensor

As shown in figure 4.51, the desired outcome only can be done when the transmitter and receiver are coupled as close as possible, thus proving the diagnostic that the amplification circuit at the input of the first op-amp of the LM324N (Quad Operational Amplifier).

Next, another problem encounter is that different manufacturer of the same chip which in this case is the LM324N. The LM324N for National Semiconductor has a ground as its –Vcc while the one from STMicroelectronics has a negative voltage as its Vcc. Hence, different manufacturers has different kind of pin configuration for the same chip and datasheet have to be read wisely in order to avoid any chip damage and time wasting.

On the other hand, the next circuit in which the output voltage from attenuated circuit is fed into the PIC faces a problem of not being able work under sunlight, hence making this designed circuit almost futile to be used as a reverse parking sensor circuit.

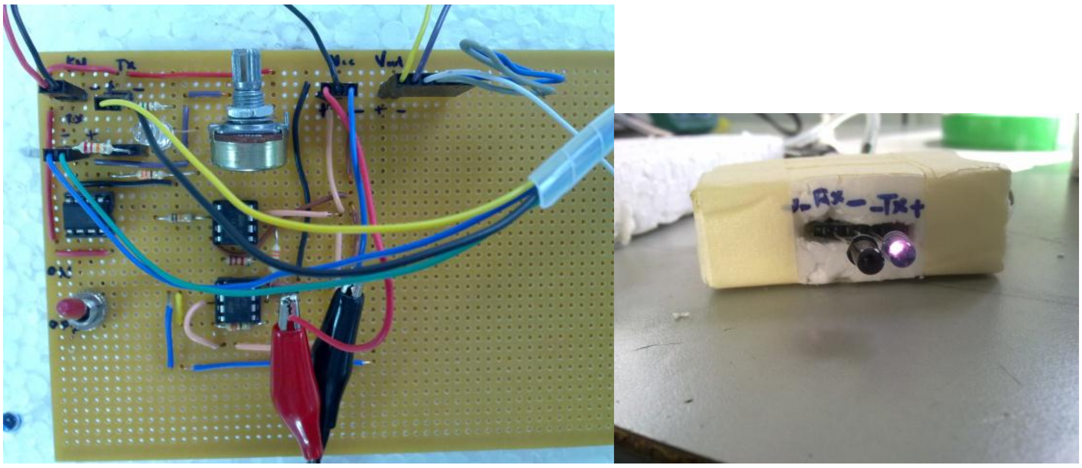

Figure 4.53 Outcome Circuit of Reverse Parking Sensor Circuit 2

Another problem also occurs as the circuit can't detect obstacles further than 17cm even if the circuit is run in the absence of sunlight and fluorescence light. However, this circuit at least can work better than the first one as it detected obstacles and output voltage to the attenuator with an attenuation of 0.2dB.

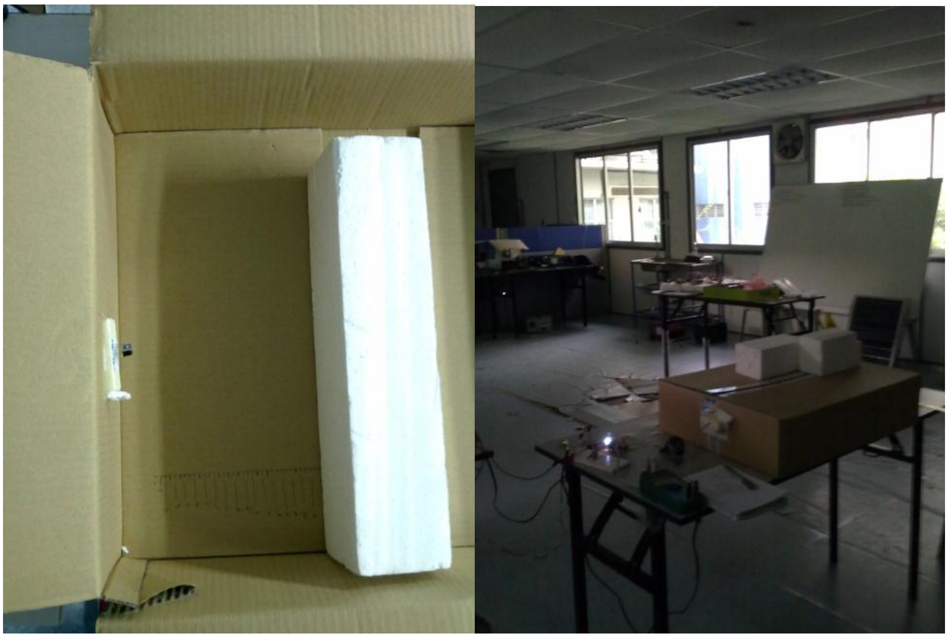

Figure 4.54 Circuit Testing in the dark

As can be seen in figure 4.53, the circuit is tested in a box with all of the lights turned off as the photodiode can detect infrared radiation from sunlight and lamps. By doing this, all of the external factors that affect the detection of the transmitting infrared signal by the photodiode are excluded. Then only the experiment can be taken place to determine the real range of detection of the reflected infrared signal for the infrared transmitter.

Table 4.7 Distance of Obstacle vs. Voltage Generated

Distance of Obstacle from Sensors, d (cm)	Voltage generated at the output of the op-amp attenuator, V_{OUT} (V)
0 - 13	0.745
13.5	0.745~0.744
14	0.744
14.5	0.743
15	0.740
15.5	0.587
16	0.381
16.5	0.274
17	0.255

CHAPTER 5

CONCLUSION AND RECOMMENDATIONS

5.1 Conclusion

In this report of the EVICS, the discussed modules are as follow:

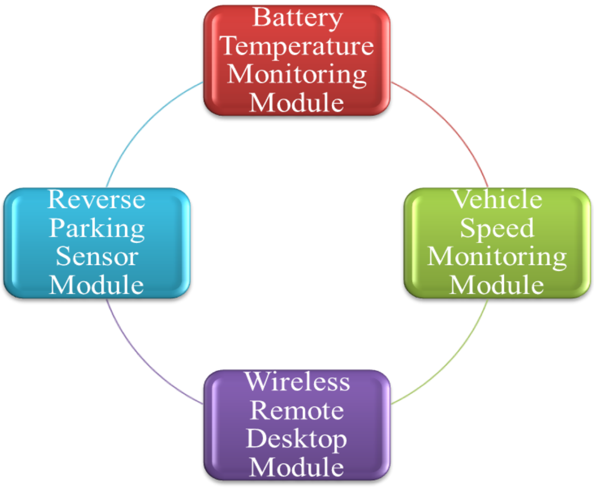

Figure 5.1 Overall Project Modules

The EVICS is a system that can be enhanced even further to optimize the usage of the Intel Atom Board and to fully monitor the entire electric vehicle operations. In this part of the project, it is unfortunate that the infrared reverse parking sensor module is unable to remain stable due to a lot of external factors, mainly because of the infrared radiation generated by the sun. Hence, this problem makes the designed circuit to be unsuitable for the usage of reverse parking sensor module. However, the good thing is that the circuit can be improved and also the other modules operating perfectly and it is able to interface with the Intel Atom Desktop Board.

From this project, there are a lot of valuable and priceless experience, such as being able to present paper publications in front of a crowd, visiting industrial sponsors, participate in competition and being able to work as team to achieve a common goal which is to pioneer an electric vehicle for UTAR.

Technical skills such as programming techniques and hardware troubleshooting are sharpened even more when doing this project. Analytical and troubleshooting skills in terms of software and hardware have so been improved in course of this project.

Besides learning technical skills and knowledge, project and time management are also vital parts in this project. It is inevitable to deny that the time management for this project is done mediocrely and hence this will serve as a reminder of time management and the ability to take on many tasks must be balanced.

5.2 Recommendations

5.2.1 Ultrasonic Reverse Parking Sensor

In place of the infrared reverse parking sensors, the ultrasonic sensor can be implemented for higher stability, stronger reflected signal, higher response time and most importantly not affected by external elements such as sun radiation in the case of infrared sensors.

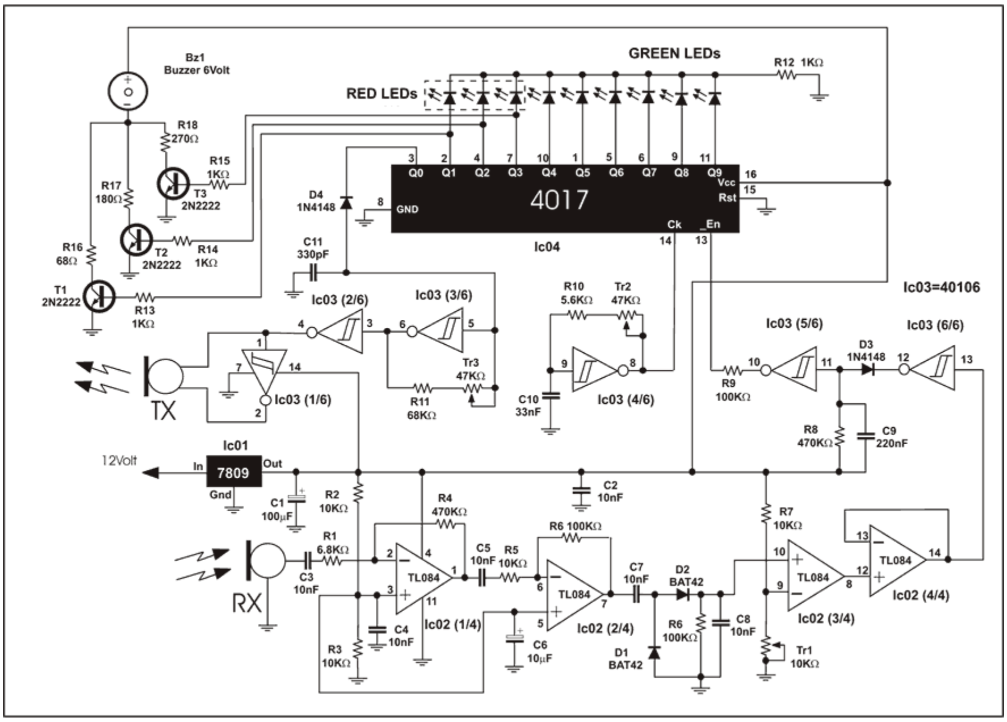

Figure 5.2 Ultrasonic Reverse Parking Sensors

5.2.2 Pulse-Width-Modulation on Cooling Fans

By using the timer function in the PIC18F microcontrollers, the speed of the fan can be adjusted automatically according to the detected temperature of the LM35. Let's say, if temperature is cool, the fans will turn slow. If the temperature is warm, the fans will turn at a medium speed. And, if the temperature is hot, consequently the fans will turn at a faster speed.

5.2.3 Digital 7 Segment Display or LCD Display of the RPM and km/h

By utilizing the displays mentioned in the title, it can replace the LEDs and show the users a more accurate value and a more presentable display unit.

5.2.4 More Sampling Using Higher Performance Microcontroller

The problem of using PIC18F2550 is that there are not much samples to be made to get a more continuous and analogue-like display for the users. Hence, a more powerful and stable microcontroller can be used to perform higher sampling rate and more sampling of the input parameters.

REFERENCES

Chong, W.S. (Ed.). (2009). *Battery car management system protocol*. Kuala Lumpur: Universiti Tunku Abdul Rahman

Comair Rotron., (n.d.). *Establishing cooling requirements: air flow vs pressure*. Retrieved from http://www.comairrotron.com/engineering_notes_02.asp

Discover. (2009, February). *Temperature effects on battery performance & life.* Retrieved from http://www.discover-energy.com/files/shared/Discover_temperature_effects_charging.pdf

EV1. *Revenge of the ev1.* Retrieved from http://www.ev1.org/

Gan, G.D., Gan, Y.H., Yoong, M.K., Vincent Cheah, B.K., Leong, C.K., Phuan, Z.Y. & Dr. Chew, K.W. (2010). Studies of electric motor for light-weight electric vehicle. *Proceedings of the Malaysian universities transportation research forum and conference: green transportation for future generation* (pp. 135-148). Putrajaya: Universiti Tenaga Nasional. ISBN 978-967-5770-08-1

Intel. (2009). *Intel desktop board d510mo*. Retrieved from http://www.intel.com/Products/Desktop/Motherboards/D510MO/D510MO-overview.htm

Korthof, D. (2005, July 6). *Zero emission vehicle (zev): no tailpipe emissions.* Retrieved from http://drivingthefuture.com/zevhist.htm

Leitman, S., & Brant, B. (2009). *Build Your Own Electric Vehicle* (2nd ed.). The McGraw-Hill. pg 54

Leitman, S., & Brant, B. (2009). *Build Your Own Electric Vehicle* (2nd ed.). The McGraw-Hill. Pg57

Mehrad, E., Yimin, G., Gay, S. E., & Ali, E. (2005). *Modern Electric, Hybrid Electric, and Fuel Vehicles*. Florida: CRC Press.

National Semiconductor. (2000, November). *Lm35 precision centigrade temperature sensors*. Retrieved from http://www.national.com/ds/LM/LM35.pdf

Norton, R.L. (2008). *Kinematics and dynamics of machinery (si units)*. Worcester, Massachusetts: McGraw Hill Higher Education

Phuan, Z. Y.,Gan, G.D., Gan, Y.H., Yoong, M.K., Vincent Cheah, B.K., Leong, C.K. & Dr. Chew, K.W. (2010). Design of battery pack for electric vehicle based on lithium-Ion technology. *Proceedings of the Malaysian universities transportation research forum and conference: green transportation for future generation* (pp. 127-134). Putrajaya: Universiti Tenaga Nasional. ISBN 978-967-5770-08-1.

Tan, Paul. (2009, December 10). *Proton and lg developing electric cars* [Web log message]. Retrieved from http://paultan.org/2009/12/10/proton-and-lg-developing-electric-cars

Tan, Paul. (2010, October 15). *Hybrid car tax exemption to be extended to end of 2011* [Web log message]. Retrieved from http://paultan.org/2010/10/15/hybrid-car-tax-exemption-to-be-extended-to-end-of-2011/

Telegraph, Motoring News. (2009, January 40). *Fastest electric car in the world unveiled.*
Retrieved from http://www.telegraph.co.uk/motoring/news/4396891/Fastest-electric-car-in-the-world-unveiled.html

Tesla, Motors. (2010). *Roadster features and specs.* Retrieved from http://www.teslamotors.com/roadster/specs

Thompson, M. *Electric vehicle battery information*. Retrieved from http://www.madkatz.com/ev/battery.html

APPENDICES

APPENDIX A

Conference Paper Publications:

- Malaysian Universities Transportation Research Forum and Conference, MUTRFC 2010:
  1. Studies of Electric Motor for Light-Weight Electric Vehicle
  2. Studies on Electric Car Chassis and Design Principle (Abstract only)
  3. Design of Battery Pack for Electric Vehicle Based on Lithium Ion Technology (Abstract only)
  4. Case Study on EV Controller and Battery Management System (Abstract only)

- IEEE STUDENT 2010 Conference:
  1. Studies of Regenerative Braking in Electric Vehicle
  2. Ultra Fast Charging System on Lithium Ion Battery

Studies of Electric Motors for Light-Weight Electric Vehicle

Gan Guo Dong [1]*, Gan Yu Han[2], Leong Chee Ken[3], Phuan Zheng Yi[4], Vincent Cheah Beng Keat[5], Yoong Mun Kiat[6], Dr. Chew Kuew Wai[7]

ABSTRACT:

In the development of the electric vehicle (EV), the parameters of electric motor, such as its torque, maximum speed, rotation per minute (rpm) and etc played an important role in determining the performance of a good EV. The electric motor is the heart of the EV which offers the driving element that moves the EV in various conditions. The electric motor comes in different shapes, driving methods, types and functions. However, the problems faced lies in the selection of the perfect electric motor for a four-seater, urban-bound vehicle that can muscle out the sufficient torque and deliver wide range of speed. Also, maintaining high efficiency in the long run to overcome the dominance of the combustion engine. The solutions are to do engineering research in the field of electric motor. Various experiments are performed to determine the motor parameters. In this paper, the arguments between the usage of DC motor and AC motor have been briefly discussed. The suitability of DC motor for light weight EV have been investigated and discussed.

Keywords: DC/AC motor, torque, maximum speed, rotation per minute (rpm), light weight EV.

1 Student, Universiti Tunku Abdul Rahman, Setapak, 53100 Kuala Lumpur, MALAYSIA
2 Student, Universiti Tunku Abdul Rahman, Setapak, 53100 Kuala Lumpur, MALAYSIA
[3] Student, Universiti Tunku Abdul Rahman, Setapak, 53100 Kuala Lumpur, MALAYSIA
[4] Student, Universiti Tunku Abdul Rahman, Setapak, 53100 Kuala Lumpur, MALAYSIA
[5] Student, Universiti Tunku Abdul Rahman, Setapak, 53100 Kuala Lumpur, MALAYSIA
[6] Student, Universiti Tunku Abdul Rahman, Setapak, 53100 Kuala Lumpur, MALAYSIA
[7] Assistant Professor, Universiti Tunku Abdul Rahman, Setapak, 53100 Kuala Lumpur, MALAYSIA

**Correspondence Author: Gan Guo Dong, Universiti Tunku Abdul Rahman, Malaysia. Tel: +60122068462. Email: kenny_ggd@hotmail.com*

INTRODUCTION

According to a new study from the Centre for Entrepreneurship and Technology at University of California, Berkeley, electric cars could comprise 64-86% of US light vehicle sales by 2030[3]. As seen in Fig.4, the study shows rapid adoption for electric vehicles with switchable batteries, quantifies how the electrification of the U.S. transportation system will decrease America's dependence on foreign oil, increase employment, and reduce the environmental impact of transportation emissions. From this study, the electric vehicle and the development of high performance electric motor is a force to be reckoned with. Thus, development of the electric vehicle industry depends on the heart of every electric vehicle (EV) which is the drive train or also known as electric propulsion system (EPS) and this EPS greatly affects the performance of the EV. EPS plays a role in transferring energies in either direction as required, under control of the driver at all times. Due to diversity of EVs, the design of electric motor and propulsion system has to be carried out at system level, which should take EV types, performance, configuration and electric motor parameter into consideration. And, among the EPS-system, it is very important to select the proper type of motor with suitable rating because it is the crucial step in designing the overall system.

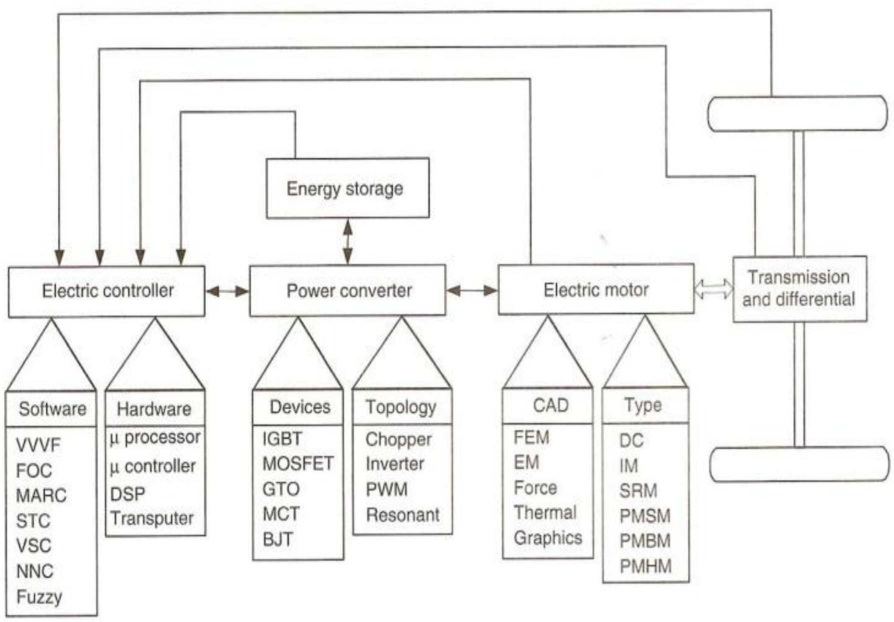

Figure 1. Functional Block Diagram of a Typical Electric Propulsion System. [2]

For the electric motor, many criteria such as efficiency, cost, reliability, power density, maturity of technology and controllability must be taken into consideration. Usually, electric cars are driven by large electric motors usually rated between 3.5 and 28 horsepower. For those accustomed to gas engines, this may not seem like much power, but the rating systems used for gas engines and electric motors are so different that the numbering system is almost meaningless [6]. Gas engines are rated at their peak hp, electric motors are rated at their continuous hp. The peak hp of an electric motor is usually 8 to 10 times its continuous rating. Electric vehicle drive motors can be divided into two basic groups, DC or direct current motors, and AC or alternating current motors.

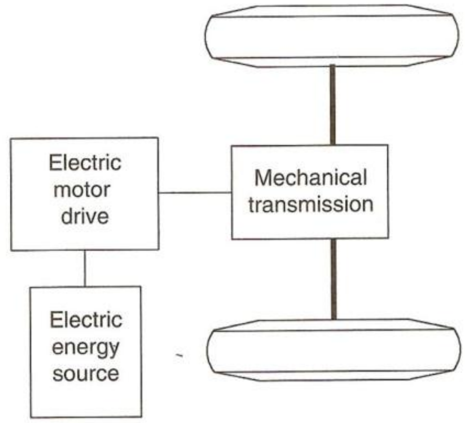

Figure 2. Primary EV Power Train [2]

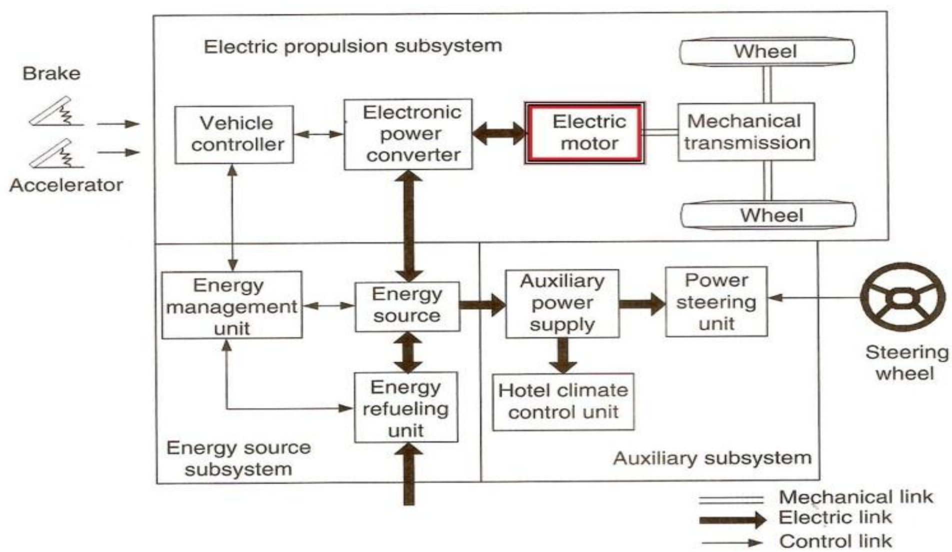

Figure 3. Conceptual Illustration of General EV Configuration [2]

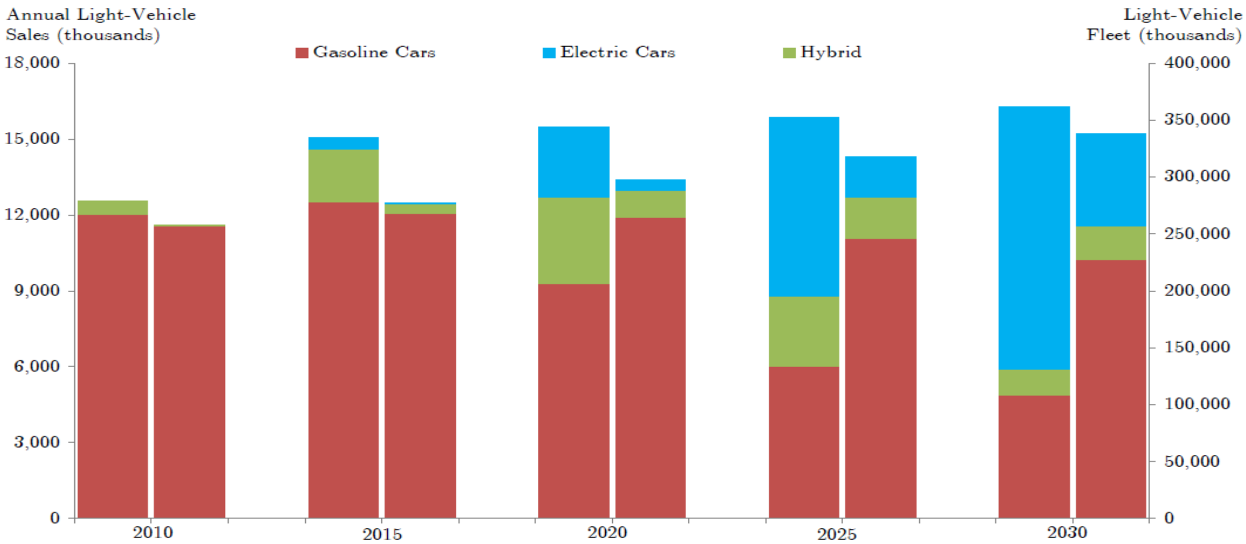

Figure 4. US Light Vehicle Sales and Fleet Composition under Baseline Scenario

LITERATURE REVIEW

EV Demands and Design Outline of EPS

TABLE I

EV'S BASIC REQUIREMENT ON ELECTRIC DRIVE TRAIN AND THEIR IMPLICATIONS ON PERFORMANCE

Requirement	Implications
High torque at low speeds and constant power at high speed.	Driving performance.
Continuous and smooth drive control.	Comfort.
High efficiency, regenerative braking.	Longer driving range.
High specific power and specific torque.	Overall efficiency and consistency.
Maintenance free.	Safety and maintenance cost.
Reasonable Cost.	Price and Budget.

With this, a description of motor parameters and control strategy can be discussed and also to identify the parameters according to the performance requirement. Lastly, optimization can be made to improve the drive train and efficiency.

Characteristics of Electric Motor for EV

In EV, the vehicle performance is completely determined by the torque-speed characteristic of the motor which is much closer to the ideal as compared to ICE (Internal Combustion Engine). In order to meet EV requirement, operation entirely in constant power is needed. However, operation fully in constant power may be impossible for any practical vehicle. For EVs, the desired output characteristics of electric motor drives are illustrated in Fig.5. It can be observed that the electric motor is expected to be able to produce a high torque at low speed for starting and acceleration because as it increase to the base speed, the voltage increases to its rated voltage while the flux remain constant. Also, electric motor generates a high power at high speed for cruising due to the fact that beyond the base speed, the voltage remains constant and the flux is weakened. The result is constant output power while the torque declines hyperbolically with speed. Thus, a single-gear transmission will be enough for a light-weight EV [2]. In Fig.5, as we know from above, the electric motor can generate constant rated torque up to its base speed. At this speed, the motor reaches its rated power limit. The operation beyond the base speed up to the maximum speed is limited to the constant power region. This region of the constant power operation depends primarily on the particular motor type and its control strategy.

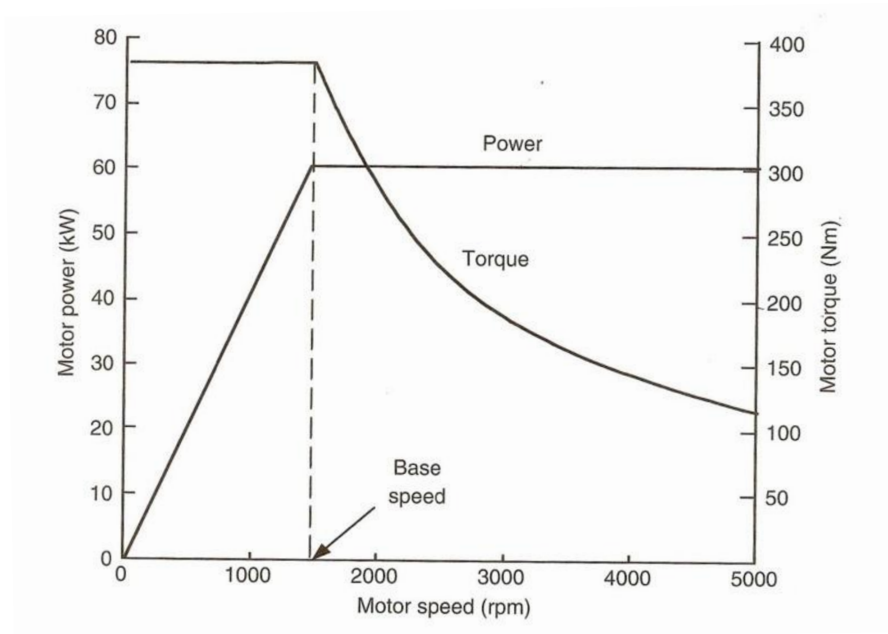

Figure 5. Typical Performance Characteristics of Electric Motor for Traction. [2]

From the output characteristics of electric motor for EVs, the following valuable results can be concluded as follows: a) the power requirement (rated power) for acceleration performance (acceleration time and acceleration distance) decreases as constant power region ratio increases. b) Conversely, the torque requirement (rated torque) for acceleration increases as constant power region ratio increases. This results in a larger motor size and volume. c) The maximum speed of electric motor has a pronounced effect on the required torque of the motor. Low speed motors with the extended constant power speed range have a much higher rated shaft torque. Consequently, they need more iron and copper to support this higher flux and torque. d) As motor power decreases (due to extending the range of constant power operation), the required torque is increasing. Therefore, although the converter power requirement (hence the converter cost) will decrease when increasing the constant power range, the motor size, volume, and cost will increase. e) Increasing the maximum speed of the motor can reduce the motor size by allowing gearing to increase shaft torque. However, the motor maximum speed cannot be increased indefinitely without incurring more cost and transmission requirements. Thus, there is multitude of system level conflicts when extending the constant power range [4].

Next, it is the tractive effort of the electric motor is discussed. The tractive effort which is also known as tractive force is described as the pulling force exerted by a vehicle. The tractive effort generated by a traction motor on driven wheels and vehicle velocity are expressed as:

$$F_t = \frac{T_m \, i_g i_o \eta}{r_d} \; (N) \qquad (1)$$

And

$$V = \frac{\pi \, N_m \, r_d}{30 \, i_g \, i_o} \; (m/s) \qquad (2)$$

where T_m and N_m are respectively the motor torque output and speed (rpm), i_g is the gear ratio of transmission, i_o is the gear ratio of final drive, η is the efficiency of the whole driveline from the motor to the driven wheels and r_d is the radius of the drive wheels [2].

The efficiency of an electric motor varies with the operating conditions on the speed-torque curve as shown in Fig.6 below where the most efficient operating area exist. Thus, the EPS design should be at least be as close as possible to the area with the most efficiency [2].

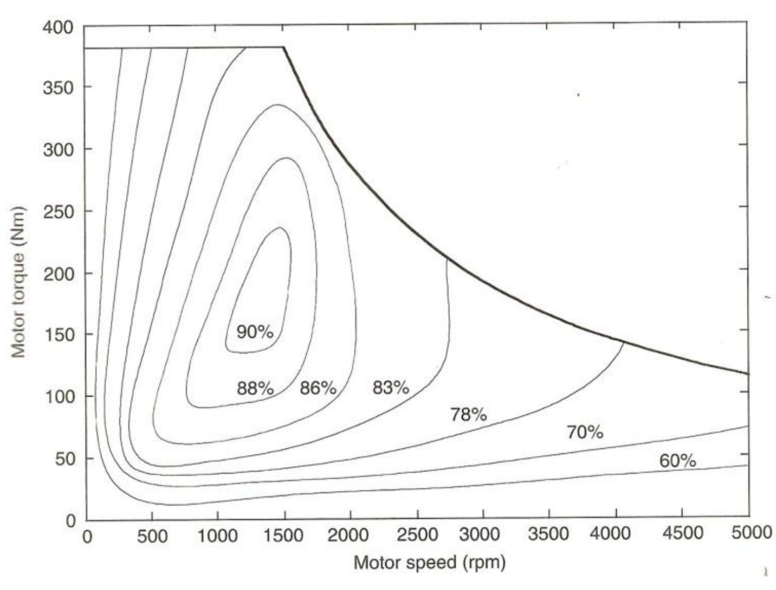

Figure 6. Typical Electric Motor Efficiency Characteristics[2]

AC Motor and DC Motor

In this section of the paper, the basic principles of the many types of electric motor are discussed. Furthermore, the advantages and disadvantages of each type of the AC and DC electric motors are further discussed.

1) DC Motor

DC motors have a long history in EV use. The most commonly used version is what is known as a series-wound motor, which means the armature and field windings are wired in series. Other designs include shunt-wound, compound-wound, and permanent magnet motors. One of the advantages of using the DC motor is that the design concept of the DC motor is easy to understand due to the maturity of this technology in electric vehicle industry [7]. Thus, making it easy for us to troubleshoot the problems related to DC motors. Besides that, DC motors provide simple and cheaper drive design that is also easier to manufacture. Varying the speed can be meaning a variation in a large enough potentiometer. Whether it is using Pulse Width Modulation (PWM) or Silicon Controlled Rectifier (SCR), the speed and torque can be easily controlled. The other good thing about the DC motor is that it has a direct and easy way in controlling speed and torque [8]. Speed is proportional to armature voltage of the motor while the torque is proportional to the supplied current. However, DC motors have their drawbacks which include high maintenance due to the commutator and brushes which will wear in time and causes dust from brushes to accumulate and soon deteriorate the motor efficiency.

2) AC Motor

At the present time AC motors are most commonly found in commercially built EVs, as they require more sophisticated and complex control systems than DC motors. AC control systems on the horizon and will likely become available soon in the future as it is good prospect to venture in [8]. One of the advantages of the AC motor is its reliable operation. The design of an AC motor requires no brushes and commutators which mean that it has low maintenance. Thus, no brushes to be replaced and no dust accumulation form the brushes. Owing to the fact that the there are no commutators and brushes, there will be no frictional losses and thus the overall efficiency is higher than the DC motor. Even though the AC motor technology in electric vehicle is still growing, the AC motor has a distinctive advantage which is the regenerative effect which can be used to recharge the battery of EV when the car slows down [8]. However, there are also disadvantages to the AC motor. One of them is the cost of the motor and its driver circuit. The speed control and torque control of the AC motor is expensive due to the complexity of the circuit. Converter circuits are needed to convert the battery's DC-to-AC and also single-phase to three-phase. The standard AC motors can't be operated in speeds less than about 1/3 of base speed due to thermal considerations [9].

Comparative Study on the Specific Type of Electric Motor for EV

In this section, there will be further comparisons between electric motors and their advantages and drawbacks of implementing them in the EV.

1) Brushed DC Motor

The brushed series DC motor is the most affordable and readily available current production motor. Brushed DC motors are good in achieving high torque at low speed and their torque–speed characteristics suitable for the high starting torque situation and high load conditions. And, these motors are easy to control their speed through variation of voltage levels. The characteristic of series, shunt and compound motors are shown in Fig.7. Series motors are good in applications requiring high starting torque and heavy torque overload. Shunt motors have better controllability than series motors. Shunt motors also known as separately excited motors are suited for field weakened operation, due to its decoupled torque and flux control characteristics. Moreover, a range of extended constant power operation is obtained by separate field weakening [4].

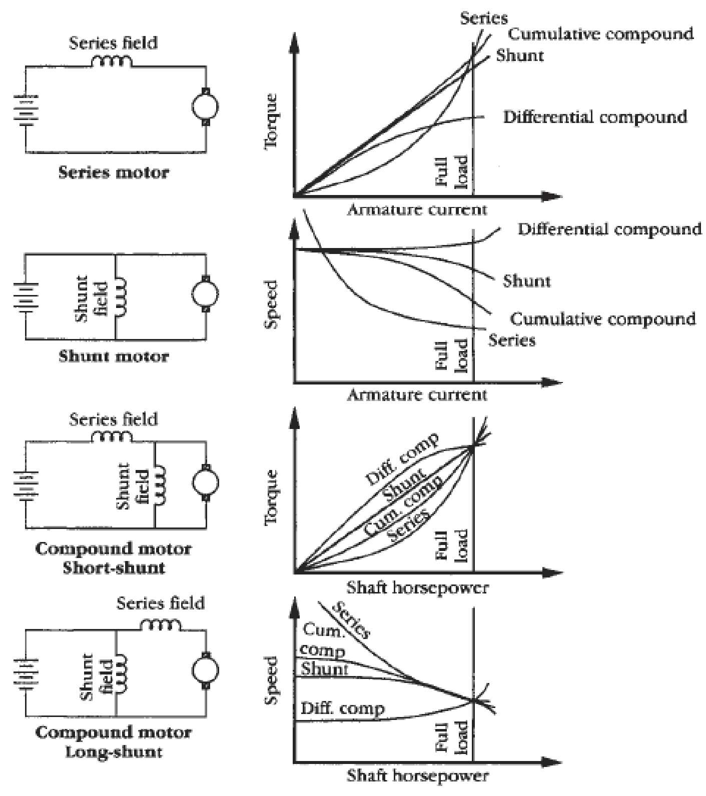

Figure 7. Characteristics of DC Motor Types

Moreover, the speed characteristics of DC motors can be observed in the Fig. 8 below.

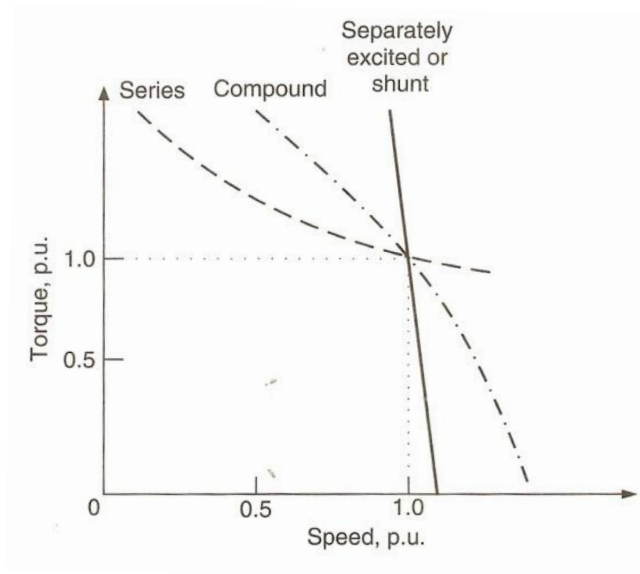

Figure 8. Speed Characteristics of DC motors[2]

On the other hand, permanent magnet motors are very efficient, but only in a very narrow rpm band, and quickly lose their efficiency in the varying speeds of normal driving. Permanent magnet motors resemble the shunt motor in their torque, speed, reversing, and regenerative braking characteristics. However, the permanent magnet motors have starting torques several times that of shunt motors, and their speed versus load characteristics are more linear and easier to predict [4] [8].

2) Brushless DC Motor (BLDC)

In a BLDC, the brush-system/commutator assembly is replaced by an intelligent electronic controller and making the BLDC the most efficient of all electric motor. The controller performs the same power-distribution found in a brushed DC-motor, only without using a commutator/brush system. The controller may contain a bank of MOSFET devices to drive high-current DC power, and a microcontroller to precisely orchestrate the rapid-changing current-timings. Because the controller must follow the rotor, the controller needs some means of determining the rotor's orientation/position (relative to the stator coils.) Some designs use Hall Effect sensors to directly measure the rotor's position. Others measure the back EMF in the undriven coils to infer the rotor position, eliminating the need for separate Hall Effect sensors, and therefore are often called "sensorless" controllers.

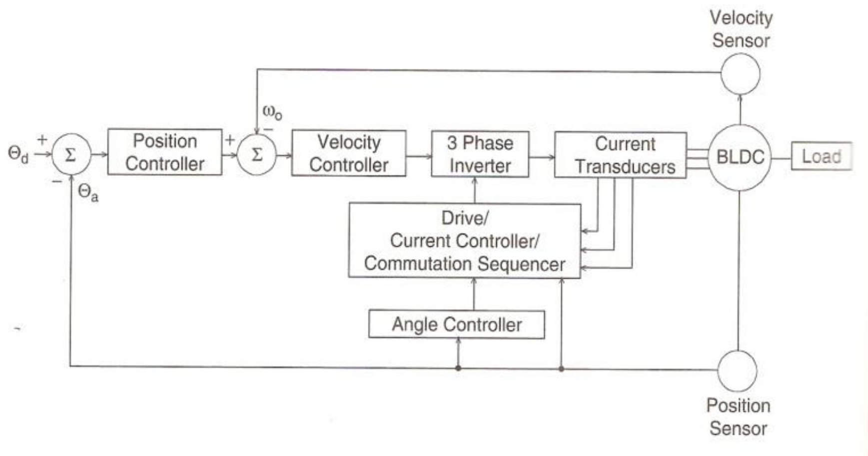

Figure 9. Basic Block Diagram of a Classical Speed and Position Control for BLDC [1]

BLDC motors can be constructed in two different physical configurations: In the 'conventional' configuration, the permanent magnets are mounted on the spinning armature (rotor) and the stator coils surround the rotor. In the 'outrunner' configuration, the radial relationship between the coils and magnets are reversed; the stator coils form the center (core) of the motor, while the permanent magnets spin on an overhanging rotor which surrounds the core. In all BLDC motors, the stator-coils are stationary and thus making current circulation only in the stator and not the rotor, making the rotor to not heat up. This will further ease the cooling design for the BLDC as the stator in conventional configuration is on the periphery of the motor and it will be easier to cool when the stator heats up. Improvement of efficiency can be done using the inverted rotor topology/"outrunner" (where the rotor rotates on the outside of the stator) has a larger magnetic field. The additional radius provides higher torque and power density and leads to better efficiency.

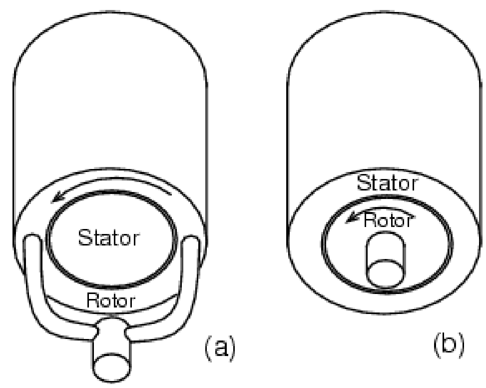

Figure 10. (a) outrunner configuration. (b) conventional configuration

3) AC Induction Motor (IM)

Squirrel cage IM have been the most suitable candidate due to their reliability, robustness, almost maintenance-free characteristics, low manufacturing cost and the ability to work in various conditions. The IMs are the only AC motor that has the most mature technology in EV industry and having several features such as lightweight, small volume, low maintenance, high reliability and efficiency. Besides, the IM offers a higher efficiency in the regenerative effect.

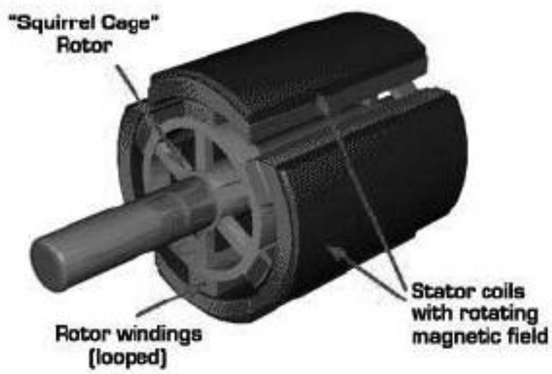

Figure 11. AC Squirrel Cage IM [8]

The absence of brush friction allows the motors to have higher maximum speed, and the higher rating of speed enable these motors to develop high output. Thus, IM does not have so much of the speed limitation as in the dc motors. Frequency of the voltage is varied to offer the speed control of the IM. Extended speed range operation beyond base speed is accomplished by flux weakening, once the motor has reached its rated power capability. Field orientation control (FOC) of IM can decouple its torque control from field control. This allows the motor to behave in the same manner as a separately excited dc motor [4] [10]. A properly designed IM, with field oriented control can achieve field weakened range of 3-5 times the base speed [4]. However, the controllers of IMs are at higher cost than the ones of DC motors. Moreover, the breakdown torque limits its extended constant-power operation. At the critical speed, the breakdown torque is reached and any attempt to operate the motor at the maximum current beyond this speed will stall the motor. Although FOC may extend constant power operation, it results in an increased breakdown torque thereby resulting in an over-sizing of the motor. In addition, efficiency at a high speed range may suffer in addition to the fact that its efficiency is lower than that of permanent magnetic (PM) motors and switched reluctance motors (SRMs) due to the absence of rotor winding and rotor copper losses [4].

4) Switched Reluctance Motor (SRM)

The SRM is an interesting candidate in the EV industry due to the high performance, low cost, rugged structure, fault tolerant, outstanding torque-speed characteristics and reliable converter topology. The design of SRM is similar as the stepper motor. Also, SRM drives can run in extremely long constant power range and the torque-speed characteristic matches with the needs of the EV [4]. SRM has high starting torque and high torque-inertia ratio. The simplicity of the design owes to the rotor without any windings, magnets, commutators or brushes. The fault tolerance of SRM is also extremely good. Owing to its simple construction and low rotor inertia, SRM has very rapid acceleration and extremely high speed operation. And, SRM is suitable for single gear transmission in EV propulsion due to its wide speed range operation. One important feature of the SRM is the different number of poles on the stator and the rotor. The windings of diametrically opposite stator poles are connected in a series to form the electric phases of the motor. For each electric phase, a power electronic circuit with one or two electronic switches is necessary for the control of unidirectional current flowing during appropriate intervals for the torque production. Exciting the stator coils in sequence produces the torque in the motor. This requires an inverter (i.e. a set of low cost electronic switches such MOSFETs or IGBTs) that drives the motor from the battery's DC voltage supply [11].

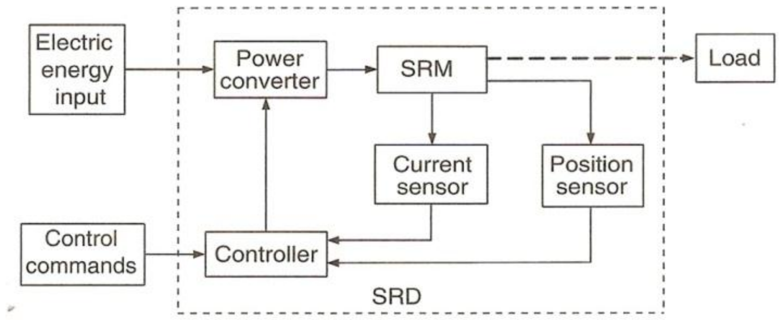

Figure 12. SRM Drive System [2]

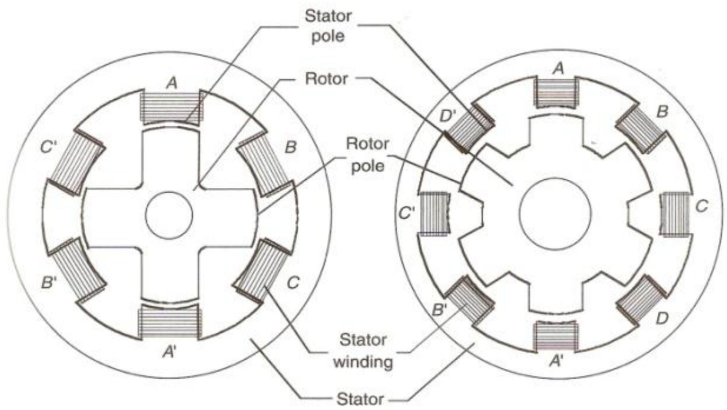

Figure 13. Cross Section of Common SRM [2]

5) Comparisons between Motors

DC motor will continue to be used in EVs because DC motor drives are available at the lowest cost. From the point of view of efficiency, BLDC motors are the best choice as BLDCs have several advantages over brushed DC-motors, including higher reliability, longer lifetime (no brush erosion), elimination of ionizing sparks from the commutator, and overall reduction of electromagnetic interference (EMI.). However, among the four types of motors discussed, the lightest of all is the SRM which is a bonus point for EVs. If the choice of motor for EVs is determined by weight, efficiency and cost, it is clear that SRM is the victor. Besides of the efficiency, weight and cost, SRM also have the upper hand in cooling, maximum speed, fault tolerance, and reliability. However, of the four major electric EV motors, BLDC motor has the highest torque density, but if compared to SRM which have better speed-torque characteristic for traction application. Even though the BLDC has a higher efficiency than SRM, taking into that the SRM's fault tolerance plays a big role in EV. SRM are naturally fault tolerant. As for IM and BLDC motors, their electromechanical energy conversion is interdependent upon proper excitation. While, SRM drives have discrete phase windings and thus phase windings are independent of each other. Therefore, if one phase in the SRM fails the SRM drive can still operate at a lower performance until repair work is done on it. Additionally, the converter topology used for an SRM protects it from serious electrical fault of shoot-through, which is not eliminated fully in IM and PM BLDC motor drives [4].

METHODOLOGY

Market Research and Case Studies

Investigation and research is done on all of electric vehicles that are available in the current market and also the up and rising technologies. The main objective is to observe and explore on the various type of electric motor that are used in the drive train of the electric vehicle. Furthermore, determine the value of parameters, such as torque, rpm, input power and the nominal requirement for voltage and current.

Various Types of Motor Testing

- Measurement of Winding Resistance
- Magnetization Characteristics
- No Load Test
- Full Load Test

These tests are to determine the profile of the motor and the load capacity of the motor.

MATLAB Simulation

The simulation will determine the characteristic of the motor in the drive train and the compatibility of it in the EV's system itself.

RESULT ANALYSIS

Market Research and Case Studies

1998 Peugeot Partner

Motor Specifications:

- 28kW DC separate excited Motor
- Motor Torque: 180Nm
- Motor Speed: 6500rpm

Figure 14. Peugeot Partner

MATLAB Simulation

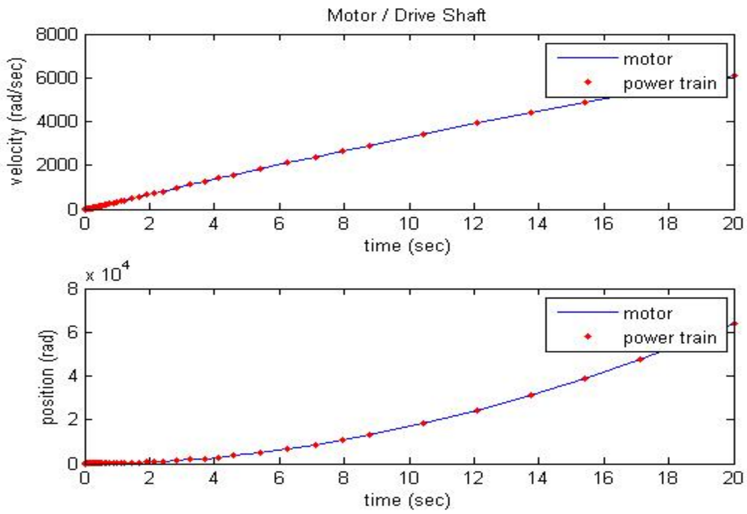

Figure 15. An Example of the Resulted Simulation of the EV Drive Train for MATLAB

CONCLUSION

As the comparisons stated, the DC motors seems to be more mature in the industry of electric vehicles and less expensive in constructing the prototype itself. AC motor driver circuit is very complicated and the components are expensive since the technology is not yet mature. DC motor driver offers a more straightforward approach to speed and torque control while BLDCs are maturing to replace DC brushed motors to overcome the problems of high maintenance. However, even though AC motor controller technology is not yet mature in the electric vehicle industry, thus making the cost very high. There are several car companies are pushing their way and creating their own path in developing this technology as the AC motor are still can be improved further and someday overtake DC motors in the EV industry. However, the SRM which is a very powerful candidate in the EV motor struggle proves to have the upper hand in nearly every category of the comparisons:

a) Lower weight than BLDC and IM.
b) Lower cost than BLDC and IM due to the absence of winding and rare-earth permanent magnets.
c) Fault tolerance and safety.
d) Higher reliability and efficiency than brushed-DC motor.

The only losing points of SRM are the cost of manufacturing is lower than brushed DC motors, the efficiency of BLDC is higher than SRM and the lacking of maturity of SRM in the EV industry as most car companies opt for BLDC and IM while EV enthusiasts favour the low cost brushed DC motor.

REFERENCES

[1] Handbook of Automotive Power Electronics and Motor Drives, Edited by Ali Emadi, CRC Press, Taylor & Francis Group, 2005.

[2] Ehsani, Mehrdad. (2005). Modern electric, hybrid electric, and fuel cell vehicles. CRC.

[3] Becker, T. A., & Sidhu, I. (2009). Electric vehicle in the us - a new model with forecast to 2030.

[4] Xue, X. D., Cheng, K. W. E., & Cheung, N. C. (2008). Selection of electric motor drives for electric vehicles.

[5] Cheng, Y., & Duan, F. The Design principle of electric motors and drive systems for electric vehicles. 802-805.

[6] Halstead, J. (2005, October 25). *Electric car motors*. Retrieved from http://www.evconvert.com/eve/electric-car-motors

[7] Rippel, W. (2007, January 9). Induction versus dc brushless motors. Retrieved from http://www.teslamotors.com/blog4/?p=45

[8] Larminie, J., & Lowry, J. (2003). *electric vehicle technology explained*. John Wiley & Sons.

[9] Leitman, S., & Brant, B. (2009). *Build your own electric vehicle*. McGraw Hill.

[10] Boley, B. L. (1996). *Overview of motor types tutorial*. Retrieved from http://www.oddparts.com/acsi/motortut.htm

[11] Ehsani, M., Gao, Y., & Gay, S. (2003). Characterization of electric motor drives for traction applications. 891-896.

[12] Cho, C. Peter, & Johnson, Ralph H. Electric motors in vehicle applications. 193-198.

[13] Hashemnia, N., & Asaei, B. (2008). Comparative study of using different electric motors in the electric vehicles.

[14] Keoun, Bradley C. Designing an electric vehicle conversion. 303 - 308.

[15] Buja, G. (2008). Light electric vehicles.

[16] Honda, Y., Nakamura, T., Higaki, T., & Takeda, Y. (1997). Motor design considerations and test results of an interior permanent magnet synchronous motor for electric vehicles. 75-82.

MUTRFC 2010
Malaysian Universities Transportation Research Forum and Conference
21th December 2010
Universiti Tenaga Nasional, Putrajaya

A STUDY ON ELECTRIC CAR CHASSIS AND DESIGN PRINCIPLE

Gan Yu Han[1]*, Gan Guo Dong[2], Leong Chee Ken [3], Phuan Zheng Yi[4], Vincent Cheah Beng Keat[5], Yoong Mun Kiat[6], Dr. Chew Kuew Wai[7]

ABSTRACT:

In this project, the placement of components in an electric car (EV) and the system chassis design will be studied and explained. The scope covered is divided into 5 main portions:

Part 1: Placement of important components such as Lithium-ion polymer batteries, DC brushless motor, controller and driver circuits strategically in the chassis of an electric car.

Part 2: Study to maintain balance, aerodynamic and spacing optimization in the design of an electric car.

Part 3: Important criteria to be considered in the positioning of batteries, motor and controller in the chassis such as the size, weight, type of components used, specification requirements, etc.

Part 4: Balancing the front and back weight ratio of the car to ensure stability and safety of the driver and passengers.

Part 5: Design of good air ventilation and heat dissipation to prolong the lifetime of expensive equipments such as batteries and provide safety to the users.

Commercially available electric vehicles and prototypes still do not have a defined standard of component placements unlike engine vehicles. Therefore, these studies will provide a fundamental platform for further studies on commercially available electric cars in the market.

Keywords: balance, stability, safety, heat dissipation, spacing optimization

DESIGN OF BATTERY PACK FOR ELECTRIC VEHICLE BASED ON LITHIUM-ION TECHNOLOGY

Z.Y Phuan*[1], G.D Gan[2], C.K Leong[3], B.K Cheah[4], M.K Yoong[5], Y.H Gan[6] and K.W Chew[7]

ABSTRACT:

In these modern days, electric vehicles are well known for its efficiency, it would be a cost saving choice compared to the ICE car, due to its advantages such as silent engine, zero emission which are totally green to the environment. However the selection of a suitable battery type such as lead acid, NiMH, Lithium ion in the long run plays a very important role in the construction or design of the electric vehicle due to its function and also the physical aspects. In terms of the functionality, the vehicle must be able to provide sufficient energy to allow the car to move or accelerate and at the same time, having a long lifespan or constant power supplied to the vehicle. Taking this into consideration, lithium ion battery have been selected as the main power source when designing an electric car, this can be viewed from the characteristics of a lithium ion battery such as fast charging rate, light weight, high capacity and long charge-discharge cycle, etc. Hence the design of battery pack using lithium ion battery inclusive of its compartment design, ventilation and the monitoring system will be discussed in this paper.

*Keywords **:** Lithium Ion, fast charging rate, charge-discharge cycle*

CASE STUDY ON EV CONTROLLER AND BATTERY MANAGEMENT SYSTEM

Vincent Cheah Beng Keat1*, Gan Yu Han2, Leong Chee Ken 3, Phuan Zheng Yi4, Gan Guo Dong5, Yoong Mun Kiat6, Dr. Chew Kuew Wai7

ABSTRACT:

The application for the designed Pulse Width Modulation Motor Control circuit including Battery Management System is in the field of battery powered cars. This new move towards renewable energy and environmental friendliness is definitely a goal worth aiming for as the Earth's natural resources continue to diminish. Battery powered vehicles are indeed a very important component in the future of electrical and electronics engineering in this nation. This is evident considering Proton's latest offering, the Proton Saga EV Green Propulsion, and is Malaysia's first very electric vehicle. It is hoped that through the execution of this assignment, we as engineering students may someday contribute towards the technological development in the field of electronics of our very own country, Malaysia.

In an Electrical Vehicle (EV) design, the power management system and controller plays an important role as a 'brain' of the EV, to ensure the car can run smoothly and in order. The main functions of a controller is basically to control the main contactor and kill switch contactor, incorporating appropriate safety measures and interlocks, control the reversing contactor, incorporating appropriate safety measures and interlocks, power the vacuum pump in the EV braking.

STU10032- Studies of Regenerative Braking In Electric Vehicle

*M.K Yoong** , G.D Gan, *Y.H Gan, C.K.Leong, Z.Y Phuan, B.K Cheah. K. W Chew*

Faculty of Engineering and Science, University Tunku Abdul Rahman, Setapak, Kuala Lumpur, 53100
*Email: yoongmunkiat@hotmail.com

Abstract -Generally in electric and gasoline cars, the braking system is based on the hydraulic braking technology. However, this traditional braking methodology causes a lot of energy wastage since it produces unwanted heat during braking. Hence, the invention of regenerative braking in electric car nowadays is getting popular due to its technology that helps in saving energy and with higher efficiency to boost up the acceleration of the car. In regenerative braking, the motor act as a generator. It transfers the energy generated which is in the form of kinetic energy to restore the battery or capacitor energy in order to prolong the range or driving distance. Meanwhile, in regenerative braking system, the brake controller monitors the speed of the wheels and calculates the torque required hence the excessive energy from the rotational force can be converted into the electricity when the motor acts like generator, the generated electricity will be fed back into the batteries. The reasons of choosing regenerative braking is because of its advantages over conventional break such as energy conservation, wear reduction, fuel consumption, more efficient in braking, and it meet up the concept “go green” as it produce zero carbon dioxide. Besides ,there are more advance technology now implementing in regenerative braking to improve the car efficiency such as using flywheel to save more energy thru the wheel and ultracapacitor with DC-DC converter to boost up the car acceleration and provide better performance for regenerative system for the electric car. In this paper, the working principle and some braking controller for the regenerative braking have been studied to promote the efficiency and to realize the energy saving in the electric vehicle.

Keywords: regenerative braking, generator, brake controller, energy conservation, flywheel, ultra capacitor.

I. INTRODUCTION

THE invention of EV is a miracle since it produces “ZERO EMMISION” to the air which means there is no toxic gasses release from the car that cause the ozone layer in our earth polluted. Nowadays, the population of EV starts to increase according to the demand in the market. Besides, the enforcement of the government toward the production of electric car is getting more serious. Every step is taken to save the earth from the excessive air pollution and the recession on the natural resources such as oils and natural gasses in the earth. In twentieth century, vehicular technology such as control technology and integrative technology have been aggressively developed. Somehow, the limitation of driving range still becomes an obstacle for the development of electric vehicles. Regenerative braking has become one of the ways to solve the driving range as this method can increase an EV’s driving range by 8-25%.[13,14] This technology had mostly replaced the traditional braking system in the cars. The traditional braking system always utilizes mechanical friction method to dissipate kinetic as heat energy in order to achieve the effect of stopping. Studies show that in urban driving about one third to one half of the energy required for operation of a vehicle is consumed in braking [11, 12]. Base on the energy perspective, the kinetic energy of EV is surplus energy when the electric motorcycle is in the braking state since it dissipated the energy as heat and causes a loss of the overall energy. This wasted energy can actually convert to a useful energy for a car especially in hybrid and electric car. Therefore regenerative braking had been implemented in the car braking system. However, the total energy saves dependent on driving condition. Normally it will be more effective in city driving rather than highway where little braking occurs. There are several advantages of regenerative braking taken over the traditional braking system such as;

1. More control over the braking
2. More efficient and effective in stop-and-go driving conditions
3. The brakes work in reverse, which might help at the ramp
4. Better fuel economy
5. Reduced carbon dioxide
6. Save energy and go green
7. Prevents wear on mechanical brake systems

In this work, the working principle and some braking controller for the regenerative braking have been reviewed.

II. REGENERATIVE BRAKING SYSTEM

A. *Working principle*

Regenerative braking is a braking method that uses the mechanical energy from the motor to convert into electrical energy and regenerated back into the supply source. The regenerative braking improves the efficiency of the car by converting kinetic energy to thermal energy through frictional braking. The vehicle can convert a good fraction of its kinetic energy to charge up the battery, using the same principle as an alternator. In regenerative braking system for EV, it use motor to slow down the car when the driver apply force on the brake pedal, then the electric motor works in reverse direction thus slowing the car. While running backwards, the motor acts as the generator to recharge the batteries as shown in figure 2. While in normal running condition where the motor turning forward and taken energy from the battery as shown in figure 1. By using regenerative braking method, it vastly reduces the reliance on fuel, boosting economy and lowering emissions [**1**] [2]. These types of brakes work effective in condition such as stop-and-go driving situations in urban city. The regenerative braking system can provide the majority of the total braking force when there are in low-speed, stop-and-go traffic where little deceleration is required. In any vehicles that use these kinds of brakes, the brake controller can do much more than just monitoring the speed of the wheel. It can be used to calculate the torque, rotational force and generated electricity to be fed back into the batteries. During the braking operation, the brake controller directs the electricity produced by the motor into the batteries or capacitors [**1**] [2], The advanced algorithms in the motor controller give it complete control of the motor torque for both driving and regenerative braking. A torque command is derived from the position of the throttle pedal. The motor controller converts this torque command into the appropriate 3-phase voltage and current waveforms to produce the commanded torque in the motor in the most efficient way. The torque command can be positive or negative. When the torque serves to slow the vehicle then energy is returned to the battery, regenerative is achieved.

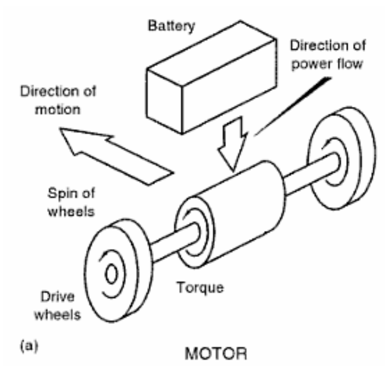

Figure 1: Car in moving forward condition [11]

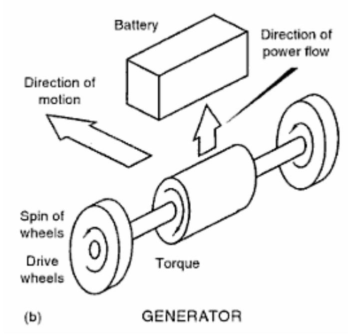

Figure 2: regenerative action during braking [11]

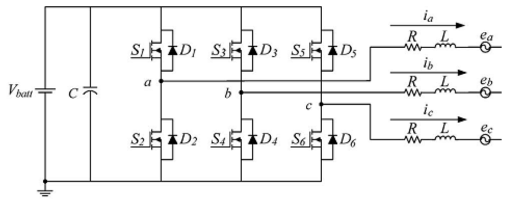

Figure 3: Basic control circuit of three phase motor [16]

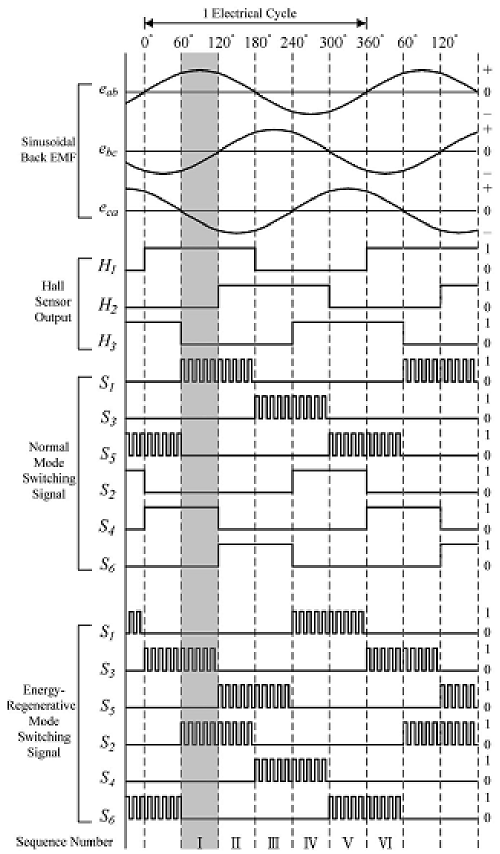

(b)

Figure 3(b) shows the characteristics of Hall sensor signals, back EMFs, and switching signal sequences of normal and energy-regenerative modes [16]

Fig. 3 shows the basic control circuit used in the regenerative braking system. It consisted of power electronic components such as IGBT, thyristor, diodes and resistors. Base on the figure;

- R and L are the armature resistance and inductance
- ea, eb, and ec are the armature back EMFs of the phase a, b, and c.
- ia, ib, and ic are the armature currents of the phase a, b, and c.

Fig. 3(b) shows the switching sequences of the normal and energy-regenerative modes for the Brushless DC Motor (BLDCM). Base on Fig. 3(b);

- eab ebc, and eca are the line-to-line armature back EMFs
- H1 − H3 are the commutation signals (Hall sensor signals)
- S1 − S6 are the switching signals of the six power switches

During the normal mode, the high side switches S1, S3, and S5 are operated in pulse width modulation (PWM) switching mode; the low side switches S2, S4, and S6 are operated in normal high or low. To the contrary, all the switches are operated in PWM switching mode during the energy-regenerative mode. [16]

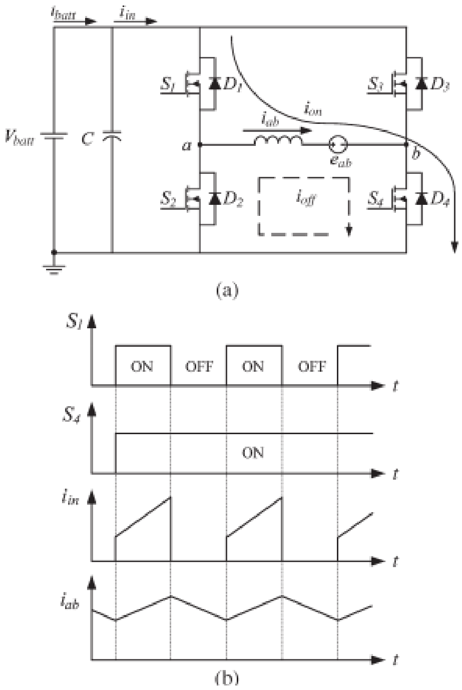

Figure 4: The state 1 under normal condition (a) Equivalent circuit (b) Waveform of input and phase current, switching signal S1 and S4 [16]

- Normal Mode

Fig. 4(a) which shows one of six state intervals (state I) and its equivalent circuit. During state I, the conduction mode represents that the switches S1 and S4 are turned on simultaneously. The inductor current iab would be increased by the energized current loop ion of the winding. Since the magnetic field of the winding is increased due to iab increase, a reverse induction voltage eab has to resist the variation of the magnetic field according to Lenz’s Law. This is represent the armature back EMF of the motor. During another mode (freewheeling mode), the switch S1 is turned off, and S4 is still on such that the inductor current will flow into the freewheeling diode D2 and the switch S4,which makes a discharging current path ioff. The corresponding sequences of S1, S4, input current iin and phase current iab are shown in Fig. 4(b). [16]

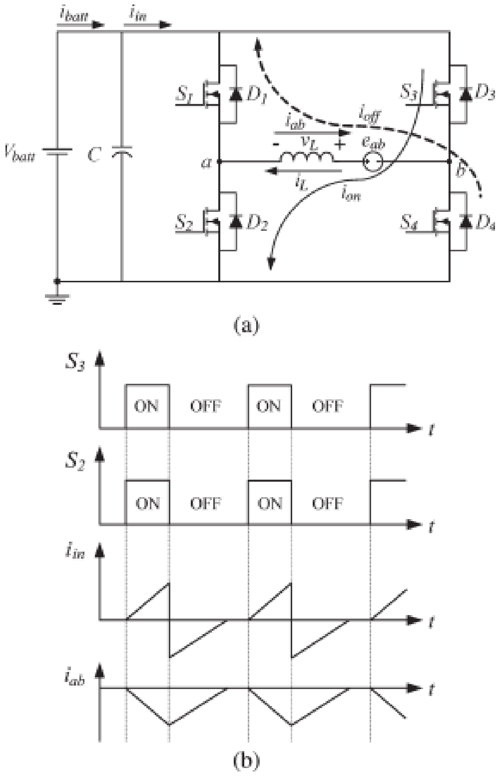

Figure 5: The state 1 under energy regenerative mode (a) Equivalent circuit (b) Waveform of input and phase current, switching signal of S_2 and S_3 [16]

- Energy-Regenerative Mode

The EV receives a brake signal; the motor operation changed from the normal mode into the energy-regenerative mode. The switching sequence is originally in the state I, as shown in Fig. 3(b). Thus, the operating principle of the energy regenerative mode for the duration of the state I is analyzed. Fig. 5(a) shows the equivalent circuit of the energy regenerative mode. When the motor goes into the energy-regenerative mode, the back EMF eab becomes a voltage source. It has to change the switching sequence to the energy regenerative mode; it can be done by switching on the switches S2 and S3. During the turn-on period of S2 and S3, the voltage vL is equal to Vbatt +

eab, and the current iin is equal to −iab,or ion, because of the winding energizing. On the contrary, during the turn-off period of S2 and S3, the current iin, which flows through the freewheeling diodes D1 and D4, is equal to iab and makes a current path ioff return to the battery. The corresponding sequences of S2, S3, the input current iin and the phase current iab are shown in Fig. 5(b). [16]

III. IMPROVEMENT IN REGENERATIVE BRAKING SYSTEM

A. Implementation of flywheel in regenerative braking system

A flywheel is an inertia energy storage device or known as electro-mechanical battery. It is use to absorb mechanical energy and serve as a storage reservoir. Flywheel is supported by magnet floating bear in vacuum and converts electric energy into kinetic energy and also kinetic energy into electric energy through the same motor/generator. Basically it store energy during the period when the supply of energy is more than the requirement and release it during the period when the requirement of energy is more than the supply. In regenerative braking system, flywheel is used to smoothen out variations in the speed of a shaft caused by torque fluctuations. It functions when the source of the driving torque or load torque is fluctuating in nature. Flywheel design can be improve by increasing its angular velocity and delivers the stored energy by decreasing its velocity. The specific energy of flywheels increases proportionally as the weight of rotating material is reduced, when compared in terms of equal mechanical strength of the flywheel.[15] There are some reasons for choosing Flywheels [15];

- It is a pure mechanical device without external power input
- No chemical reaction like chemical battery and zero emission so it is categorized as ecologically clean nature.
- Long cycle life means that it have longer life span
- High cycle efficiency of around 90%
- Low effect on life cycle although in fast charging
- Long maintenance period of more than 10 years therefore it is more reliable and low maintenance cost
- Flexibility in design and operation

B. Implementation of ultra capacitor and DC-DC converter in regenerative braking

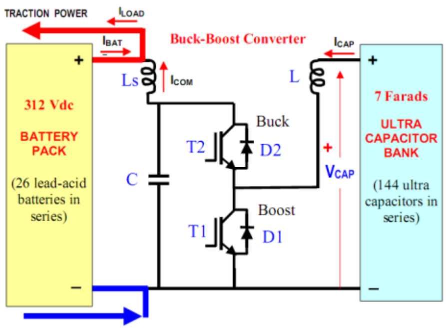

Figure 6: Flywheel regenerative braking

In the ultracapacitor system, the 3 main components are the bidirectional DC-DC converter based on the insulated gate bipolar transistors(IGBTs). The smoothing inductor LS and the ultra capacitor bank. The equipment is connected in parallel to the main of the battery. During acceleration, the capacitor voltage is allowed to discharge from full charge to one-third of its nominal voltage. During deceleration, the energy is recovered and charge up the ultracapacitor. For the DC-DC converter which is the buck-boost circuit . The boost operation is used for acceleration while buck operation is use for deceleration which will charge up the capacitor. The operation of the circuit is basically divided into two states which are boost and buck. By switching T1 on and off at a controlled duty cycle during Boost operation, the amount of energy required from the capacitor will flow to the battery. When T1 is ON, energy is taken from the capacitor, and stored in the inductor L. When T1 is OFF, the energy stored in L is transferred int o C, through D2, and then into the battery pack[4]. During Buck operation, the energy of the battery is covert to the ultracapacitor. This operation is done by controlling the pulse width modulation operation on T2. When T2 is switched ON, the energy from the battery will flow to the ultracapacitor while L stores part of this energy. When T2 is OFF, the remaining energy stored in L is transferred inside the ultra capacitor[4].

Advantages of using the circuit [4];

- DC-DC conveter design using IGBTs and water cooling system to reduce weight and size.
- Inductor LS design using aluminium coil, this coil is made wih flat plates so it reduce skin effect and minimized the losses and weight plus with air core it eliminates the saturation problem
- The voltage cell balancing protect overvoltage condition in a single capacitor when the whole package is near its maximum voltage

Ultracapacitor plays an important role in the system as this new technology has the abilities such as [4]:

- Store as much 20 times more energy compare to electrolytic capacitor
- Charge and discharge without performance degradation
- Improve the transient performance in EV car
- Fast and sudden battery discharge during acceleration or breaking can be avoided
- Provide additional supply to the car and prolong its distance.

IV. CONCLUSION

Regenerative braking is one of the most important systems in electric vehicle since it has the ability to save the wastes energy up to 8-25%. This amount of saved energy can be use to extend our range journey and power up the accessories in the car. The regenerative braking system has been improved by the advanced power electronic component such as ultracapacitor, DC-DC converter (Buck-Boost) and flywheel. The ultracapacitor that help in improving the transient state of the car during starting, provide a smooth charging characteristic for the battery and improve the overall performance of the electric vehicle system. The Buck-Boost converter helps maintaining the power management in the regenerative braking system such as boosting the acceleration. Finally, the flywheel is used to enhance the power recovery process on the wheel. In conclusion, the regenerative braking is a brilliant concept that has been developed by the automotive engineers. If this system is fully utilized and further improve in the future, a new generation of electric vehicle will be invented.

REFERENCES

[1] Yong Chen, Quanshi Chen, Yong Huang, Journal Of Asian Electric Vehicles (2004), 511-515

[2] Naohisa Hashimoto, Manabu Omae , Hiroshi Shimizu, Journal Of Asian Electric Vehicles (2004), 557-563

[3] Xinbo Chen , Gang Wan , Guobao Ning, Journal Of Asian Electric Vehicles ,(2009)1-5

[4] Juan W. Dixon, Micah Ortúzar and Eduardo Wiechmann IEEE AESS Systems Magazine Wiechmann, Journal Of Asian Electric Vehicles(2002),16-21

[5] Jun Takehara, and Kuniaki Miyaoka, EV Mini-Van Featuring Series Conjunction of Ultracapacitors and

[6] Dixon, J. (2010). Energy Storage for Electric Vehicles. Industrial Technology (ICIT), 2010 IEEE International Conference, (pp. 20 - 26).

[7] Tien-Chi Chen, T.-C. C.-S. (2009). Driving and Regenerative Braking of Brushless DC Motor for. *Journal Of Asian Electric Vehicles* , 1-11.

[8] C. C. Chan, “The state of the art of electric, hybrid, and fuel cell vehicles,” Proceedings of the IEEE, vol. 95, no. 4, pp. 704-718,April, 2007.

[9] H. Wu, S. Cheng and S. Cui, “A controller of brushless DC motor for electric vehicle,” IEEE Trans. on Magnetic, vol. 40, no. 1, pp. 509-513, January 2005.

[10] E.Fuhs, E. (2009). *hybrid vehicle and the future of personal transportation* . CRC press.

[11] Yinmin Gao, Liping Chen, Mehrdad Ehsani, Investigation of the Effectiveness of Regenerative Braking for EV and HEV. SAE InternationalSP-1466.1999-01-2910. 1999.

[12] Mehrdad Ehsani, Yimin Gao, Karen L Butler, Application of Electrically Peaking Hybrid (ELPH) Propulsion System To A Full Size Passenger Car WithSimulated Design Verification. IEEE Transaction On Vehicular Technology. Vol.48, No.6, Nov. 1999.

[13]Cao Binggang, Zhang Chuanwei, BaiZhifeng, Trend of Development of Technology for Electric Vehicles. Journalof Xi'an Jiaotong University.2004,38(1): 1-5.

[14]Binggang Cao, Z. B. (2005). Research on Control for Regenerative Braking of Electric Vehicle. *IEEE* , 92-97. [15] Dixon, J. (2010). Energy Storage for Electric Vehicles. *Industrial Technology (ICIT), 2010 IEEE International Conference*, (pp. 20 - 26).

[16] Ming-Ji Yang, H.-L. J.-Y.-K. (june 2009). A Cost-Effective Method of Electric Brake With Energy Regeneration for Electric Vehicles. *IEEE TRANSACTIONS ON INDUSTRIAL ELECTRONICS, VOL. 56, NO. 6* , 2203-221

Ultra Fast Charging System on Lithium Ion Battery

C.K.Leong*, *Y.H Gan, G.D Gan, Z.Y Phuan, M.K Yoong, B.K Cheah. K.W Chew*

Faculty Of Engineering And Science, University Tunku Abdul Rahman, Setapak Kuala Lumpur, 53100

ID:STU10028

***Abstract*— Even with the advancement of the high technology nowadays, the popularity of electric vehicle is still limited and unable to make it a common usage. The main reason is due to the limitation of the battery pack which is bulky, heavy, slow charging, short lifespan and toxicity hazardous. Among these problems, slow charging speed becomes the main consideration when purchasing an electric vehicle. Hence, different charging methods have to be studied thoroughly to seek for the best solution to overcome these problems. In today's competitive battery charging method, a lot of charger manufacturers claim that they can amazingly short charge times of 30 minutes or less. In this project, different charging method such as Constant Voltage charging, Constant Current charging, Pulsed charge etc, have been studied and compared to optimize the charging time suitable for different kind of battery pack.**

I. INTRODUCTION

N today's technology of Electric Vehicle (EV), the effort put on the research to improve the current EV cars is getting serious. Engineers and scientist has work hard to obtain better improvements. The major problem on EV cars now is the batteries charging and lifespan cycle. With the fast pace of everyday life, people wants everything to be quick. Charging an EV car at a station for several hours every few hundred kilometers is not liable and a waste of time. People would just rather use a normal petroleum car which can be refuel within 10 minutes. This problems has made the EV cars to be weak in the area of power despite the technology we have now. Some companies has also claimed that they can charge a battery under five minutes [1] which a breakthrough for EV cars. But the production has yet to be seen in the market.

Charging a lithium ion battery is simple, but charging it quickly might have some problems. These problems consist of lifespan cycles, heat dissipation of battery, ventilation of battery and efficiency if charging. The studied done, many types of fast charging has been studied throughout the years to improve on this matter. Improvement and optimization is now being done on batteries. Lithium-Ion batteries are chosen for powering up the EV car.

II. CHEMISTRY

Lithium polymer battery makes use of lithium cobalt dioxide as the positive electrode and a highly crystallized specialty carbon at the negative electrode to generate a reaction. Both reactions are mediated by electrolyte. Liquid electrolyte in lithium polymer battery consist of LiPF6 (Lithium Hexafluorophosphate) and organic solvents[2]. During charging, the current pumped inside the battery will then charged the electrode with electrons. The capacity of electrons is being expanded when charging. But when charging, the electrodes will then release gaseous which will expand the surface of the lithium-Ion battery and eventually the lifespan of the battery drop.

Full Chemical Reactions For Charging

$LiCoO2 + Cn \leftrightarrow Li(1\text{-}x)CoO2 + CnLix$

III. CHARGING STATE

The terminology of charging fast battery also has phases to consider. The first phase is where the charging rate can be exponentially fast for the first 70 percent of the battery charging. After that, it will go into the second phase with the balance charge will be controlled and have to be slowed down. In the second phase of the charge cycle, the charge current must be lowered. The efficiency to absorb charge is progressively reduced as the battery moves to a higher state-of-charge. If the charge current remains too high in the later part of the charge cycle, the excess energy turns into heat and high cell pressure.

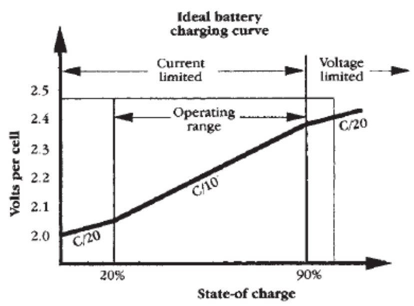

Figure 1.1 - Charging State Of Battery
Source: Build Your Own Electric Car 2nd Edition Mc Graw Hill [3]

Eventually, venting will occur, releasing oxygen and hydrogen. Not only do the escaping gases deplete the electrolyte, they are highly flammable. Such happening must not be found in a battery charging as this will cause the lifespan of the battery to be shorter and easier to be damaged.

IV. FAST CHARGING

The key to fast charging is about fast. Some chargers which are able in the market can not meet the standard of fast charging which is defined by Advanced Lead Acid Battery Consortium (ALABC)[3] which states that fast charging means charging a battery in full capacity without damaging the battery within 4 hours and 80% charge return in no more than 15 minutes or 50% charge return in no more than 5 minutes . Fast charging has to be controlled at all times to avoid over-charging of the battery which will cause the battery to be heated up and then gaseous will expand the surface of the battery.

For improvement in this, study has shown that charging the lithium-ion battery using a pulse charge will decrease the defects on the lithium battery. The positive current charge will charge the battery and the negative charge will reduce the gas release from the electrodes.

But for charging Li-Ion batteries at safest and fast way is the pulse-charging which is also commonly used in charging electric vehicle. Pulsed chargers feed the charge current to the battery in pulses. The charging rate (based on the average current) can be precisely controlled by varying the width of the pulses, typically about one second. During the charging process, a short rest period of 20 to 30 milliseconds, between pulses allow the chemical actions in the battery to be stabilized by equalizing the reaction throughout the bulk of the electrode before recommencing the charge.[4] This enables the chemical reaction to keep pace with the rate of inputting the electrical energy. This method can also reduce unwanted chemical reactions at the electrode surface such as gas formation, crystal growth and passivation. At this stage, it is possible to charge the battery at high current flow which makes charging faster for battery without any damage of gas release.

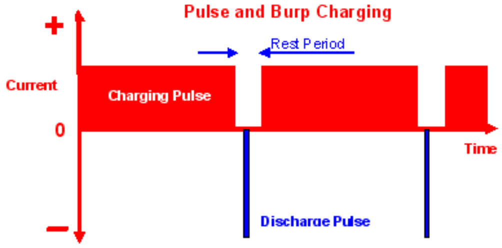

Figure 1.2 –Pulse Charging
Source: Unknown

V. BATTERY LIFESPAN

There are many ways that we can prolong the lifespan of the battery. Lifespan of a battery in EV cars plays an important role because customers want to have confident on the product. This is where car manufacturer has to ensure that the battery supplier can guarantee the lifespan of the battery in despite of the costly battery price.

One of the ways to prolong the lifetime of a battery is to limit the time at which the battery stays at 4.20/cell. Prolonged high voltage will cause corrosion, especially at elevated temperatures. 3.92V/cell is the best upper voltage threshold for cobalt-based lithium-ion. Charging batteries to this voltage level has been shown to double cycle life. Lithium-ion systems for defense applications make use of the lower voltage threshold. The negative is reduced capacity.

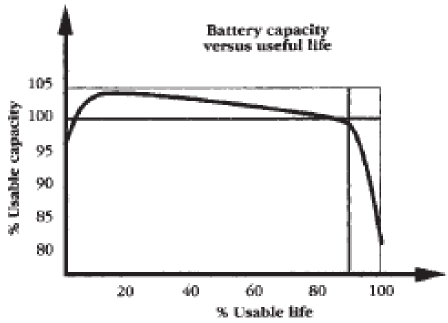

Figure 1.3 –Lifespan Of A Battery
Source: Build Your Own Electric Car 2nd Edition Mc Graw Hill [3]

The charging current of Li-ion should be moderate (0.5C for cobalt-based lithium-ion). The lower charge current reduces the time in which the cell resides at 4.20V. It should be noted that a 0.5C charge only adds marginally to the charge time over 1C because the topping charge will be shorter. A high current charge tends to push the voltage up and forces it into the voltage limit prematurely.

VI. CONCLUSION

As a conclusion, Fast charging system for the Electric Vehicle is possible and more research needs to be done to optimize the current chargers in the market for more efficient and safe charging for Electric Vehicle in the future.

REFERENCES

[1] Toshiba, Japan – The Associated Press 2010
[2] B. G. Kim, F. P. Tredeau, Z. M. Salameh “Fast Chargebility Lithium Polymer Batteries” Dept. Electrical and Computing Eng., Univ. Massachusetts, Lowell, 2008
[3] S.Leitman, B.Brant “Build Your Own Electric Vehicle” Mc Graw Hill (2008) (pg 210)
[4] M.W Cheng, S.M Wang, Y.S Lee, S.H Hsiao “Fuzzy Controlled Fast Charging System for Lithium Ion Batteries” Dept. of Electronic Eng. Fu Jen Catholic Univ. Taipei, Taiwan (2009)

APPENDIX B: News of IEEE Student 2010Conference and Sponsorship from Yokohama

4 UTAR NEWS DECEMBER 2010

Sitting in the second row (from left), Dr. Tan (fourth), Prof. Chuah (sixth), Prof. Lee (seventh) and Ling (eighth) with participants, speakers and organising committee members

First IEEE student conference in UTAR

UTAR Student Branch of the Institute of Electrical and Electronics Engineers (IEEE) organised its first conference at UTAR campus in Petaling Jaya on 20 and 21 November 2010.

Titled "Sustainable Utilization and Development in Engineering and Technology or in short STUDENT 2010, it was also the last event held at the venue as the building that housed it was to be returned to the property owner.

Officiated by UTAR President Ir. Prof. Dato' Dr. Chuah Hean Teik, the conference was organised to provide a channel for tertiary education students to present their projects and get recognition for their professional and technical achievements by IEEE and the industry.

"All the papers accepted for presentation at the conference will be published in IEEE Explore Digital Library," said Conference Director Taylor Ling Jia Zun.

The two-day conference, which saw 31 papers presented in eight sessions, attracted over 60 participants, among whom were those from India, China, Singapore and Pakistan.

UTAR Vice President (R&D and Commercialisation) Prof. Dr. Lee Sze Wei, and Chair of UTAR Centre for Vehicular Technology and the chairman of the steering committee of the conference Asst. Prof. Dr. Tan Ching Seong were also present at the opening ceremony. The conference emphasised sustainability in the application of engineering ideas and covered a wide range of research themes including alternative energy, healthcare science and technology, artificial intelligence, robotics and automation, and vehicular technology.

UTAR NEWS OCTOBER 2010

PAGE 5

Yokohama Industries seeks ties

Three delegates from Yokohama Industries Berhad visited UTAR Kuala Lumpur Campus on 4 October 2010.

Located in a 32-acre site in Semenyih, Selangor, Yokohama Industries Berhad is one of the largest battery manufacturers in Malaysia.

The delegates were its Chief Executive Officer Dr. Patrick Yong, Head of Centre for Electrochemical Research G. Balasubramaniam and Head of Corporate Communications Michelle Yong.

Present to meet the delegates were UTAR Vice President (R&D and Commercialisation) Prof. Dr. Lee Sze Wei, Dean of the Faculty of Engineering and Science Assoc. Prof. Dr. Wang Chan Chin, Deputy Dean Asst. Prof. Dr. Tan Yong Chai and several other faculty and staff members.

The two parties explored the possibility of collaboration in research, student adoption programme, and subsidies and scholarships.

From right: Dr. Tan YC, Dr. Tan CS, Balasubramaniam, Yong, Dr. Yong, Prof. Lee and other UTAR staff

Chair of Centre for Vehicular Technology Asst. Prof. Dr. Tan Ching Seong also presented slides on the research areas of the centre.

"One of the main purposes of my visit is to get to know relevant young talents [in UTAR] earlier and offer them an opportunity to learn together with the industry," said Dr. Yong during the discussion.

Dr. Yong added that Yokohama Industries was planning to engage undergraduates to work part-time and provide them with a monthly allowance.

The meeting was a fruitful one. Besides engaging UTAR students to work part-time in Yokohama Industries, both parties were keen on collaborative research on electric vehicles.

The delegates also indicated their keen interest to establish closer links with UTAR in other related matters in the future.

Dr. Yong looking at the solar collector at Kuala Lumpur Campus

APPENDIX C: Pictures from Malaysian Universities Transportation Research Forum and Conference (MUTRFC 2010)

APPENDIX D: Pictures of Innovate Malaysia 2011 Intel Platform Project Design Competition (Preliminary Round-Top23)

APPENDIX E: Innovate Malaysia 2011 Intel Platform Project Design Competition (Top 5 Finalist)

Competition Finalists

Competition finalists have been shortlisted! Congratulations to the teams! The finalists will enter to the grand finale, where the first prize, second prize, third prize, and consolation prizes will be decided during the event.

Note that the lists below are sorted by team ID. The teams may further improve their projects to compete during the grand finale.

Intel Track

Team	University	Project Title
MY011	MMU (Cyberjaya)	SMART Transit System
MY021	MMU (Melaka)	Smart Office
MY031	UTAR	Digital Speed Limit Monitoring System
MY035	MMU (Melaka)	Brain Computer Interface Control of Electrical Powered Wheelchair
MY071	UTAR	Electric Car Intelligent Controller System

APPENDIX F: Tai Kwong Yokohama Battery Industries Sdn. Bhd. Sponsorships

APPENDIX G: Response Time Table for LM35 Temperature Sensor

Output Voltage, V	*Temperature, Celcius*
0.22	22
0.37	37
0.484	48.4
0.526	52.6
0.563	56.3
0.571	57.1
0.585	58.5
0.59	59
0.594	59.4
0.597	59.7
0.601	60.1
0.604	60.4
0.609	60.9
0.612	61.2
0.616	61.6
0.619	61.9
0.624	62.4
0.63	63
0.633	63.3
0.638	63.8
0.64	64
0.645	64.5
0.649	64.9
0.652	65.2
0.656	65.6
0.659	65.9
0.662	66.2
0.665	66.5
0.668	66.8
0.67	67
0.671	67.1
0.672	67.2
0.672	67.2
0.673	67.3
0.674	67.4
0.675	67.5
0.677	67.7
0.678	67.8
0.679	67.9
0.681	68.1
0.682	68.2

0.683	68.3
0.684	68.4
0.686	68.6
0.687	68.7
0.689	68.9
0.69	69
0.691	69.1
0.692	69.2
0.694	69.4
0.695	69.5
0.697	69.7
0.698	69.8
0.699	69.9
0.7	70
0.701	70.1
0.702	70.2
0.703	70.3
0.704	70.4
0.705	70.5
0.707	70.7
0.707	70.7
0.708	70.8
0.709	70.9
0.71	71
0.711	71.1
0.711	71.1
0.711	71.1
0.712	71.2
0.713	71.3
0.714	71.4
0.715	71.5
0.716	71.6
0.716	71.6
0.716	71.6
0.717	71.7
0.718	71.8
0.718	71.8
0.718	71.8
0.719	71.9
0.719	71.9
0.72	72
0.721	72.1
0.721	72.1
0.721	72.1
0.722	72.2

0.722	72.2
0.723	72.3
0.723	72.3
0.724	72.4
0.725	72.5
0.725	72.5
0.726	72.6
0.726	72.6
0.726	72.6
0.727	72.7
0.727	72.7
0.728	72.8
0.728	72.8
0.729	72.9
0.729	72.9
0.73	73
0.73	73
0.731	73.1
0.731	73.1
0.731	73.1
0.732	73.2
0.732	73.2
0.733	73.3
0.733	73.3
0.734	73.4
0.734	73.4
0.734	73.4
0.735	73.5
0.735	73.5
0.736	73.6
0.736	73.6
0.737	73.7
0.737	73.7
0.737	73.7
0.738	73.8
0.738	73.8
0.738	73.8
0.739	73.9
0.739	73.9
0.74	74
0.74	74
0.74	74
0.741	74.1
0.741	74.1
0.741	74.1

0.741	74.1
0.741	74.1
0.742	74.2
0.742	74.2
0.742	74.2
0.743	74.3
0.743	74.3
0.743	74.3
0.743	74.3
0.744	74.4
0.744	74.4
0.744	74.4
0.744	74.4
0.744	74.4
0.744	74.4
0.744	74.4
0.745	74.5
0.745	74.5
0.745	74.5
0.745	74.5
0.745	74.5
0.745	74.5
0.745	74.5
0.745	74.5
0.745	74.5
0.746	74.6
0.746	74.6
0.746	74.6
0.746	74.6
0.746	74.6
0.746	74.6
0.746	74.6
0.746	74.6
0.746	74.6
0.746	74.6
0.746	74.6
0.746	74.6
0.747	74.7
0.747	74.7
0.747	74.7
0.747	74.7
0.747	74.7
0.747	74.7
0.747	74.7
0.747	74.7

0.747	74.7
0.747	74.7
0.747	74.7
0.747	74.7
0.747	74.7
0.747	74.7
0.747	74.7
0.748	74.8
0.748	74.8
0.748	74.8
0.748	74.8
0.748	74.8
0.748	74.8
0.748	74.8
0.748	74.8
0.748	74.8
0.748	74.8
0.748	74.8
0.748	74.8
0.748	74.8
0.749	74.9
0.749	74.9
0.749	74.9
0.749	74.9
0.749	74.9